UNIVERSITY of NAPLES FEDERICO II

PH.D. PROGRAMME in

MATERIALS and STRUCTURES ENGINEERING

XX CYCLE

PH.D. THESIS

RAFFAELLO FICO

LIMIT STATES DESIGN of CONCRETE STRUCTURES REINFORCED with FRP BARS

COORDINATOR

Prof. DOMENICO ACIERNO

TUTOR

Dr. ANDREA PROTA

UNIVERSITY OF NAPLES FEDERICO II

PH.D. PROGRAMME IN MATERIALS and STRUCTURES ENGINEERING
COORDINATOR PROF. DOMENICO ACIERNO
XX CYCLE

PH.D. THESIS

RAFFAELLO FICO

LIMIT STATES DESIGN of CONCRETE STRUCTURES REINFORCED with FRP BARS

TUTOR Dr. ANDREA PROTA

"*Memento audere semper"*

G. D'annunzio

ACKNOWLEDGMENTS

To Dr. Manfredi, my major professor, I express my sincere thanks for making this work possible. His valuable teachings will be engraved in my mind forever.

I am very grateful to Dr. Prota for his assistance and devotion; his experience and observations helped me a lot to focus on my work. I have learned many things from him during the last three years.

I wish to express sincere appreciation to Dr. Nanni for animating my enthusiasm each time that I met him. A special thank goes to Dr. Parretti for supporting me any time that I asked.

I would like to thank my dearest parents for making me believe in my dreams and for constantly supporting me to achieve them. I would like to extend my deepest regards to my beloved brothers and sister for being there with me throughout.

My deepest thank goes to the friends (they know who they are) that shared with me the most significant moments of these years.

Finally, I would like to thank all friends and colleagues at the Department of Structural Engineering who have contributed in numerous ways to make this program an enjoyable one.

INDEX

Chapter I: INTRODUCTION

1.1 BACKGROUND

Design Guidelines CNR-DT 203/2006, "*Guide for the Design and Construction of Concrete Structures Reinforced with Fiber-Reinforced Polymer Bars*", have been lately developed under the auspices of the National Research Council (CNR). The new document (see front page in Figure 1) adds to the series of documents recently issued by the CNR on the structural use of fiber reinforced polymer (FRP) composites, started with the publication of CNR-DT 200/2004, pertaining to the use of externally bonded systems for strengthening concrete and masonry structures.

The approach followed is that of the limit states semi-probabilistic method, like all the main current guidelines, while the format adopted is that of 'principles' and 'practical rules', in compliance with the classical style of Eurocodes. It is also conceived with an informative and educational spirit, which is crucial for the dissemination, in the professional sphere, of the mechanical and technological knowledge needed for an aware and competent use of such materials.

A guideline, by its nature, is not a binding regulation, but merely represents an aid for practitioners interested in the field of composites. Nevertheless, the responsibility of the operated choices remains with the designer.

The document is the result of a remarkable joint effort of researchers from 7 Italian universities and practitioners involved in this emerging and promising field, of the technical managers of major production and application companies, and of the representatives of public and private companies that use FRP as reinforced concrete (RC) reinforcement (see Figure 2). Thus, the resulting FRP code naturally encompasses all the experience and knowledge gained in ten years of countless studies, researches and applications of FRP in Italy, joined to the learning gathered from the available international codes on the design of FRP RC structures.

After its publication, the document n. 203/2006 was subject to a public hearing between February and May 2006. Following the public hearing, some modifications and/or integrations have been made to the document including corrections of typos,

additions of subjects that had not been dealt with in the original version, and elimination of others deemed not to be relevant.

The updated document has been approved as a final version on 18/06/2007 by the "Advisory Committee on Technical Recommendation for Construction".

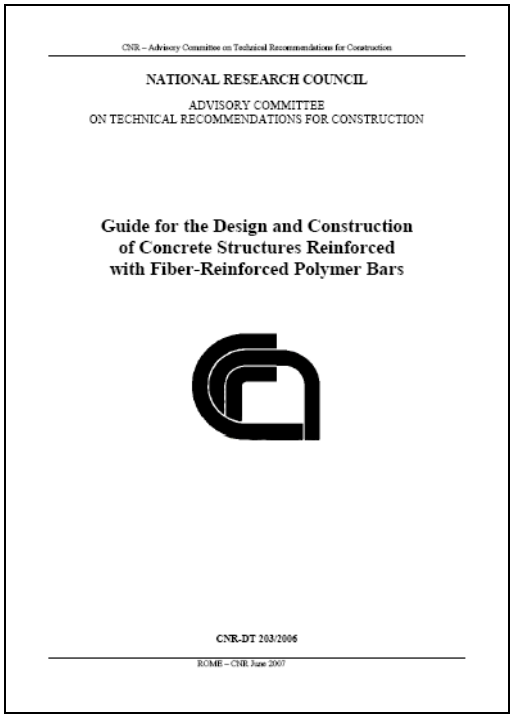
CNR – Advisory Committee on Technical Recommendations for Construction

NATIONAL RESEARCH COUNCIL

ADVISORY COMMITTEE
ON TECHNICAL RECOMMENDATIONS FOR CONSTRUCTION

Guide for the Design and Construction of Concrete Structures Reinforced with Fiber-Reinforced Polymer Bars

CNR-DT 203/2006

ROME – CNR June 2007

Figure 1 - Front Page of CNR-DT 203/2006

Task Group	Contents
University of Bologna	Materials
Polytechnic of Milan	Basis of Design
University of Naples "Federico II"	Appendix A (manufacturing techniques of FRP bars)
University of Rome "La Sapienza"	Appendix B (test methods for characterizing FRP bars)
University of Rome "Tor Vergata"	
University of Salerno	Appendix C (technical data sheet for FRP bars)
University of Sannio - Benevento	
ATP Pultrusion - Angri (SA)	Appendix D (tasks and responsibilities of professionals)
Hughes Brothers - Nebraska, U.S.A.	
Interbau S.r.l.- Milan	Appendix E (deflections and crack widths)
Sireg - Arcore (MI)	

Figure 2 - Task Group and Contents of CNR-DT 203/2006

1.2 OBJECTIVES

The thesis project is to assess the main concepts that are the basis of the document CNR-DT 203/2006, analyzing the limit state design of concrete structures reinforced with FRP bars and grids, and in particular:

- The ultimate limit states design, both for flexure and shear;
- The serviceability limit states design, specifically the deflection control;
- Test methods for characterizing FRP bars.

1.3 THESIS ORGANIZATION

- Chapter 2 presents more details on the mechanical and material properties of FRP bars, as well as on the main approaches used by the existing guidelines for the design of FRP RC structures;
- Chapter 3 presents the ultimate limit state design principles for flexure at the basis of document CNR-DT 203/2006, going also into details of the reliability-based calibration of partial safety factors applied to assess the reliability levels of the Italian guidelines.
- Chapter 4 presents the serviceability limit states flexural design of FRP RC elements; in particular, the deflection control of FRP RC members depending on the bond between FRP reinforcement and concrete is investigated based on a consistent set of experimental data.
- Chapter 5 focuses on the assessment of Eurocode-like design equations for the evaluation of the shear strength of FRP RC members, as proposed by the CNR-DT 203, verified through comparison with the equations given by ACI, CSA and JSCE guidelines, considering a large database of members with and without shear reinforcement failed in shear.
- Chapter 6 presents the investigation of mechanical characteristics and geometrical properties of large-scale GFRP bars according to the Appendix B of the CNR-DT 203/2006 (and to ACI 440.3R-04). Furthermore, ad-hoc test set-up procedures to facilitate the testing of such large-scale bars are presented.
- Chapter 7 summarizes the main conclusions and the overall findings of this thesis project with recommendations for further actions to be taken.

Chapter II: LITERATURE REVIEW

2.1 HISTORY of FRP REINFORCEMENT

FRP composites are the latest version of the very old idea of making better composite material by combining two different materials (Nanni, 1999), that can be traced back to the use of straw as reinforcement in bricks used by ancient civilizations (e.g. Egyptians in 800).

The development of FRP reinforcement can be found in the expanded use of composites after World War II: the automotive industry first introduced composites in early 1950's and since then many components of today's vehicles are being made out of composites. The aerospace industry began to use FRP composites as lightweight material with acceptable strength and stiffness which reduced the weight of aircraft structures such as pressure vessels and containers. Today's modern jets use large components made out of composites as they are less susceptible to fatigue than traditional metals. Other industries like naval, defense and sporting goods have used advanced composite materials on a widespread basis: pultrusion offered a fast and economical method of forming constant profile parts, and pultruded composites were being used to make golf clubs and fishing poles.

Only in the 1960s, however, these materials were seriously considered for use as reinforcement in concrete. The expansion of the national highway system in the 1950s increased the need to provide year-round maintenance; it became common to apply deicing salts on highway bridges; as a result, reinforcing steel in these structures and those subject to marine salt experienced extensive corrosion, and thus became a major concern (almost 40% of the highway bridges in the US are structurally deficient or functionally no longer in use, ASCE Report card 2005). Various solutions were investigated, including galvanized coatings, electro-static-spray fusion-bonded (powder resin) coatings, polymer-impregnated concrete, epoxy coatings, and glass FRP (GFRP) reinforcing bars (ACI 440R.1R-06, 2006); yet the FRP reinforcing bar was not considered a viable solution and was not commercially available until the late 1970s.

In 1983, the first project funded by the U.S. Department of Transportation (USDOT) was on "Transfer of Composite Technology to Design and Construction of Bridges" (Plecnik and Ahmad 1988). Marshall-Vega Inc. led the initial development of GFRP reinforcing bars in the U.S. Initially, GFRP bars were considered a viable alternative to steel as reinforcement for polymer concrete due to the incompatibility of thermal expansion characteristics between polymer concrete and steel. In the late 1970s, International Grating Inc. entered the North American FRP reinforcement market. Marshall-Vega and International Grating led the research and development of FRP reinforcing bars into the 1980s.

Parallel research was also being conducted on FRPs in Europe and Japan. In Europe, construction of the prestressed FRP Bridge in Germany in 1986 was the beginning of use of FRP (Meier 1992). The European BRITE/EURAM Project, "Fibre Composite Elements and Techniques as Nonmetallic Reinforcement," conducted extensive testing and analysis of the FRP materials from 1991 to 1996 (Taerwe 1997). More recently, EUROCRETE has headed the European effort with research and demonstration projects. In Japan more than 100 commercial projects involving FRP reinforcement were undertaken up to the mid-1990s (ACI Committee 440, 2001).

The 1980s market demanded nonmetallic reinforcement for specific advanced technology; the largest demand for electrically nonconductive reinforcement was in facilities for MRI (Magnetic Resonance Imager) medical equipment. FRP reinforcement became the standard in this type of construction. Other uses developed as the advantages of FRP reinforcement became better known and desired, specifically in seawall construction, substation reactor bases, airport runways, and electronics laboratories (Brown and Bartholomew 1996).

2.2 PROPERTIES of FRP BARS

The mechanical properties of FRP bars are typically quite different from those of steel bars and depend mainly on both matrix and fibers type, as well as on their volume fraction, but generally FRP bars have lower weight, lower Young's modulus but higher strength than steel. The most commonly available fiber types are the carbon (CFRP), the glass (GFRP) and the aramid (AFRP) fibers.

Table 1 lists some of the advantages and disadvantages of FRP reinforcement for concrete structures when compared with conventional steel reinforcement, as reported by ACI 440.1R-06.

The determination of both the geometrical and mechanical properties of FRP bars requires the use of specific procedures (ASTM D 618, ACI 440.3R-04).

FRP bars have density ranging from one fifth to one forth than that of steel; the reduced weight eases the handling of FRP bars on the project site (ACI Committee 440, 2001).

The tensile properties of FRP are what make them an attractive alternative to steel reinforcement. When loaded in tension, FRP bars do not exhibit any plastic behavior (yielding) before rupture. Therefore FRP reinforcement is not recommended for moment frames or zones where moment redistribution is required. Table 2 gives the most common tensile properties of reinforcing bars, in compliance with the values reported by ACI 440.1R-06. Figure 1 depicts the typical stress-strain behavior of FRP bars compared to that of steel bars.

The CNR-DT 203-2006, instead, prescribes that all types of FRP bars can be used provided that the characteristic strength is not lower than 400 MPa, and the average value of the Young's modulus of elasticity in the longitudinal direction is not lower than 100 GPa for CFRP bars, 35 GPa for GFRP bars, and 65 GPa for AFRP bars; the compressive modulus of elasticity of FRP reinforcing bars appears to be smaller than its tensile modulus of elasticity, in fact most of FRP RC design guidelines suggest not to rely upon strength and stiffness contributions provided by the compressed FRP bars (further research is needed in this area).

The longitudinal coefficient of thermal expansion is dominated by fiber properties, while the transverse coefficient is dominated by the resin; typical values of the coefficient of thermal expansion in the longitudinal and transversal directions, α_l and α_t, respectively, of composite bars with a fibers volume fraction ranging between 50% and 70%, are reported in Table 3 (CNR-DT 203, 2006); higher values of the transversal coefficients of thermal expansion, combined with the Poisson's effect in the case of compressed reinforcements, can be responsible for circumferential tensile stresses that allow the formation of cracks in the radial direction that may endanger the concrete-FRP bond.

FRP reinforcing bars are susceptible to static fatigue phenomenon ("creep rupture"), which is a progressive reduction of strength under long term loads. In general, carbon fibers are the least susceptible to creep rupture, whereas aramid fibers are moderately susceptible, and the glass fibers are the most susceptible (ACI Committee 440, 2001); such phenomenon is also highly influenced by environmental factors, such as temperature and moisture.

The bond between the FRP bar and the surrounding concrete is ensured by propagation of stresses whose values depend on bar geometry, chemical and physical characteristics of its surface as well as concrete compressive strength. The latter parameter is less important for FRP bars than for steel bars. An extensive investigation on bond is given in Chapter 4.

Table 1 - Advantages and Disadvantages of FRP Reinforcement

Advantages of FRP reinforcement	**Disadvantages of FRP reinforcement**
High longitudinal tensile strength (varies with sign and direction of loading relative to fibers)	**No yielding before brittle rupture**
Corrosion resistance (not dependent on a coating)	**Low transverse strength** (varies with sign and direction of loading relative to fibers)
Nonmagnetic	**Low modulus of elasticity** (varies with type of reinforcing fiber)
High fatigue endurance (varies with type of reinforcing fiber)	**Susceptibility of damage to polymeric resins and fibers under ultraviolet radiation exposure**
Lightweight (about 1/5 to 1/4 the density of steel)	**Low durability of glass fibers in a moist environment**
Low thermal and electric conductivity (for glass and aramid fibers)	**Low durability of some glass and aramid fibers in an alkaline environment**
	High coefficient of thermal expansion perpendicular to the fibers, relative to concrete
	May be susceptible to fire depending on matrix type and concrete cover thickness

Table 2 - Typical Tensile Properties of Reinforcing FRP Bars*

	Steel	GFRP	CFRP	AFRP
Nominal yield stress, MPa	**276** to **517**	**N/A**	**N/A**	**N/A**
Tensile strength, MPa	**483** to **690**	**483** to **1600**	**600** to **3690**	**1720** to **2540**
Elastic modulus, GPa	**200**	**35** to **51**	**120** to **580**	**41** to **125**
Yield strain, %	**0.14** to **0.25**	**N/A**	**N/A**	**N/A**
Rupture strain, %	**6.0** to **12.0**	**1.2** to **3.1**	**0.5** to **1.7**	**1.9** to **4.4**

*Typical values for fiber volume fractions ranging from 0.5 to 0.7.

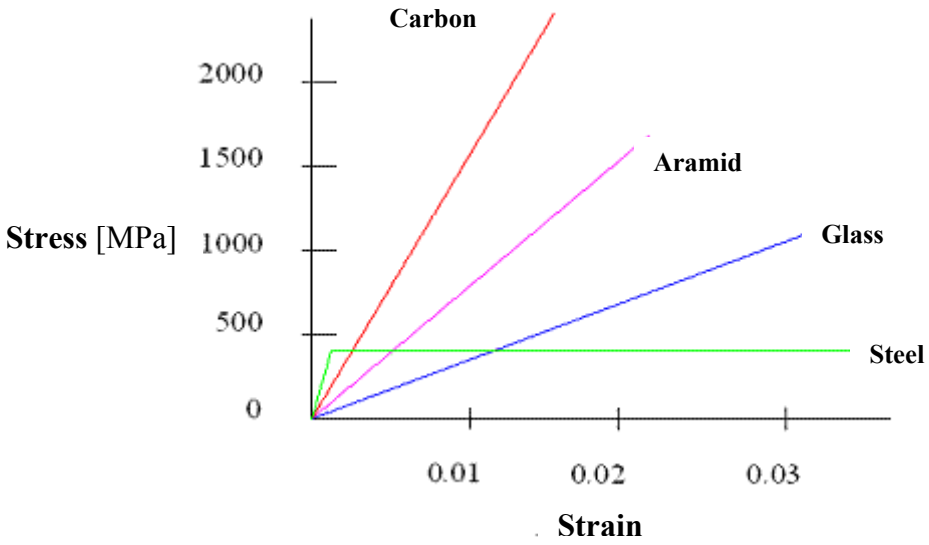

Figure 1 - Stress-strain Curves of Typical Reinforcing Bars

Table 3 - Coefficients of Thermal Expansion

Bar	α_l $[10^{-6}\,°C^{-1}]$	α_t $[10^{-6}\,°C^{-1}]$
AFRP	**-6.0 ÷ -2.0**	**60.0 ÷ 80.0**
CFRP	**-2.0 ÷ 0.0**	**23.0 ÷ 32.0**
GFRP	**6.0 ÷ 10.0**	**21.0 ÷ 23.0**

2.3 FORMS of FRP REINFORCEMENT

Typical FRP reinforcement products are grids, bars, fabrics, and ropes. The bars have various types of cross-sectional shapes (square, round, solid, and hollow) and deformation systems (exterior wound fibers, sand coatings, and separately formed

deformations). A sample of different cross sectional shapes and deformation systems of FRP reinforcing bars is shown in Figure 2.

One of the principle advantages of FRP reinforcement is the ability to configure the reinforcement to meet specific performance and design objectives. For example, FRP reinforcement may be configured in rods, bars, plates, and strands. Within these categories, the surface texture of the FRP reinforcement may be modified to increase or decrease the bond with the surrounding concrete. Unlike conventional steel reinforcement, there are no standardized shapes, surface configurations, fiber orientation, constituent materials and proportions for the final products. Similarly, there is no standardization of the methods of production, e.g., pultrusion, braiding, filament winding, or FRP preparation for a specific application.

Figure 2 - Sample FRP Reinforcement Configurations

2.4 TYPICAL APPLICATIONS

The use of FRP in concrete for anti-corrosion purposes is expected to find applications in structures in or near marine environments, in or near the ground, in chemical and other industrial plants, in places where good quality concrete can not be achieved and in thin structural elements. Most initial applications of FRP reinforcement in concrete were built in Japan, where many demonstration projects were developed in the early 90's, like floating marine structures (Figure 3), pontoon bridges (Figure 4), non-magnetic structures such as tracks for linear motors (Figure 5), bridge decks (Figure 6) and ground anchors (Figure 7).

Figure 3 - Use of Leadline Elements for the Tensioning of Diagonals of a Floating Marine Structure, Japan

Figure 4 - Use of FRP Tendons in the Pontoon Bridge at Takahiko Three Country Club, Japan

Figure 5 - Magnetic Levitation Railway System in Japan

Figure 6 - Use of CFRP Bars in a Stress Ribbon Bridge at the Southern Yard Country Club, Japan

Figure 7 - Use of Technora Elements as Ground Anchors along the Meishin Expressway, Japan

Research and development is now actively taking place in many countries, most prominently in North America and Europe. In Europe, the EUROCRETE project installed the first completely FRP reinforced footbridge in 1996 (Figure 8).

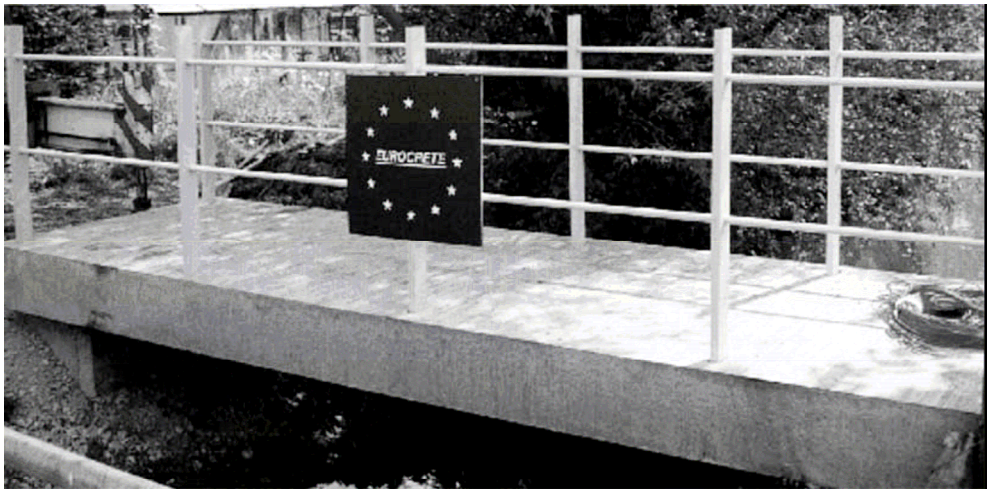

Figure 8 - The First Concrete Footbridge in Europe with Only FRP Reinforcement (EUROCRETE Project)

In North America, Canada is currently the Country leader in the use of FRP bars, mainly as reinforcement of RC bridge decks (Benmokrane, Desgagne, and Lackey 2004); Figure 9 and Figure 10 show some recent bridge applications in USA and Canada (the corresponding reference has been reported when available).

The use of GFRP bars in MRI hospital room additions is becoming commonplace as well (Figure 11).

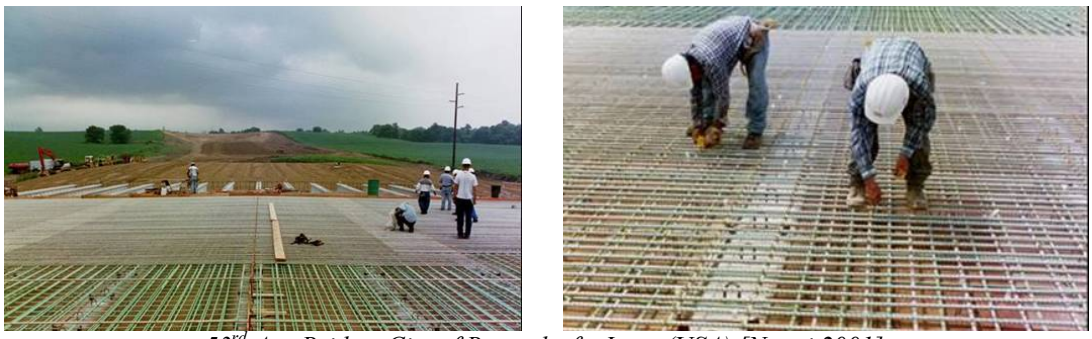

53rd Ave Bridge, City of Bettendorf – Iowa (USA) [Nanni 2001]

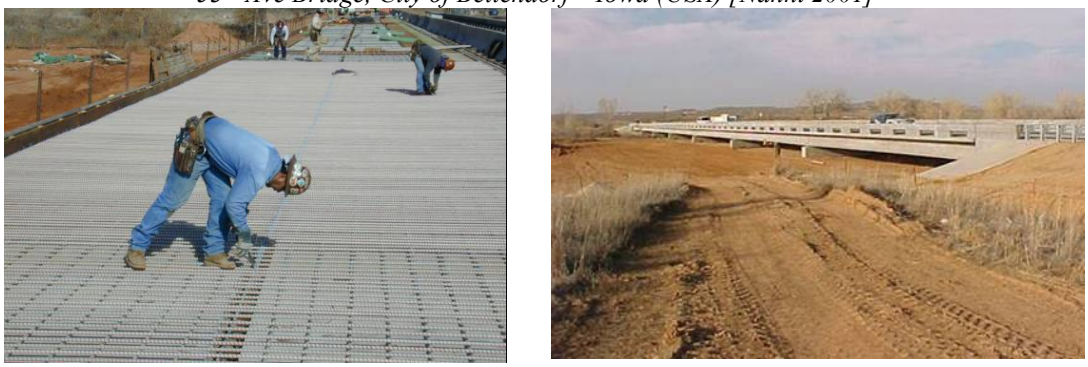

Sierrita de la Cruz Creek Bridge, Potter County – Texas (USA) [Bradberry 2001]


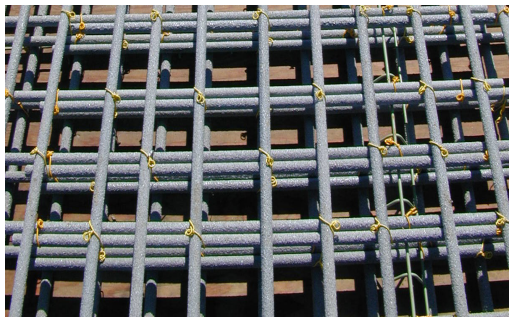

GFRP Bridge Deck, Morristown – Vermont (USA) [2002]

Figure 9 - Recent Applications of FRP RC Bridge Decks in USA


Trout River Bridge, AICAN Highway – British Columbia [2004]


GFRP Bridge Deck, Cookshire-Eaton – Quebec [2003]


Crowchild Bridge Deck, Calgary, Alberta [Rizkalla 1997]

GFRP Bridge Deck, Wotton, Quebec [Rizkalla 1997]

Figure 10 - Recent Applications of FRP RC Bridge Decks in Canada

Lincoln General Hospital, Lincoln – NE (USA)


York Hospital, Trauma Center (USA)

Figure 11 - Recent Constructions of FRP RC Hospital Rooms for MRI

Finally, tunnel works where GFRP reinforcement is used in the portion of the concrete wall to be excavated by the tunnel boring machine (TBM) called soft-eye have become common in many major metropolitan areas of the world, including Asia (for example, Bangkok, Figure 12; Hong Kong, and New Delhi) and Europe (for example, London and Berlin). A detailed description of this application type is given in Chapter 6.

At present, the higher cost of FRP materials suggests that FRP use will be confined to applications where the unique characteristics of the material are the most appropriate. Efficiencies in construction and reduction in fabrication costs will expand their potential market.

Figure 12 - Tunnelling Boring Application, Bangkok MRTA – Thailand
(courtesy: **http://www.fortius.be**)

2.5 REVIEW of EXISTING GUIDELINES DESIGN PHILOSOPHY on FRP RC

Design guidelines for FRP RC structures have been developed in Japan (JSCE, 1997), Canada (ISIS, 2001; CSA-S806, 2002), USA (ACI 440.1R-01, 2001; ACI 440.1R-03, 2003; ACI 440.1R-06, 2006), and Europe (Clarke et al., 1996); Table 4 gives a summary of the historical development of the existing documents ruling the design of internal FRP RC structures.

Table 4 - Chronological Development of Documents for Internal FRP Reinforcement

1970s	**1996**	**1997**
Use of fiber reinforcement in concrete	The European Committee for Concrete (EUROCRETE) published a set of design recommendations for FRP RC	The Japan Society of Civil Engineers (JSCE) published a set of design recommendations for FRP RC
1999	**2000**	**2001**
The Swedish National code for FRP RC was published	The Canadian Standard Association (CSA) published a set of design recommendations for FRP RC Bridges (CAN/CSA S6-00)	The ISIS Canada published a manual on the use of internal FRP reinforcement The American Concrete Institute (ACI) Committee 440 published the first version of design recommendations for internal FRP reinforcement (440.1R)
2002	**2003**	**2006**
The CSA published a set of design recommendations for FRP RC Buildings (CAN/CSA S806-02) CUR Building & Infrastructure published a set of design recommendations for FRP RC (The Netherlands)	ACI Committee 440 published the second version of guidelines 440.1R	The National Research Council (CNR) published the Italian design recommendations for internal FRP reinforcement (CNR-DT 203/2006) ACI Committee 440 published the third version of guidelines 440.1R

The recommendations ruling the design of FRP RC structures currently available are mainly given in the form of modifications to existing steel RC codes of practice, which predominantly use the limit state design approach. Such modifications consist of basic principles, strongly influenced by the mechanical properties of FRP reinforcement, and empirical equations based on experimental investigations on FRP RC elements.

With respect to steel, when dealing with FRP reinforcement the amount of reinforcement to be used has to be determined by a different approach, due to the lower stiffness and the high strength of composite materials. In fact, for FRP reinforcement, the strength to stiffness ratio is an order of magnitude greater than that of steel, and this affects the distribution of stresses along the section.

Hence, when considering a balanced section, a condition desired for steel RC design, the neutral axis depth for FRP RC sections would be very close to the compressive end. This implies that for such a section, a larger amount of the cross section is subjected to tensile stresses and the compressive zone is subjected to a greater strain gradient. Hence, for similar cross sections to that of steel, much larger deflections and less shear strength are expected (Pilakoutas et al., 2002).

The following sentence reported in the ACI 440.1R-06 (2006) can be considered as a principle that is universally accepted by the referenced guidelines: "*These design recommendations are based on limit state design principles in that an FRP-reinforced concrete member is designed based on its required strength and then checked for fatigue endurance, creep rupture endurance, and serviceability criteria. In many instances, serviceability criteria or fatigue and creep rupture endurance limits may control the design of concrete members reinforced for flexure with FRP bars (especially AFRP and GFRP that exhibit low stiffness)*".

Nevertheless, also significant differences occur among the available FRP RC documents; for example, when considering the limit state philosophy, two main design approaches may be distinguished; if one takes into account the inequality:

$$R \geq S \tag{2.1}$$

where R is the resistance of member and S is the load effect, the two different design approaches are:

- The American-like design approach, where Eq. (2.1) becomes:

$$\phi R_n \geq S_u , \tag{2.2}$$

R_n being the nominal strength of member (depending on the characteristic strength of materials); ϕ is a strength reduction factor and S_u is the corresponding design load effect, obtained by amplifying the applied loads by appropriate coefficients, α;

- The Eurocode-like design approach, where Eq. (2.1) turns into:

$$R_u \geq S_d , \tag{2.3}$$

where R_u is the ultimate resistance of member, computed as a function of the design strength of material, derived multiplying the characteristic materials strength by material safety factors; and S_d is the design load effect, analogous to S_u.

In conclusion the reduction applied on the resistance by the American Standards through the ϕ factor in the Eurocode-like Standards corresponds to the reduction applied on the materials resistance; in other words the nominal value of resistance computed in the American Standard is function of the Eurocode-like characteristic (namely *guaranteed* in ACI codes) values of material strengths.

In particular for the flexural design, all available guidelines on FRP RC structures distinguish between two types of flexural failure, depending on the reinforcement ratio of balanced failure, ρ_{fb}, to be checked in the design procedure; if the actual reinforcement ratio, ρ_f, is less than ρ_{fb}, it is assumed that flexural failure occurs due to rupture of FRP reinforcement, whereas if ρ_f is greater than ρ_{fb}, then it is assumed that the element will fail due to concrete crushing. In the ideal situation where ρ_f is equal to ρ_{fb}, the concrete element is balanced and hence, flexural failure would occur due to simultaneous concrete crushing and rupture of the FRP reinforcement. It should be noted that, for FRP RC structures, the concept of balanced failure is not the same as in steel RC construction, since FRP reinforcement does not yield and, hence, a balanced FRP RC element will still fail in a sudden, brittle manner; accordingly, a concrete crushing failure can be considered as the ductile mode of failure of an FRP RC section. Following a brief overview of the aforementioned guidelines is given.

2.5.1 European Design Guidelines

The European design guidelines by Clarke et al (1996) are based on modifications to British (BS8110, 1997) and European RC codes of practice (ENV 1992-1-1, 1992). The guidelines include a set of partial safety factors for the material strength and stiffness that take into consideration both the short and long term structural behavior of FRP reinforcement; and hence, the adopted values are relatively high when compared with the values adopted by other guidelines. The guidelines do not make any distinction between the two types of flexural failure and in addition, they do not provide clear indications about the predominant failure mode, which would result from the application of these partial safety factors.

The recently issued Italian guidelines CNR-DT 203/2006 will be discussed in details within the thesis.

2.5.2 Japanese Design Guidelines

The Japan Society of Civil Engineers (JSCE) design guidelines (JSCE, 1997) are based on modifications of the Japanese steel RC code of practice, and can be applied for the design of concrete reinforced or prestressed with FRP reinforcement; the analytical and experimental phases for FRP construction are sufficiently complete (ACI 440.1R-06, 2006). The JSCE places in between the two design philosophies reported, considering both material and member safety factors, that are slightly higher than the ones used for steel reinforcement; although the model adopted for the flexural design covers both types of flexural failure, there is no information about the predominant mode of flexural failure that would result from the application of the proposed partial safety factors. The guideline may also be utilised as a reference document, since it gives general information about different types of FRP reinforcement, quality specifications, and characterization tests for FRP materials.

2.5.3 Canadian Design Guidelines

The Canadian Standard Association (CSA) design guidelines CAN/CSA-S806-02 (2002) are the most recently issued Canadian guidelines on the design and construction of building components with FRP. In addition to the design of concrete elements reinforced or prestressed with FRP, the guidelines also include information about characterization tests for FRP internal reinforcement. The guideline was

approved, in 2004, as a national standard of Canada, and is intended to be used in conjunction with the national building code of Canada (CSA A23.3, 2004).

The document prescribes that "*the factored resistance of a member, its cross-sections, and its connections shall be taken as the resistance calculated in accordance with the requirements and assumptions of this Standard, multiplied by the appropriate material resistance factors…Where specified, the factored member resistance shall be calculated using the factored resistance of the component materials with the application of an additional member resistance factor as appropriate*". In other words, the Canadian approach is that of material safety factors, with the exception of special cases (i.e. stability in compressed members; sway resisting columns; and flexure and axial load interaction and slenderness effects).

As for the predominant mode of failure, the CSA S806-02 remarks that "*all FRP reinforced concrete sections shall be designed in such a way that failure of the section is initiated by crushing of the concrete in the compression zone*".

The Canadian network of centres of excellence on intelligent sensing for innovative structures has also published a design manual that contains design provisions for FRP RC structures (ISIS, 2001). The guidelines also provide information about the mechanical characteristics of commercially available FRP reinforcement. This guideline is also based on modifications to existing steel RC codes of practice, assuming that the predominant mode of failure is flexural, which would be sustained due to either concrete crushing (compressive failure) or rupture of the most outer layer of FRP reinforcement (tensile failure).

2.5.4 American Design Guidelines

The American Concrete Institute (ACI) design guidelines for structural concrete reinforced with FRP Bars (ACI 440.1R-06, 2006) are primarily based on modifications of the ACI-318 steel code of practice (ACI 318-02, 2002).

The document only addresses non-prestressed FRP reinforcement (concrete structures prestressed with FRP tendons are covered in ACI 440.4R). The basis for this document is the knowledge gained from worldwide experimental research,

analytical research work, and field applications of FRP reinforcement. The recommendations in this document are intended to be conservative.

The ACI 440.1R design philosophy is based on the concept that "*the brittle behavior of both FRP reinforcement and concrete allows consideration to be given to either FRP rupture or concrete crushing as the mechanisms that control failure…both failure modes (FRP rupture and concrete crushing) are acceptable in governing the design of flexural members reinforced with FRP bars provided that strength and serviceability criteria are satisfied…to compensate for the lack of ductility, the member should possess a higher reserve of strength. The margin of safety suggested by this guide against failure is therefore higher than that used in traditional steel-reinforced concrete design.* Nevertheless, based on the findings of Nanni (1993), the concrete crushing failure mode is marginally more desirable for flexural members reinforced with FRP bars, since by experiencing concrete crushing a flexural member does exhibit some plastic behavior before failure.

The ACI440.1R guideline uses different values of strength reduction factors for each type of flexural failure, while - for the shear design - it adopted the value of φ used by ACI318 for steel reinforcement. In addition, environmental reduction factors are applied on the FRP tensile strength to account for the long-term behavior of FRPs.

As for shear, an exhaustive assessment of the different existing design approaches is given in Chapter 5.

However, for FRP RC structures the specific mechanical characteristics of the FRP rebars are expected to result in serviceability limit states (SLS)-governed design; the following SLS for FRP RC members are universally considered:

- materials stress limitations;
- deflections (short and long term);
- crack width and spacing.

A detailed description of the CNR-DT 203/2006 on serviceability (specifically on deflection and bond) is reported in Chapter 4.

The CSA S806-02 only prescribes that FRP reinforced concrete members subjected to flexure shall be designed to have adequate stiffness in order to limit deflections or

any deformations that may adversely affect the strength or serviceability of a structure.

The ACI 440.1R design guideline (ACI 440.1R-06, 2006) provides different limits for each type of FRP reinforcement, which should not be exceeded under sustained and cyclic loading. The Japanese recommendations limit the tensile stresses to the value of 80% of the characteristic creep-failure strength of the FRP reinforcement, and it is noted that the stress limitation should not be greater than 70% of the characteristic tensile strength of the FRP reinforcement. ISIS Canada applies a reduction factor, F, to the material resistance factors. Values of the factor F account for the ratio of sustained to live load as well as for the type of FRP reinforcement.

The limits on deflections for steel RC elements are equally applicable to FRP RC; whereas the ratios of effective span to depth are not. ACI 440.1R-03 (2003) considers that these ratios are not conservative for FRP RC and recommends further studies. ISIS Canada (2001) proposes an equation for the effective span to depth ratio.

Finally, when FRP reinforcement is used corrosion is not the main issue because the rebars are designed to be highly durable; however, crack widths, w, have to be controlled to satisfy the requirements of appearance and specialized performance. Table 5 reports the maximum values for design crack width in FRP RC members, w_{max}, taken from several codes of practice.

Table 5 - Crack Width Limitations for FRP RC Elements

Code	Exposure	w_{max} [mm]
JSCE **CNR-DT 203/2006**	**-**	**0.5**
ACI 440.1R 06 **CSA S806-02**	**Interior**	**0.7**
ACI 440.1R 06 **CSA S806-02**	**Exterior**	**0.5**

For bond of FRP reinforcement in concrete elements some code proposals have been recently formulated in the national codes of practice; from the design point of view, the study of concrete structures reinforced with FRP rebars has been initially

developed by extending and modifying existing methods applied to the design of steel reinforced concrete structures. Therefore, studies have been often developed by comparing performances obtained by using steel rebars and by using FRP rods while the production technologies have been oriented towards the fabrication of composite rebars which were, at least in shape and dimensions, similar to deformed steel rebars. Very different code formulations have been thus derived by the referenced guidelines.

Finally, areas where currently there is limited knowledge of the performance of FRP reinforcement include fire resistance, durability in outdoor or severe exposure conditions, bond fatigue, and bond lengths for lap splices. Further research is needed to provide additional information in these areas (ACI 440.1R-06, 2006).

Chapter III
ULTIMATE FLEXURAL BEHAVIOR

3.1 INTRODUCTION

In this chapter the general principles prescribed in the CNR-DT 203/2006 for the design of FRP RC elements is presented; the case of uniaxial bending, e.g. when the loading axis coincides with a symmetry axis of the reinforced element cross section, is examined. In particular, a reliability-based calibration of partial safety factors was applied to assess the reliability levels of the ultimate limit state (ULS) design according to the Italian guidelines.

3.2 GENERAL PRINCIPLES

According to the CNR-DT 203/2006 document the design of concrete structures reinforced with FRP bars shall satisfy strength and serviceability requirements, not relying upon strength and stiffness contributions provided by the compressed FRP bars; the conventional serviceability and the corresponding levels of the design loads shall be considered according to the current building codes (D.M.LL.PP. 09/01/1996 or Eurocode 2, 2004).

The following inequality shall always be met:

$$E_d \leq R_d \tag{3.1}$$

where E_d and R_d are the factored design values of the demand and the corresponding factored capacity, respectively, within the limit state being considered. The design values are obtained from the characteristic values through suitable partial factors, to be chosen according to the current building code, or indicated in the CNR-DT 203 with reference to specific issues. In fact, strength and strain properties of the FRP bars are quantified by the corresponding characteristic values; only the stiffness parameters (Young's modulus of elasticity) are evaluated through the corresponding average values.

The design value, X_d, of the generic strength and/or strain property of a material, in particular of a FRP bar, can be expressed as follows:

$$X_d = \eta \frac{X_k}{\gamma_m} \tag{3.2}$$

where X_k is the characteristic value of the property being considered, η is a conversion factor accounting for special design problems, and γ_m is the material partial factor. The conversion factor η is obtained by multiplying the environmental conversion factor, η_a, by the conversion factor due to long-term effects, η_l. Possible values to be assigned to such factors are reported in Table 1 and Table 2, respectively. Values obtained from experimental tests can be assigned when available. Such values are obtained by testing FRP bars to a constant stress equal to the maximum stress at serviceability for environmental conditions similar to that encountered by the structure in its life and by evaluating the bar residual strength over time in compliance with the standard ISO TC 71/SC 6 N (2005).

Table 1 - Environmental Conversion Factor η_a for Different Exposure Conditions of the Structure and Different Fiber Types

Exposure conditions	Type of fiber / matrix*	η_a
Concrete not-exposed to moisture	Carbon / Vinylester or epoxy	1.0
	Glass / Vinylesters or epoxy	0.8
	Aramid / Vinylesters or epoxy	0.9
Concrete exposed to moisture	Carbon / Vinylesters or epoxy	0.9
	Glass / Vinylesters or epoxy	0.7
	Aramid / Vinylesters or epoxy	0.8

* The use of a polyester matrix is allowed only for temporary structures.

Table 2 - Conversion Factor for Long-Term Effects η_l for Different Types of FRP

Loading mode	Type of fiber / matrix	η_l (SLS)	η_l (ULS)
Quasi-permanent and/or cyclic (creep, relaxation and fatigue)	Glass / Vinylesters or epoxy	0.30	1.00
	Aramid / Vinylesters or epoxy	0.50	1.00
	Carbon / Vinylesters or epoxy	0.90	1.00

If FRP bars are used for temporary structures (serviceability less than one year), the environmental conversion factor η_a can be assumed equal to 1.00.

The design strength R_d can be expressed as follows:

$$R_d = \frac{1}{\gamma_{Rd}} R\left\{X_{d,i}; a_{d,i}\right\} \tag{3.3}$$

where $R\{\cdot\}$ is a function depending upon the specific mechanical model considered (e.g. flexure, shear) and γ_{Rd} is a partial factor covering uncertainties in the capacity model; unless otherwise specified, such factor shall be set equal to 1. The arguments of the function $R\{\cdot\}$ are typically the mechanical and geometrical parameters, whose design and nominal values are $X_{d,i}$ and $a_{d,i}$, respectively.

3.3 PARTIAL FACTORS

For ultimate limit states, the partial factor γ_m for FRP bars, denoted by γ_f, shall be set equal to 1.5, whereas for serviceability limit states (SLS), the value to be assigned to the partial factor is $\gamma_f = 1$. The partial factor $\gamma_c = 1.6$ prescribed by the referenced building codes shall be assigned for concrete.

3.4 RELIABILITY STUDY

The overall aim of the structural reliability analysis is to quantify the reliability of cross sections under consideration of the uncertainties associated with the resistances and loads. This section focuses on the reliability analysis of flexural simply supported GFRP-RC members; in particular, a reliability-based calibration of partial safety factors has been applied to assess the reliability levels of the flexural design equations as given by the CNR-DT 203/2006 guidelines, reported hereafter. This could be achieved thank to the work carried out by Dr. Santini (Santini, 2007) at the Dept. of Struct. Eng. of University of Naples "Federico II", with the assistance of the work group made by Dr. Iervolino, Dr. Prota and the writer, with the supervision of Prof. Manfredi.

3.4.1 Reliability Index

In probability-based Load and Resistance Factor Design (LFRD) the structural performance is defined by a limit state function, which can be generally expressed as (Ellingwood et al., 1982; Galambos et al., 1982):

$$G(X) = 0 \tag{3.4}$$

where X is the vector of resistance or load random variables (a random variable is a defined number associated to a given event that is unknown before the event occurs). The safety of a structural component depends on its resistance (R) and load effects (S), which can be expressed in the limit state function as the difference between the random resistance of the member, R, and the random load effect acting on the member, S:

$$G = R - S \tag{3.5}$$

if G>0 the structure is safe, otherwise it fails. The probability of failure, P_f, is equal to:

$$P_f = \Pr(R - S < 0) \tag{3.6}$$

Since R and S are treated as random variables, the outcome G will also be a random variable. In general, the limit state function can be a function of many variables, $X=(X_1,X_2,\ldots,X_m)$ representing dimensions, material properties, loads and other factors such as the analysis method.

A direct calculation of the probability of failure may be very difficult for complex limit state functions, and therefore, it is convenient to measure structural safety in terms of the reliability index, β, defined such that the probability of failure is

$$P_f = \Phi(-\beta), \tag{3.7}$$

Φ being the standard normal cumulative-distribution function (R. Ellingwood, 2003). Indicative values of P_f for some typical failure modes are (BS EN 1990:2002):

- $P_f = 10^{-5} \div 10^{-7}$ for ULS with no warning (brittle failure);
- $P_f = 10^{-4} \div 10^{-5}$ for ULS with warning (ductile failure);
- $P_f = 10^{-2} \div 10^{-3}$ for SLS with large elastic deformations or undesirable cracking.

Indicative values of β are shown in Table 3, in correspondence of P_f values, as reported by (BS EN 1990:2002):

Table 3 - β vs P_f for Normal-type Distribution

β	P_f
1,282	10^{-1}
2,326	10^{-2}
3,09	10^{-3}
3,719	10^{-4}
4,265	10^{-5}
4,753	10^{-6}
5,199	10^{-7}

In this study the First Order Reliability Method (FORM) has been used; it is based on a first order Taylor Series expansion of the limit state function, which approximates the failure surface by a tangent plane at the point of interest; this method is very useful since it is not always possible to find a closed form solution for a non-linear limit state function or a function including more than two random variables. More details on the use of such method to compute β in this study are reported in Appendix A.

In terms of resistance, *R*, and load effects, *S*, generally their Normal probability distributions (see § 3.4.4) are compared to assess the reliability of a member: the intersection area of the two bell curves shall be investigated, as reported in Figure 1, based on the assumption that the farer the two bells, the higher the member reliability; in this example the first case corresponds to a good reliability level, lacking any contact point between the two curves; in the second case a larger scattering of the two bell curves occurs with respect to case 1: the reliability level of member decreased since points under the intersection zone of the two curves imply structural failure; cases three and four are intermediate between the first and the second one.

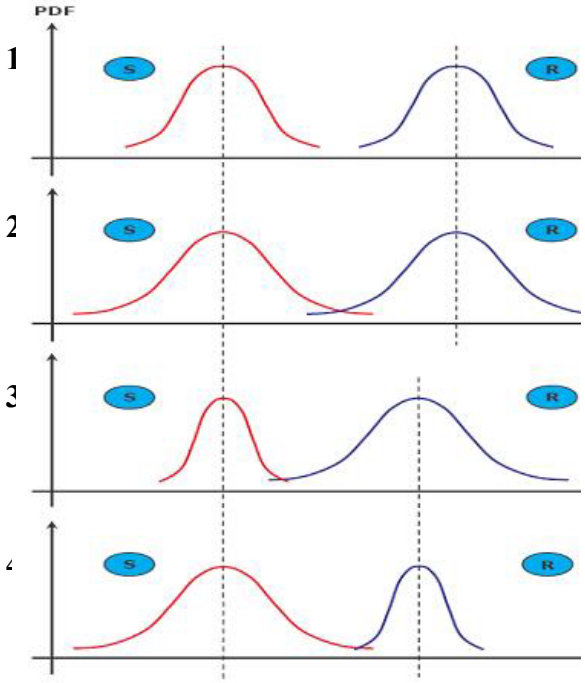

Figure 1 - Possible Distributions of *R* and *S* Probability Density Functions

In this study, all random design variables involved in the flexural design of GFRP RC members are attributed a predefined probability distribution; hence, using Monte-Carlo design simulations to create random samples, the limit state function is developed for each randomly generated design case; the solution of such a problem is sought so that the target reliability is attained with the optimal partial safety factor for the GFRP reinforcement.

3.4.2 Background

The establishment of a probability-based design framework for FRP RC structures is becoming more and more needful since despite the growing popularity of composites they are still perceived as being less reliable than conventional construction technologies, such as steel, concrete, masonry, and wood, where design methods, standards, and supporting databases already exist (Ellingwood, 2003). If several reliability research applications on externally bonded FRP structures have been carried out in literature (Plevris et al. 1995; Ellingwood 1995, 2003; Okeil et al. 2001, 2002; Monti and Santini 2002; Frangopol and Recek 2003; Di Sciuva and Lomario 2003; Spitaleri and Totaro 2006), the research in the field of internal FRP RC structures is still scarce.

La Tegola (La Tegola 1998) re-examined from a probabilistic point of view the effective distributions of actions to be adopted for the design of FRP RC structures at both ULS and SLS: higher values of strength and lower values of Young's modulus compared to steel imply that the design of FRP RC structures will be influenced almost exclusively by the SLS, whereas actual steel codes consider the same distribution of actions for the SLS and, amplified, for the ULS. Neocleous et al. (1999) evaluated the reliability levels of two GFRP RC beams for the flexural and shear failure mode, concluding that the design of such members should be based on the attainment of the desired failure mode hierarchy by applying the appropriate partial safety factors. Pilakoutas et al. (2002) examined the effect of design parameters and especially of γ_f on the flexural behavior of over-reinforced FRP RC beams, concluding that the desired mode of flexural failure is not attained by the application of γ_f alone, but it is necessary to apply limits on the design parameters considered by the models adopted to predict the design capacity.

He and Huang (2006) combined the Monte Carlo simulation procedure with the Rackwitz–Fiessler method to assess the reliability levels of the provisions for flexural capacity design of ACI 440.1R-03 and ISIS guidelines. The assessment indicated that the provisions in both guidelines are rather conservative; the reliability indexes change dramatically when failure mode is switched from one to the other, but within either failure mode, reliability indexes do not vary significantly with respect to relative reinforcement ratio.

Kulkarni (2006) developed resistance models for FRP RC decks and girders designed using ACI guidelines (ACI 440.1R-06), showing that the cross sectional properties seem not to be major factors affecting the structural reliability, whereas concrete strength, load effects and reinforcement ratio of FRP reinforcement play a significant role on the structural reliability of members.

3.4.3 Provisions on Flexural Capacity Design

According to the CNR-DT 203/2006 the design of FRP-RC members for flexure is analogous to the design of steel reinforced concrete members. The flexural capacity of concrete members reinforced with FRP bars can be calculated based on assumptions similar to those made for members reinforced with steel bars. Both

concrete crushing and FRP rupture are acceptable failure modes in governing the design of FRP-RC members provided that strength and serviceability criteria are satisfied. Assumptions in CNR-DT 203/2006 method are as follows:

Design at ultimate limit state requires that the factored ultimate moment M_{Sd} and the flexural capacity M_{Rd} of the FRP RC element satisfy the following inequality:

$$M_{Sd} \leq M_{Rd} \tag{3.8}$$

It is assumed that flexural failure takes place when one of the following conditions is met:

1. The maximum concrete compressive strain ε_{cu} as defined by the current Italian building code is reached.
2. The maximum FRP tensile strain ε_{fd} is reached; ε_{fd} is computed from the characteristic tensile strain, ε_{fk}, as follows:

$$\varepsilon_{fd} = 0.9 \cdot \eta_a \cdot \frac{\varepsilon_{fk}}{\gamma_f} \tag{3.9}$$

where the coefficient 0.9 accounts for the lower ultimate strain of specimens subjected to flexure as compared to specimens subjected to standard tensile tests.

With reference to the illustrative scheme shown in Figure 2, two types of failure may be accounted for, depending upon whether the ultimate FRP strain (area 1) or the concrete ultimate compressive strain (area 2) is reached.

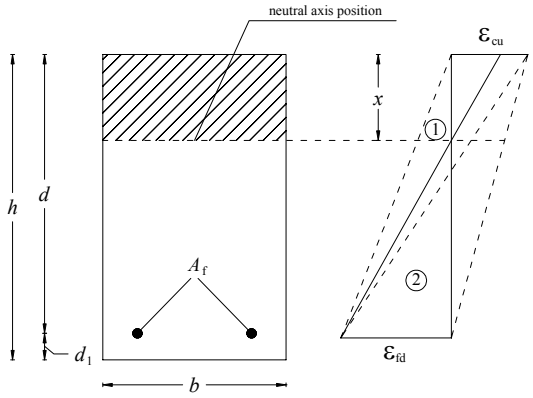

Figure 2 - Failure Modes of FRP RC Section

Failure occurring in area 1 is attained by reaching the design strain in the FRP bars: any strain diagram corresponding to such failure mode has its fixed point at the limit value of ε_{fd}, defined by the relationship (3.9).

Failure occurring in area 2 takes place due to concrete crushing, while the ultimate strain of FRP has not been attained yet. Moreover, according to the current Italian building code, design at ULS can be conducted by assuming a simplified distribution of the normal stresses for concrete ("stress block"), for elements whose failure is initiated either by the crushing of concrete or rupture of the FRP bars.

The resistance of a member is typically a function of material strength, section geometry, and dimensions. These quantities are often considered to be deterministic, while in reality there is some uncertainty associated with each quantity. Accounting for such uncertainties is achieved in three steps: first, the important variables affecting the flexural strength of GFRP-RC members are identified; second, statistical descriptors (mean, standard deviation, and distribution type) for all variables are found, creating a sample design space by considering different GFRP reinforcement ratios, thicknesses, widths, and concrete strengths; finally, Monte-Carlo simulations and comparisons with experimental results are carried out to develop a resistance model that accounts for variability in material properties, fabrication and analysis method.

3.4.4 Variables Affecting the Flexural Strength of GFRP-RC Members

The parameters that affect the flexural strength of GFRP-RC members include cross sectional properties, geometric and material properties of reinforcing GFRP bars, and concrete properties. Among all these properties, the member width, b, the effective depth, d, concrete compressive strength, f_c, are dealt with as the random variables that affect the resistance of GFRP-RC sections; the modulus of elasticity of GFRP bars, E_f, is treated as a deterministic design variable in the assessment.

The following parameters are needed to accurately describe the properties of the variables statistically:

- Mean: this is the most likely value of the observations. For a random variable, x, the mean value, μ_x, is defined as:

$$\mu_x = E[x] = \int_{-\infty}^{+\infty} x f_x(x) dx \tag{3.10}$$

- Standard deviation: Standard deviation, σ_x, estimates the spread of data from the mean and is calculated as:

$$\sigma_x = \sqrt{\int_{-\infty}^{+\infty} (x - \mu_x)^2 f_x(x) dx} \tag{3.11}$$

- Coefficient of Variation (COV): the coefficient of variation, V_x, is calculated as:

$$V_x = \frac{\sigma_x}{\mu_x} \tag{3.12}$$

- Bias: Bias is the ratio between the mean of the sample to the reported nominal value:

$$\lambda_x = \frac{\mu_x}{x_n} \tag{3.13}$$

where x_n is the nominal value of variable x.

In addition to these parameters, the description of the probability distributions is also necessary to define a variable; any random variable is defined by its probability density function (PDF), $f_x(x)$ (see Figure 3), and cumulative distribution function (CDF), $F_x(x)$ (see Figure 4).

The probability of x falling between a and b is obtained by integrating the PDF over this interval:

$$P(a < x \le b) = \int_{a}^{b} f_{\mathrm{x}}(x)dx \tag{3.14}$$

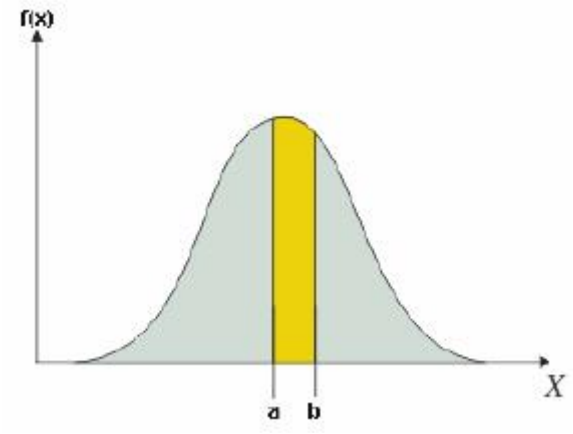

Figure 3 - PDF of *X*

The CDF describes the probability that the set of all random variables takes on a value less than or equal to a number:

$$P(X \le x) = \int_{-\infty}^{x} f_{\mathrm{x}}(x)dx = F_X(x) \tag{3.15}$$

It is clear from Eqs. (3.14) and (3.15) that:

$$f_x(x) = \frac{d}{dx} F_x(x) \tag{3.16}$$

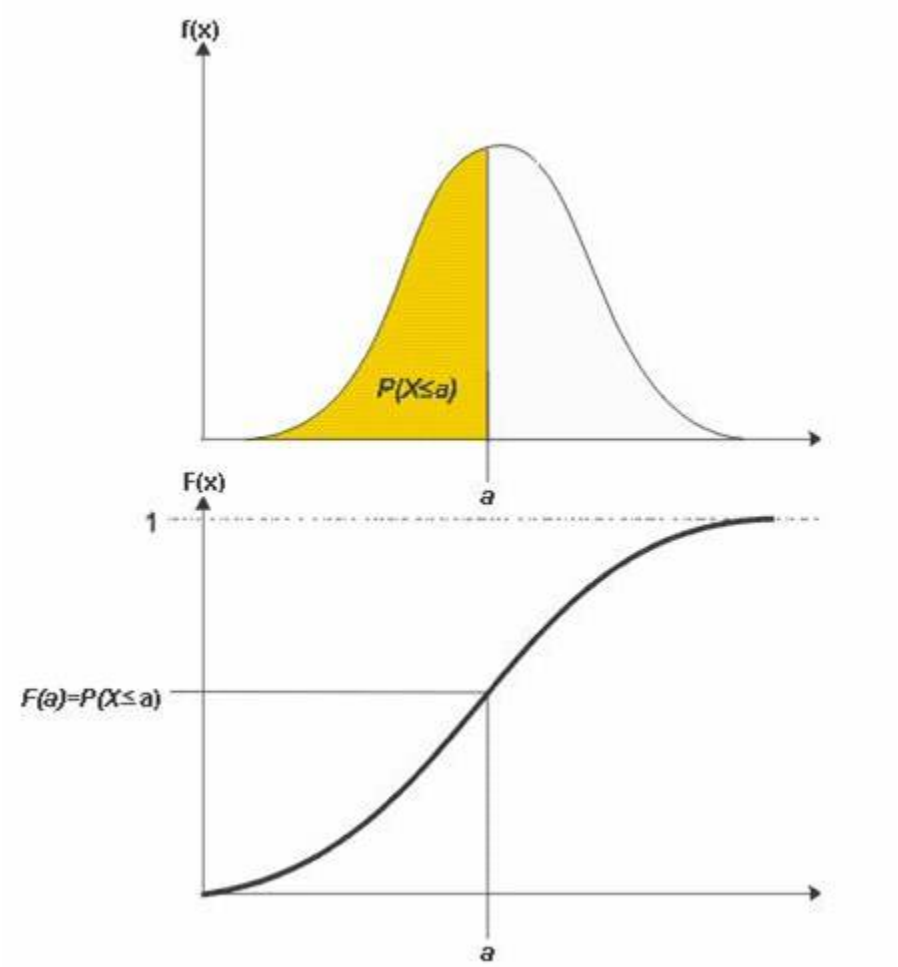

Figure 4 - Graphical Representation of Relationship between PDF and CDF

In this study, the following probability distributions have been taken into account:

- *Normal or Gaussian Distribution*: If a variable is normally distributed then two quantities have to be specified: the mean, μ_x , which coincides with the peak of the PDF curve, and the standard deviation, σ_x, which indicates the spread of the PDF curve. The PDF for a normal random variable X is given by Eq. (3.17):

$$f_X(X) = \frac{1}{\sigma_x \sqrt{2\pi}} \exp\left[-\frac{1}{2}\left(\frac{X - \mu_x}{\sigma_x} \right)^2 \right] \tag{3.17}$$

Since there is no closed-form solution for the CDF of a Normal random variable, tables have been developed to provide values of the CDF for the special case in which $\mu_x = 0$ and $\sigma_x = 1$. These tables can be used to obtain values for any general normal distribution.

- *Weibull Distribution*: In most civil engineering applications, the PDF and CDF distributions for the Weibull random variable, *X*, are given by Eqs. (3.18) and (3.19), respectively (see also Figure 5):

$$f_X(X) = m\sigma_o^{-m} X^{m-1} \exp\left[-\left(\frac{X}{\sigma_0} \right)^m \right] \tag{3.18}$$

$$F_X = 1 - \exp\left[-\left(\frac{X}{\sigma_0} \right)^m \right] \tag{3.19}$$

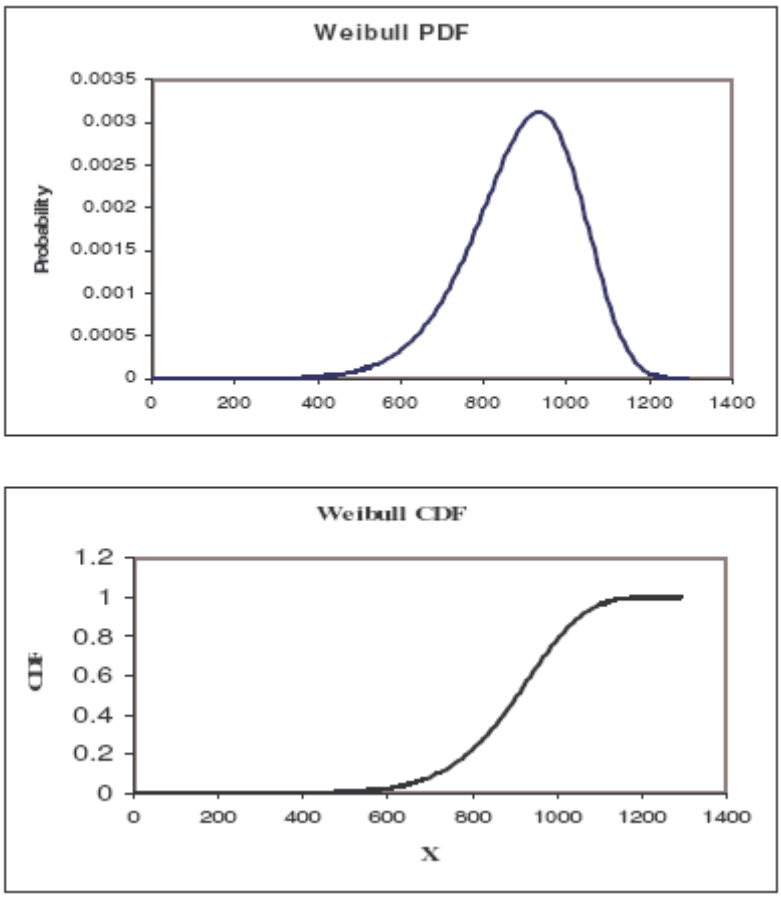

Figure 5 - Graphical Representation of Weibull Distribution

The relationships between the two Weibull parameters m and σ_0 with μ_X and σ_X are complex; therefore the following simplified equations are used:

$$m = COV^{-1.08} \tag{3.20}$$

$$\sigma_0 = \frac{\mu}{\Gamma\left(\frac{1}{m}+1\right)} \tag{3.21}$$

where $\Gamma[\,]$ is the gamma function. In Figure 5 the values $m = 8$ and $\sigma_0 = 950$ have been used.

- *Gumbel Distribution*: It is used to represent the minimum or maximum of a series of observations derived from different observations, assuming different shapes if referred to the minimum (see Figure 6) or maximum (see Figure 7).

The PDF of a Gumbel distribution is defined as:

$$f_X(X) = \frac{1}{\sigma} e^{-e^z} \tag{3.22}$$

where:

$$z = \frac{X - \mu}{\sigma}. \tag{3.23}$$

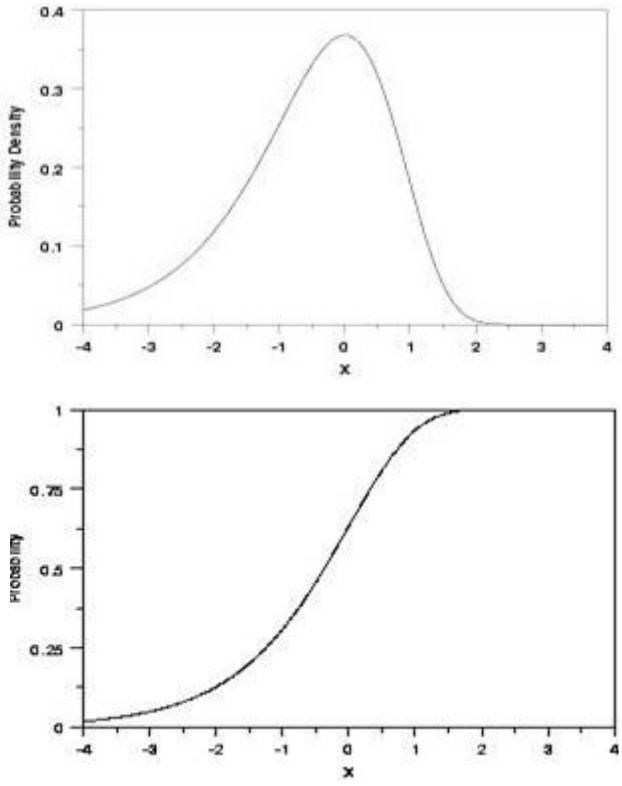

Figure 6 - Gumbel PDF and CDF Referred to Minimum Values

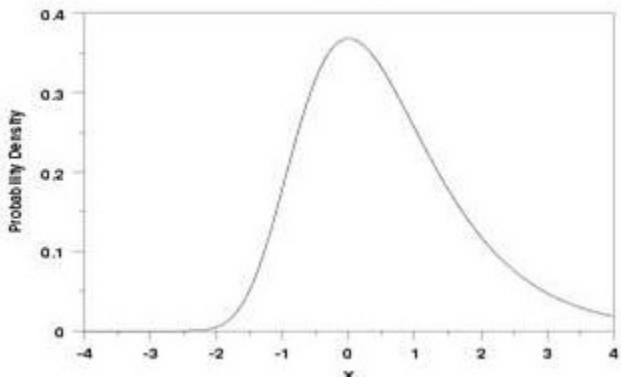

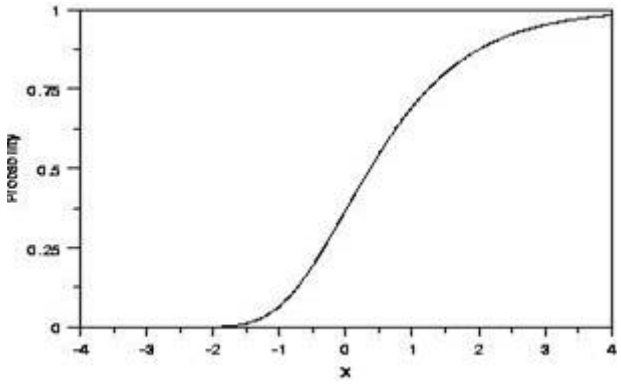

Figure 7 - Gumbel PDF and CDF Referred to Maximum Values

- *Lognormal Distribution*: It is obtained from a Normal variable Y with the following transformation:

$$X = \exp(Y)\,. \tag{3.24}$$

The Lognormal distribution represents the limit of random variables product when their number goes to infinite, regardless of their probability distribution. The PDF of a Lognormal distribution is defined as (see also Figure 8):

$$f_{\mathrm{X}}(X) = \frac{1}{\zeta\sqrt{2\pi}}\exp\left[-\frac{1}{2}\left(\frac{\ln(X)-\lambda_{\mathrm{x}}}{\zeta}\right)^2\right], x > 0\,, \tag{3.25}$$

where λ_{x} and ζ are the mean and standard deviation of ln(X), respectively, computed as:

$$\lambda_{\mathrm{x}} = \ln(\mu) - \frac{\zeta^2}{2}, \zeta = \sqrt{\ln\left[1+\left(\frac{\sigma}{\mu}\right)^2\right]}\,. \tag{3.26}$$

The Lognormal function is often used to model the concrete compressive strength (Sorensen et al., 2001), although most of researchers still refer to the Normal distribution. Here the Normal distribution will be adopted to model the concrete compressive strength.

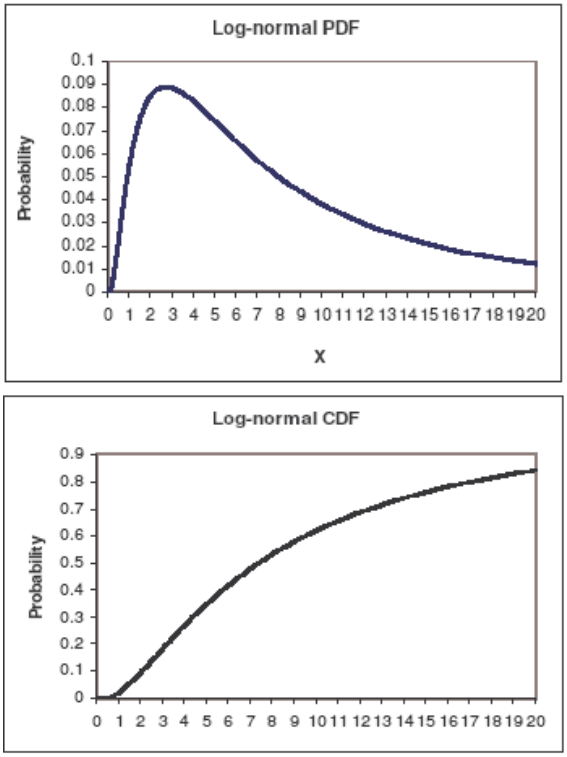

Figure 8 - Lognormal PDF and CDF

3.4.5 Statistical Properties

A literature review was carried out to select the proper statistical characteristics for each random design variable (Okeil et al. 2002, Nowak and Collins 2000, Nowak and Szerszen 2003, Ellingwood 1995), as reported hereafter:

- *Geometrical properties*: The bias and COV of *b*, *h* and *d* range between 1.00 and 1.02 and 0.5% and 7.0 %, respectively. To make the assessment more general, two extreme nominal values (A and B) were selected for each random design variable, and for each of them the relationships reported in Table 4 were considered; *d* values are proportionally related to *b*; both the geometrical variables are assumed to have Normal distribution.
- *Concrete Compressive Strength*: Statistical properties of concrete are well documented in Ellingwood et al. (1980), and Nowak and Szerszen (2003) and summarized in Table 4; two nominal values A and B were considered. The random variable describing the compressive strength of concrete, f_c, is assumed to be normally distributed.

- *Tensile Strength of GFRP Bars*: The tensile strength of GFRP reinforcement is assumed to follow the Weibull theory; this assumption is well established in the literature (Okeil et al. 2000) and has been verified experimentally through tests of composite specimens with different size and stress distribution. Data on the statistical properties of GFRP bars have been taken into account (see Table 4) according to the values suggested by Pilakoutas et al. (2002); only one nominal value was considered.

Table 4 - Statistical Properties of Main Variables

Design Variable	Minimum Nominal Value (A)	Mean μ & Standard Deviation σ	Bias & COV (%)	Maximum Nominal Value (B)	Mean μ & Standard Deviation σ	Bias & COV (%)	Probability Distribution
Base *b* [mm]	b_A	μ=b_A+2.54	1	b_B	μ=b_B+2.54	1	Normal
		σ=3.66	1.8		σ=3.66	0.7	
Effective Depth *d* [mm]	0.8·h_A	μ=d_A-4.70	1	0.95·h_B	μ=d_B-4.70	1	Normal
		σ=12.70	5.4		σ=12.70	0.9	
Concrete Strength f_{ck} [MPa]	20.67	μ=27.97	1.4	41.34	μ=46.16	1	Normal
		σ=2.85	10		σ=1.94	4	
GFRP Strength f_{fk} [MPa]	743.4	μ=810	1	E_f (GFRP bars) = 45 GPa			Weibull
		σ=40.5	5				

3.4.6 Sample Design Space

Developing the resistance models for FRP-RC members requires investigating a wide range of realistic parameters in the design space. In this study, beams and slabs are designed following the recommendations published by CNR-DT 203/2006, and then two different reliability analyses have been carried out separately by applying the same approach but defining different design spaces and deriving different conclusions.

3.4.6.1 Design Space for Beams

Two extreme nominal values (A and B) were selected for each random design variable (b, d, f_c) as reported in Table 5, as well as thirty ratios of ρ_f/ρ_{fb}, being ρ_f the

reinforcement ratio of FRP bars, and ρ_{fb} the corresponding balanced value, defined as:

$$\rho_{fb} = \frac{f_{ck} \cdot 0.85 \cdot \varepsilon_{cu}}{f_{fk} \cdot (\varepsilon_{cu} + \varepsilon_{fk})}, \tag{3.27}$$

where ε_{cu} is the maximum concrete compressive strain.

A design space made of $2^3 \cdot 30 = 240$ design cases was thus defined.

Table 5 - Nominal Values of Random Variables for Beams

Design Variable	Minimum Nominal Value (A)	Maximum Nominal Value (B)
b [mm]	200	500
d [mm]	240	1425
f_{ck} [MPa]	23.28	42.97

3.4.6.2 Design Space for Slabs

Similarly to the design space for beams, in the case of slabs three nominal values were assigned to d and two to f_c (with b=1000mm), as well as thirty ratios of ρ_f/ρ_{fb}, with a design space made of $2 \cdot 3 \cdot 30 = 180$ design cases (see Table 6).

Table 6 - Nominal Values of Random Variables for Slabs

Design Variable	Nominal Value (A)	Nominal Value (B)	Nominal Value (B)
d [mm]	100	250	400
f_{ck} [MPa]	23.28	42.97	

3.4.7 Resistance Models for Flexural Capacity of FRP-RC Members

As the flexural capacity of an FRP-RC member depends on the material and cross sectional properties, which are random design variables, its flexural capacity, M_R, is a random variable as well. Three main categories of possible sources of uncertainty can be identified when considering the nominal strength rather than the actual (random) strength (Ellingwood, 2003)

- *Material properties* (*M*): the uncertainties associated with material properties are uncertainties in the strength of the material, the modulus of elasticity, etc;

- *Fabrication* (*F*): these are the uncertainties in the overall dimensions of the member which can affect the cross-sectional area, the moment of inertia, etc.
- *Analysis* (*P*): the uncertainty resulting from the specific method of analysis used to predict behavior.

Each of these uncertainties has its own statistical properties; i.e. bias, COV, and distribution type; hence the mean value of the resistance model can be expressed as:

$$\mu_{M_R} = M_n \cdot \mu_M \cdot \mu_F \cdot \mu_P , \tag{3.28}$$

where μ_M, μ_F, and μ_P are the mean values of *M*, *F*, and *P*, respectively and M_n is the nominal flexural capacity of member.

Accordingly, the bias factor, λ_{M_R}, and the COV factor, V_{M_R}, describing the resistance model of M_R, are given as:

$$\lambda_{M_R} = \lambda_M \cdot \lambda_F \cdot \lambda_P \tag{3.29}$$

$$V_{M_R} = \sqrt{V_M^2 + V_F^2 + V_P^2} \tag{3.30}$$

where λ_M, λ_F and λ_P are the bias factors and V_M, V_F and V_P are the coefficients of variation of *M*, *F*, and *P* respectively.

As the uncertainty due to the analysis method yields significant effects on the probability of failure and consequently on the reliability index, β, the reliability study will assess such effects separately from those of *M* and *F*.

3.4.7.1 Uncertainties due to the Analysis Method

The reliability of the analysis method has been assessed by comparing experimental values of the flexural capacity available in literature, M_{exp} (Saadatmanesh 1994, Theriault and Benmokrane 1998, Pecce et al. 2000, Aiello and Ombres 2000) with the corresponding analytical values, M_{th}, derived using the analysis method proposed by the CNR-DT 203/2006, by using the following formulations:

$$\lambda_{\mathrm{P}} = \mu\left(\frac{M_{\exp}}{M_{\mathrm{th}}}\right) \tag{3.31}$$

$$V_{\mathrm{P}} = COV\left(\frac{M_{\exp}}{M_{\mathrm{th}}}\right) \tag{3.32}$$

The following values were derived:

$$\lambda_{\mathrm{P}} = 1.12 \tag{3.33}$$

$$V_{\mathrm{P}} = 15.67\% \tag{3.34}$$

The effects of uncertainties due to *M* and *F* will be computed in function of the design space selected.

3.4.7.2 Uncertainties due to Material (M) and Fabrication (F)

Monte-Carlo simulations are performed to determine λ_{M}, λ_{F}, V_{M} and V_{F} by varying randomly generated values for material properties and dimensions simultaneously; in this way a combined bias, λ_{MF}, and coefficient of variation, V_{MF}, resulted from these simulations.

The Monte-Carlo simulation method is a special technique to generate some results numerically without doing any physical testing. The probability distribution information can be effectively used to generate random numerical data. The basis of Monte-Carlo simulations is the generation of random numbers that are uniformly distributed between 0 and 1.

The procedure given below is applicable to any type of distribution function.

Consider a random variable *X* with a CDF $F_{\mathrm{X}}(x)$. To generate random values x_{i} for the random variable, the following steps should be followed:

1. Generate a sample value u_{i} for a uniformly distributed random variable between 0 and 1;
2. Calculate a sample value x_{i} from the formulation: $x_{\mathrm{i}} = F_{\mathrm{x}}^{-1}(u_{\mathrm{i}})$, where F_{x}^{-1} is the inverse of $F_{\mathrm{X}}(x)$.

Knowing the CDF and basic parameters of the distribution, random numbers can be generated for a particular variable.

The mean and standard deviation of the flexural capacities computed by using the limit state design approach illustrated in par. 3.4.3 for 50000 of randomly generated values for each design case (out of 240 for beams and 180 for slabs) is obtained. Appendix A reports, for each design case, the flexural capacity M_r, the mean and standard deviation of M_r distribution, the bias, λ_{MF}, and the COV, V_{MF}, both for beams and slabs.

The definition of the analytical model that better fits the flexural capacity trend has been attained by studying the statistical distribution obtained using the Monte-Carlo simulations; it has been concluded that the distribution type that better represents the flexural capacity trend depends on the design case and in particular on the ratio ρ_f/ρ_{fb} considered; in fact:

- For sections having $\rho_f/\rho_{fb} \leq 1$ the member failure is governed by the GFRP reinforcement failure, so that the flexural capacity trend is well represented by a Weibull-type distribution;
- For sections having $\rho_f/\rho_{fb} > 1$ the member failure is governed by the concrete crushing, hence the flexural capacity trend is well represented by a Normal-type distribution.

This is confirmed by the observation of probability charts available for both Weibull and Normal distributions; for example, for $\rho_f/\rho_{fb}=0.8$ the flexural capacity data set is better represented by a Weibull-type distribution, as shown in Figure 9:

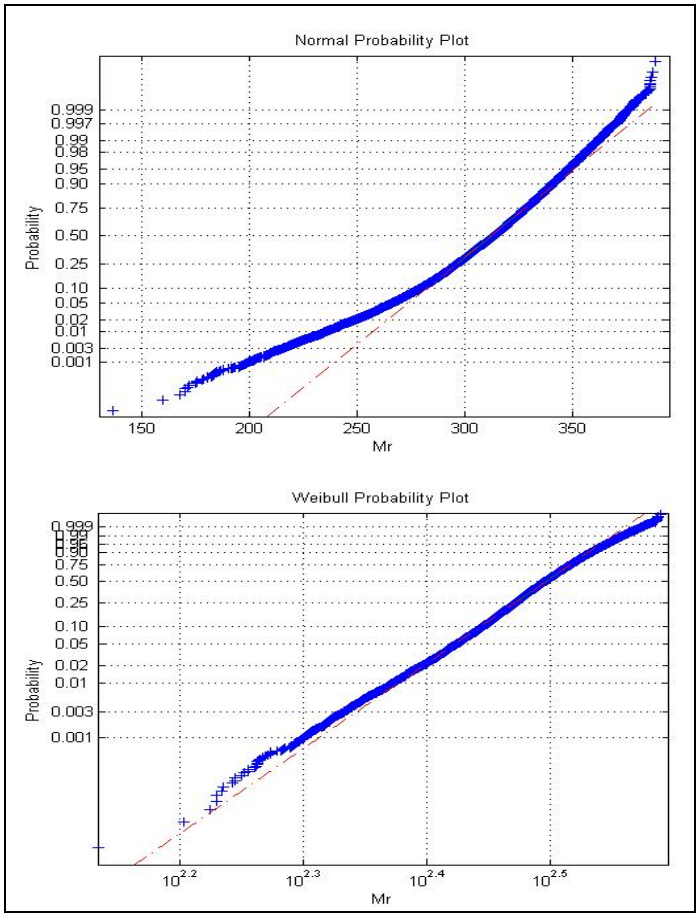

Figure 9 - Comparison between Data Sets (ρ_f/ρ_{fb}=0.8) Reported on Normal and Weibull Charts

Similarly, when considering sections with ρ_f/ρ_{fb}=1.2, the related data set will be better fitted by a Normal-type distribution rather than by a Weibull one, as shown in Figure 10.

These results are derived both for beams and slabs; therefore it can be assumed that the flexural capacity trend of the considered design cases does not depend on the specific type of member analyzed, but it only depends on the reinforcement ratio of the section.

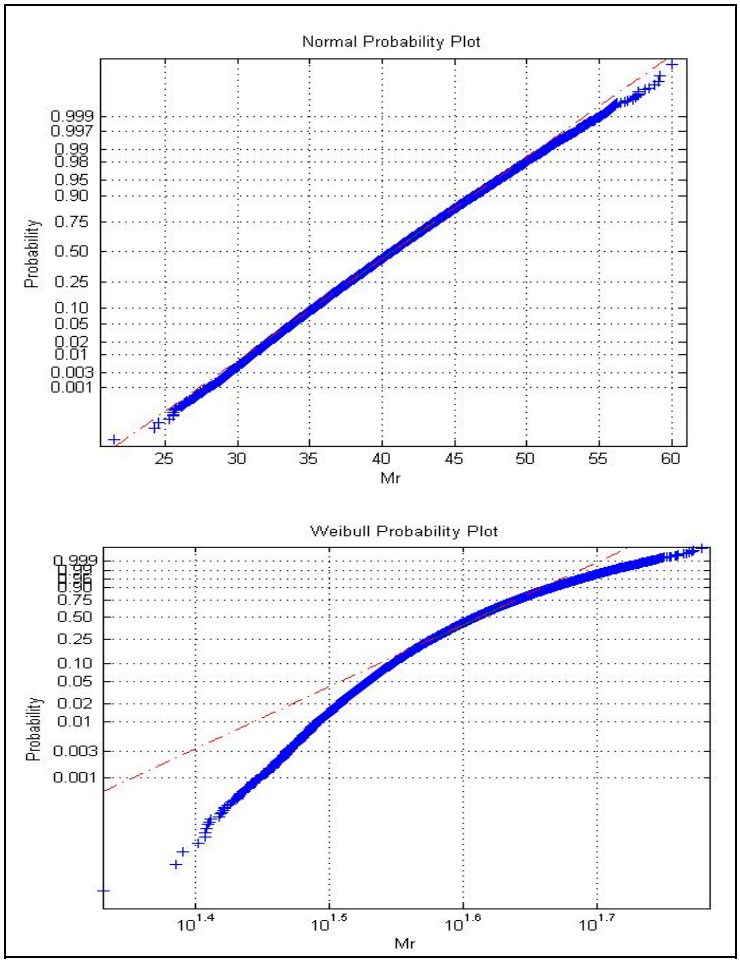

Figure 10 - Comparison between Data Sets (ρ_f/ρ_{fb}=1.2) Reported on Normal and Weibull Charts

3.4.8 Used Load Model

Dead loads (D) and live loads (L) often acting on FRP RC members of civil structures are the two load categories considered in this study.

The dead load considered in design is the gravity load due to the self weight of the structure; it is normally treated as a Normal random variable in literature (Okeil et al. 2002, Nowak and Collins 2000, Ellingwood et al. 1980, La Tegola 1998); because of the control over construction materials, it is assumed that the accuracy to estimate dead loads is higher compared to that of live loads. The works considered in this study induced to adopt a bias, λ_D, of 1.0 and a coefficient of variation, V_D , of 10 %.

The live loads, L, represent the weight of people and their possessions, furniture, movable equipments, and other non permanent objects; the area under consideration plays an important role in the statistical properties of live loads, since the magnitude

of load intensity decreases as the area contributing to the live load increases. The studies considered herein (Okeil et al. 2002, Nowak and Collins 2000, Plevris et al. 1995, Ellingwood et al. 1980, La Tegola 1998) led to assume a bias, λ_D, equal to 1.0 and a COV, V_L, equal to 25%; a Gumbel-type distribution was chosen to represent the live loads.

Table 7 summarizes the statistical properties considered for dead and live loads.

Table 7 - Statistical Properties for Dead Loads and Live Loads

Load	Bias	COV (%)	Distribution Type
Dead (*D*)	1.05	10	Normal
Live (*L*)	1	25	Gumbel

3.4.9 Reliability Analysis

The LRFD design code specifies a strength equation in the following format:

$$\phi R_n \geq \sum \gamma_{Qi} Q_i , \tag{3.35}$$

where the nominal resistance of a structural member, R_n, is reduced by a resistance factor, ϕ, while the applied loads, Q_i, are increased by the load factors, γ_{Qi}.

The values of ϕ and γ_{Qi} are set to ensure that members designed according to this design equation have a low probability of failure that is less than a small target value. The Standard Codes referenced in this study (Eurocode 2, 2004; D.M.LL.PP. 09/01/1996) prescribe that the following relationship shall be applied:

$$M_{rd} \geq \sum \gamma_{Qi} Q_i , \tag{3.36}$$

where M_{rd} is the design flexural capacity of member, computed as a function of the concrete design strength, $f_{cd} = f_{ck}/\gamma_c$, and of the GFRP reinforcement design strength, $f_{fd} = 0.9 \cdot \eta_a \cdot f_{fk}/\gamma_f$. In other words the resistance factor ϕ turns into material safety factors herein, namely γ_c and γ_f.

To evaluate the reliability index of the designed GFRP RC beams and slabs, in this study the limit state function consists of three random variables, flexural resistance,

M_R, applied bending moment due to dead load effects, M_D, and applied bending moment due to live load effects, M_L:

$$G(M_r, M_D, M_L) = M_r - (M_D + M_L); \tag{3.37}$$

the statistical properties of M_D and M_L for building loads are discussed earlier in this chapter, whereas the load demands are computed with the design equation of the current guidelines (CNR-DT 203/2006). Assuming a defined ratio of M_L/M_D, it is possible to derive the applied moment value, for example:

$$\frac{M_L}{M_D} = 1, \tag{3.38}$$

that replaced in equation:

$$\gamma_D M_D + \gamma_L M_L = M_{rd}, \tag{3.39}$$

gives:

$$M_D(\gamma_D + \gamma_L) = M_L(\gamma_D + \gamma_L) = M_{rd}, \tag{3.40}$$

or:

$$M_D = M_L = \frac{M_{rd}}{\gamma_D + \gamma_L} \tag{3.41}$$

given γ_D, γ_L and M_{rd} it is possible to derive M_D and M_L from eq. (3.41); the coefficients γ_D and γ_L prescribed by the current guidelines (D.M.LL.PP. 09/01/1996) are 1.4 and 1.5, respectively.

In the current analysis, five different ratios M_L/M_D have been considered, namely 0.5, 1, 1.5, 2, 2.5; the higher or lower predominance of M_L over M_D influences the probability distribution representing the applied moment, $M_S = M_L + M_D$, as depicted

in Figure 11. The statistical properties of M_S will be thus derived depending on the specific ratio M_L/M_D.

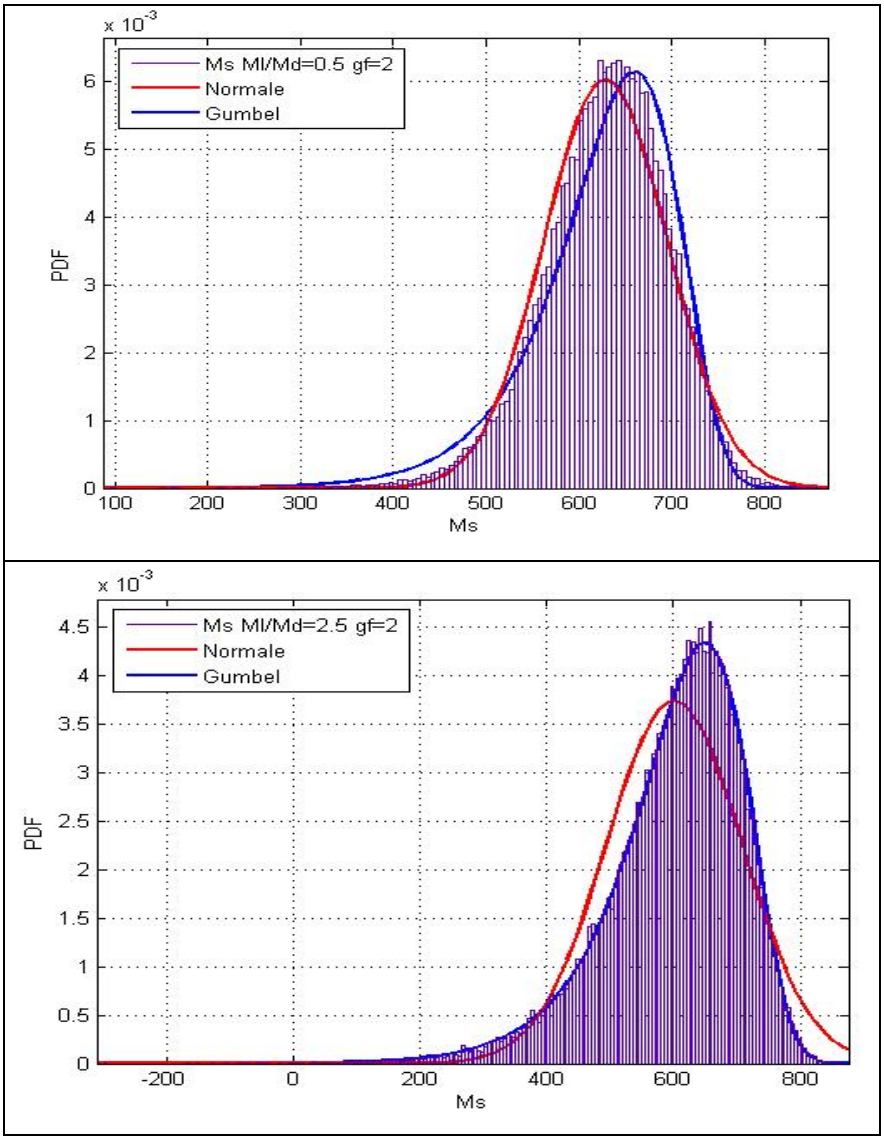

Figure 11 - PDFs of M_s for M_L/M_D=0.5 and 2.5 (γ_f=2)

The statistical properties of M_r are obtained employing the Monte-Carlo sampling already explained, computing for the randomly extracted values the flexural capacity according to the ULS design.

Finally the reliability index is computed for the design cases assumed in function of both M_L/M_D and γ_f; secondly, the uncertainties due to factors *M*, *F* and *P* are taken into account as well. This will be done separately for beams and slabs.

It must be highlighted that the reliability index will be investigated in two different ways, in compliance with the research works available in literature (see § 3.4.2), namely by distinguishing the two possible failure modes or not. In the first case, two further types of classifications can be used, that is considering the characteristic or the design values of materials. This will be better explained in the following sections.

3.4.10 Reliability Index of Beams

Following the procedure explained in the previous paragraph, the reliability index has been initially computed for each of the 240 design cases related to beams, by varying the ratios M_L/M_D and ρ_f/ρ_{fb}. The partial safety factor for FRP reinforcement suggested in the CNR-DT203, γ_f=1.5, has been considered initially.

The diagram reported in Figure 12 allows deducing the following remarks, regardless of the specific ratio M_L/M_D :

- for design cases corresponding to $\rho_f/\rho_{fb}<0.5$, the reliability index β is nearly constant and then independent of the reinforcement ratio;
- for design cases corresponding to $0.5<\rho_f/\rho_{fb}<0.9$, the reliability index β predominantly increases when the reinforcement ratio increases;
- when $0.9<\rho_f/\rho_{fb}<1.0$, the reliability index β slightly decreases when the reinforcement ratio increases;
- for design cases corresponding to $1.0<\rho_f/\rho_{fb}<2.5$ the reliability index β decreases when the reinforcement ratio increases, until a constant value for $\rho_f/\rho_{fb}>2.5$;

Summarizing, different zones can be identified, depending on ρ_f/ρ_{fb}: two edge zones of low, steady values of β corresponding to under-reinforced ($\rho_f/\rho_{fb}<0.5$) and over-reinforced sections ($\rho_f/\rho_{fb}>2.5$); a central zone with the maximum values of β corresponding to the balanced failing sections, where the materials are best exploited and then with the highest structural reliability values; and two transition zones with β variable going from under- or over-reinforced sections to balanced failing sections.

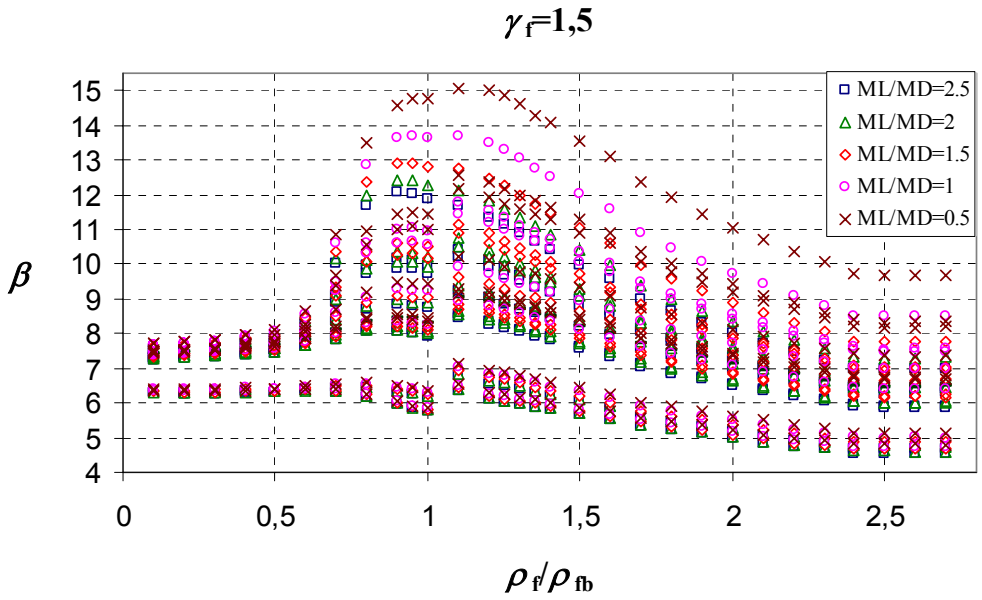

Figure 12 - Trend of β vs ρ_f/ρ_{fb} and M_L/M_D (γ_f=1.5; BEAMS)

It can also be noticed that design cases with minimum values of both the mechanical and the geometrical properties (nominal values A) have statistical distributions of M_r with higher values of COV and constant bias values. A higher COV means a higher standard deviation when fixing the mean value, so that the probability distribution bell will more scattered, with larger intersection of M_r and M_s PDF curves, and then with lower values of β, that means a higher probability of failure. In brief, lower values of mechanical and geometrical properties correspond to lower reliability and higher probability of failure.

However, the reliability index is significantly influenced by the reinforcement ratio ρ_f/ρ_{fb} and by the specific design cases taken into account, which means by the mechanical and geometrical properties considered; nevertheless, β is strongly variable within the design space considered, ranging from 4.5 to 12.2.

3.4.11 Reliability Index of Beams Depending on γ_f and on M_L/M_D

The reliability index β has been assessed also when varying γ_f, namely between 1 and 2 with steps of 0.1, with $M_L/M_D = 2.5$ and for two design cases, i.e. in correspondence of two specific values of ρ_f/ρ_{fb}, namely 0.5 and 2.3, so as to produce both GFRP failure and concrete failure of the section, respectively. Figure 13 shows the trend of M_s and M_r when varying γ_f, for the design case CB.dB.bB.R0,5.G

(Appendix A points out the meaning of design case ID name). In this specific case it can be noticed that when γ_f decreases M_s increases, such that the PDF of M_s approaches that of M_r; the intersection area between the two curves will increase and then reliability β will decrease, in compliance with the concept that reducing the limitation on the material strength (in particular that of GFRP, fixing γ_c=1.6) means increasing the probability of failure of member.

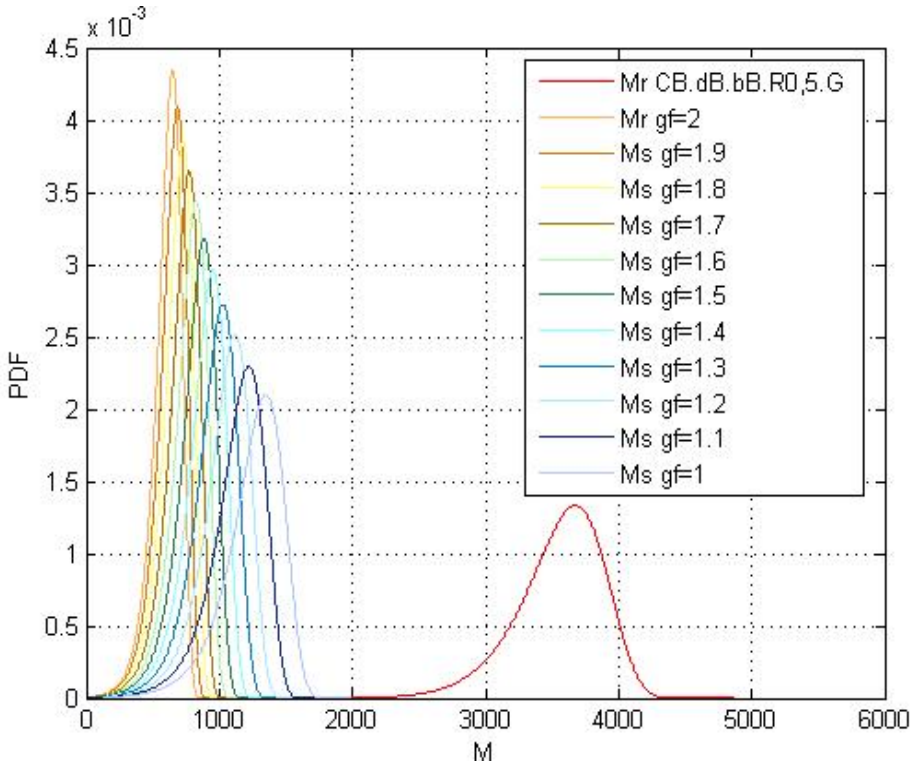

Figure 13 - PDF of M_s and M_r vs γ_f (ρ_f/ρ_{fb}=0.5; M_L/M_D=2.5; BEAMS)

The trend of β vs γ_f for the two design cases analyzed is reported in Figure 14, where the two modes of failure have been set apart and plotted separately: sections failing by GFRP rupture have a decreasing reliability when γ_f decreases, whereas sections failing by concrete crushing have an even higher reduction of reliability when γ_f decreases, although this occurs only for γ_f>1.4; when 1.0<γ_f<1.4 the weight of γ_f on these sections disappear and β settles to a constant value (≈7). The dependence on γ_f for concrete crushing sections when γ_f>1.4 occurs because with respect to the initial sorting of sections failing by concrete crushing when the characteristic strengths are accounted for, after taking into account the design values of strengths

($f_{cd} = f_{ck}/\gamma_c$; $f_{fd} = 0.9 \cdot \eta_a \cdot f_{fk}/\gamma_f$) the failure mode may switch in some cases, so that concrete crushing sections will have a dependence on γ_f when the failure mode switches to GFRP failure due to the introduction of partial safety factors γ_c and γ_f.

It can be concluded that when the failure mode is due to GFRP rupture ($\rho_f/\rho_{fb} \leq 1$) β regularly decreases when γ_f decreases as well; when the failure mode is due to concrete crushing ($\rho_f/\rho_{fb} > 1$) β still decreases when γ_f decreases, but only until a value equal to 1.4 for the specific design cases considered, below which β will get to a constant value.

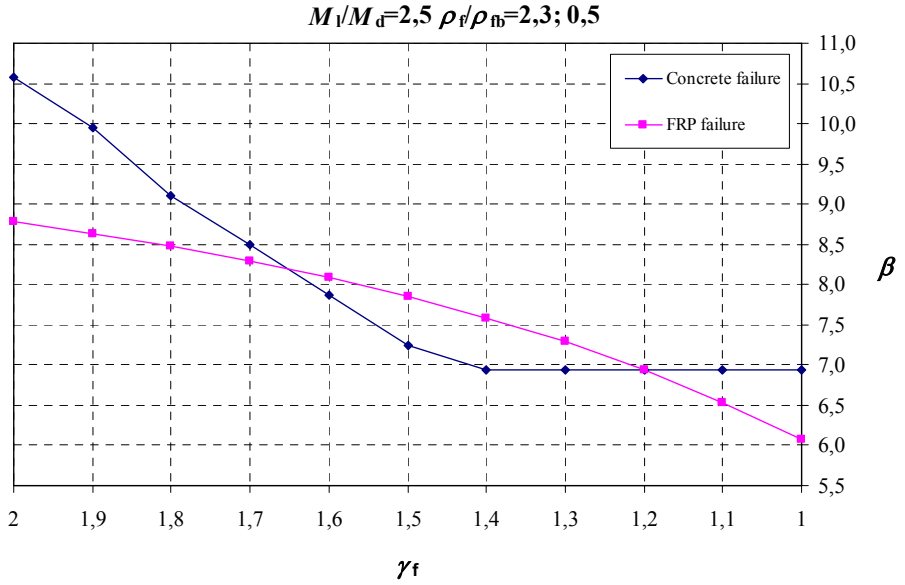

Figure 14 - Trend of β vs γ_f for M_D/M_L =2.5 and ρ_f/ρ_{fb}=0.5;2.3 [BEAMS]

3.4.12 Reliability Index of Beams Depending on γ_f, Regardless of M_L/M_D

The dependence of the reliability index on γ_f for the 240 design cases (beams) has been assessed for the five ratios M_L/M_D (1200 design cases overall); a mean value of β, β_0, was plotted in function of γ_f, as shown in Figure 15:

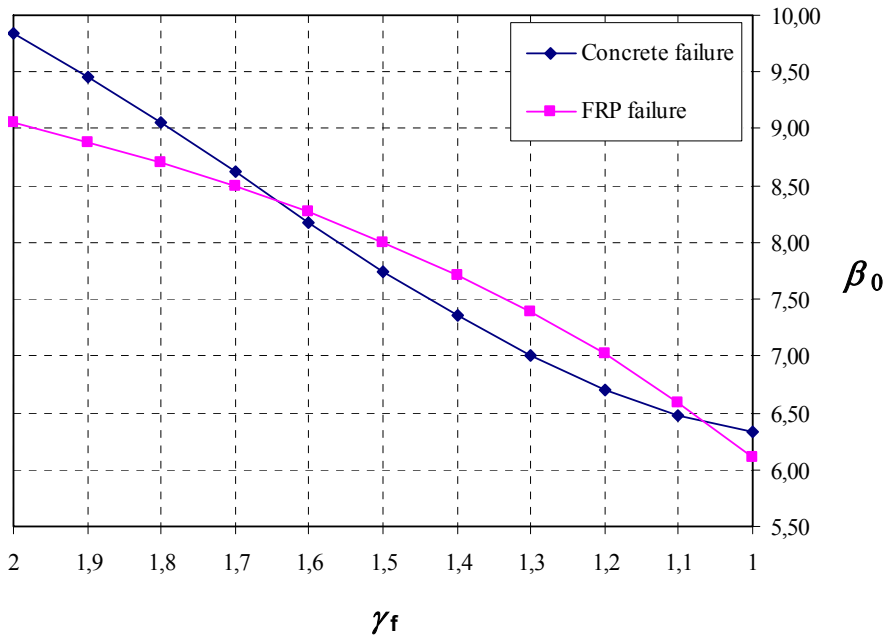

Figure 15 - β_0 vs γ_f for all M_L/M_D Ratios and all ρ_f/ρ_{fb} [f_{fk},f_{ck}; BEAMS]

The two failure modes curves intersect in two points, corresponding to $\gamma_f = 1.08$ ($\beta_0 = 6.4$) and $\gamma_f = 1.65$ ($\beta_0 = 8.3$), which can be deemed as optimum points, since they satisfy the balanced failure mode. It is believed that for the 1200 design cases considered the value of γ_f to be preferred is $\gamma_f = 1.08$, since it reduces the GFRP reinforcement strength less than the other one and together it corresponds to a satisfactory level of safety of member, being $\beta_0 > \beta_{min} = 5$ (P_f=10^{-7}), which can be deemed as the maximum threshold value for flexural RC members at ULS (see Table 3). Nevertheless, it can be also observed that points with $\gamma_f = 1.5$ correspond to a good level of safety ($\beta_0 > 7.5$), although the limitation on the strength of FRP reinforcement can be considered too penalizing and cost-ineffective.

It must be underlined that the classification proposed to plot β_0 vs γ_f, obtained by considering the ratios ρ_f/ρ_{fb} accounting for the characteristic values of material strengths, turns into the plot of Figure 16 when accounting for the design values of materials strengths: no failure mode switch takes place, concrete failures only occur for $1 < \gamma_f < 1.6$ and within this range the concrete failures do not depend on γ_f, as it is expected. Nevertheless, the optimum value of $\gamma_f = 1.04$ found with this

classification is very close to the one derived before ($\gamma_f = 1.08$), whereas points with $\gamma_f = 1.5$ correspond to a level of safety of FRP failing sections ($\beta_0 = 8.0$) higher than those failing by concrete crushing ($\beta_0 \sim 6.4$), which can be deemed a good result, since the ductile failure mode occurs more likely.

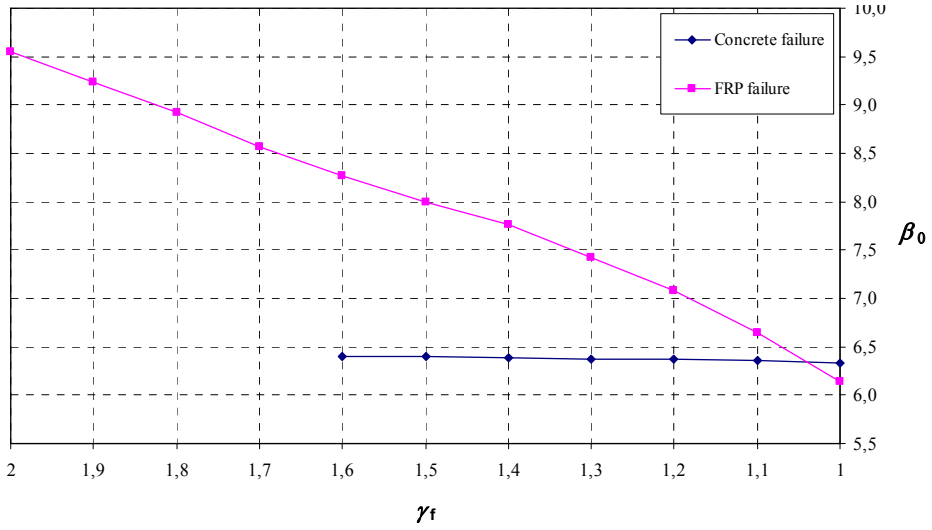

Figure 16 - β_0 vs γ_f for for all M_L/M_D Ratios and all ρ_f/ρ_{fb} [f_{fd},f_{cd}; BEAMS]

3.4.13 Reliability Index of Beams Accounting for *P*, *M* and *F*

The material properties, fabrication and analytical method influence the reliability index; such influence has been assessed for the selected beams design cases by applying the concepts examined in par. 3.4.7.1 and in par. 3.4.7.2: the *P* factor influence is independent on the design cases selected, whereas the *M* and *F* factors strictly depend on them, as reported in Appendix A; combining the values of bias and COV for all the design cases, λ_{M_R} and V_{M_R} have been derived, thus giving the diagram of Figure 17. It can be noticed that, with respect to Figure 15 trend, the trend of the two curves did not change from a qualitative standpoint; yet, accounting for the influence of the three parameters, that is carrying out a more refined and rigorous analysis, a considerable reduction in the reliability level will be brought. Moreover, no intersection between the two curves and then no optimum point is attained.

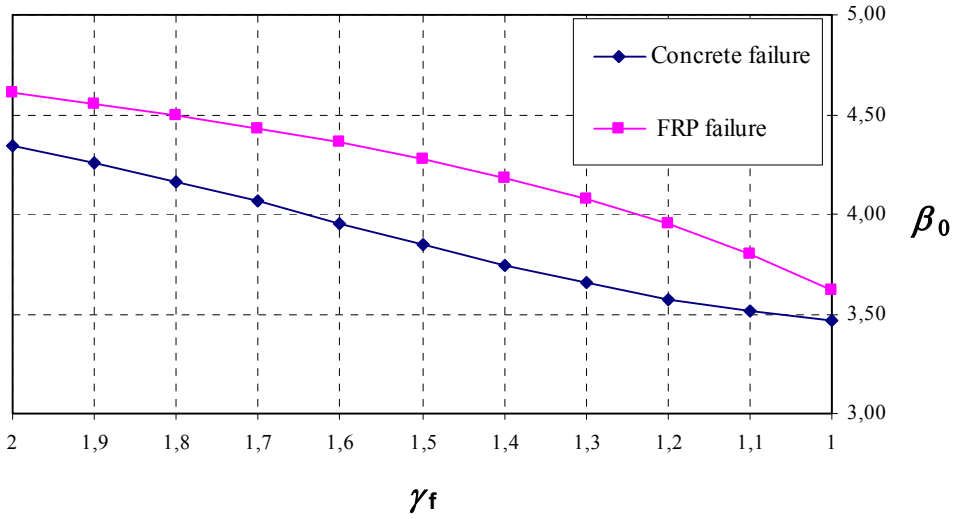

Figure 17 - β_0 vs γ_f Accounting for *P*, *M* and *F* Factors [BEAMS]

3.4.14 Reliability Index of Beams Depending on γ_f and γ_c

The dependence of the reliability index on both γ_f and γ_c was investigated as well, as reported in Figure 18, where $\beta_{0,TOT}$ refers to both failure modes. The trend of the reliability index related to the 1200 design cases can be explained as follows: for values of $\gamma_f > 1.6$ the reliability is not influenced by the specific value of γ_c, because the failure mode is governed by the FRP rupture exclusively; when $1 < \gamma_f < 1.6$, for a fixed value of γ_f, $\beta_{0,TOT}$ increases when γ_c increases, as expected, since to a higher limitation on the concrete strength developed corresponds a higher level of safety of the structure. The flattening of the three diagrams for $1 < \gamma_f < 1.6$ with respect to the trend derived when $\gamma_f > 1.6$ is due to the fact that the FRP failure decreasing trend combines with the constant trend of the concrete failure.

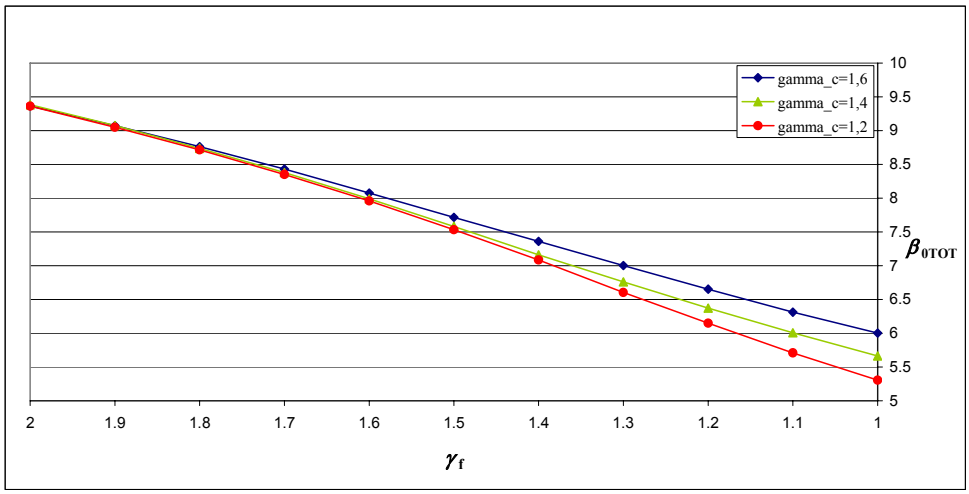

Figure 18 - β_{0TOT} vs γ_f and γ_c [BEAMS]

3.4.15 Minimum Reliability Index of Beams

A different representation of the reliability index behavior has been accomplished by minimizing the following sum of squares with respect to γ_f and γ_c:

$$\frac{1}{n_c}\sum_{m=1}^{n_c}(\beta_m - \beta_{min})^2, \quad (3.42)$$

where n_c = total number of design cases; and β_m = reliability index for case m ($\beta_{min} = 5$); the diagram depicted in Figure 19 has been derived; it shows that the value of γ_f that minimizes quantity 3.41 is lower than unity, confirming that all points with $\gamma_f > 1$ satisfy the minimum reliability index requirement.

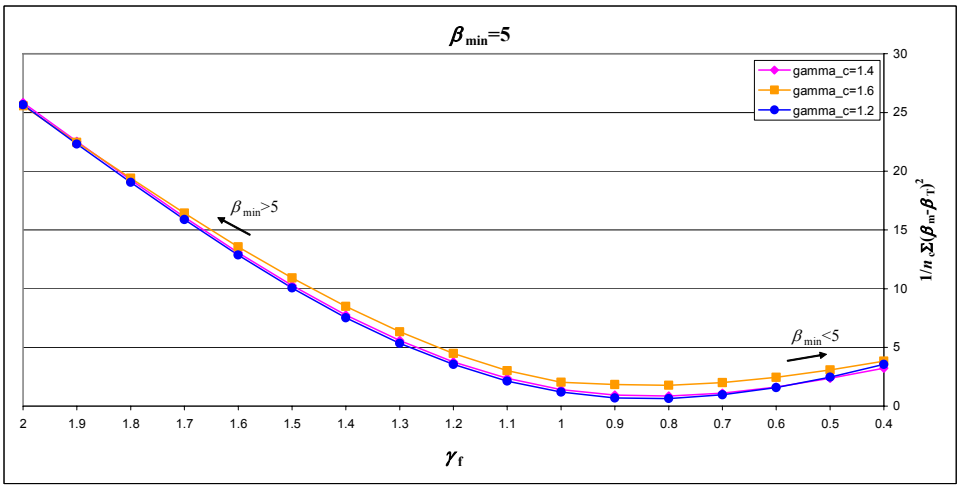

Figure 19 - Average Deviation from β_{min} vs γ_f and γ_c [BEAMS]

If varying also the values of β_{min} the trends in Figure 20 are obtained (setting γ_c=1.6). It can be noticed that while all points satisfy the minimum requirement for $3 < \beta_{min} < 6$, when $\beta_{min} = 7$ only points with $\gamma_f > 1.15$ correspond to $\beta > \beta_{min}$; whereas when $\beta_{min} = 8$ only points with $\gamma_f > 1.4$ correspond to $\beta > \beta_{min}$; this confirms that for the design space considered a good level of safety is attained for $\gamma_f = 1.5$, although better results in terms of cost effectiveness and exploitation of FRP strength could be reached.

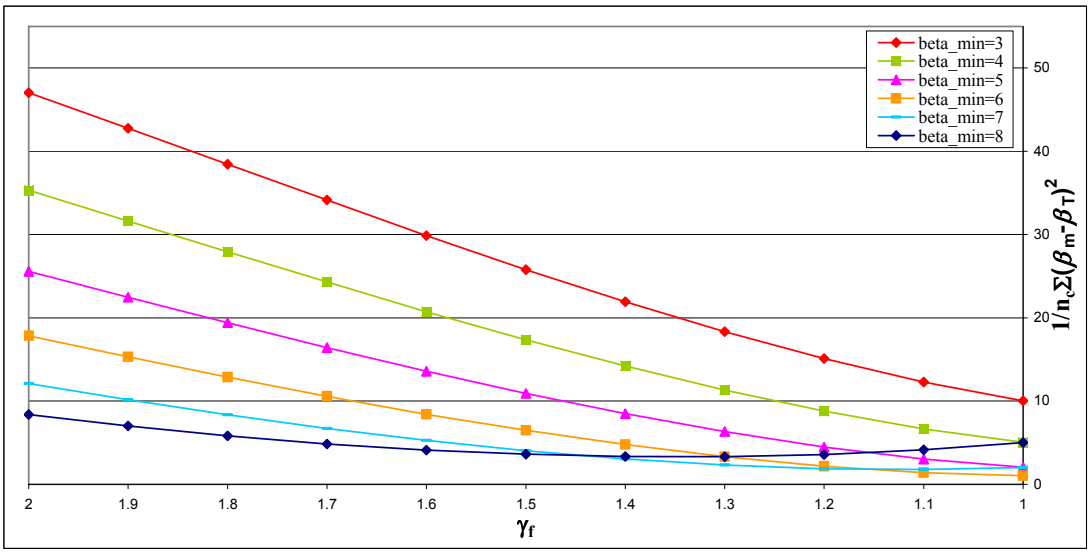

Figure 20 - Average Deviation from Different β_{min} vs γ_f and γ_c [BEAMS]

Finally, the extreme values of $\beta_{0,TOT}$ have been plotted depending on γ_f (see Figure 21, in order to show that although the minimum values of $\beta_{0,TOT}$ are lower than $\beta_{min} = 5$ (maximum threshold value for flexural RC members at ULS, with P_f=10^{-7}), in any case it satisfies the minimum threshold of Table 3, i.e. $\beta_{0,TOT\_min} > 4{,}265$, where 4,265 corresponds to the minimum threshold prescribed by BS EN 1990:2002 for flexural RC members at ULS (P_f=10^{-5}).

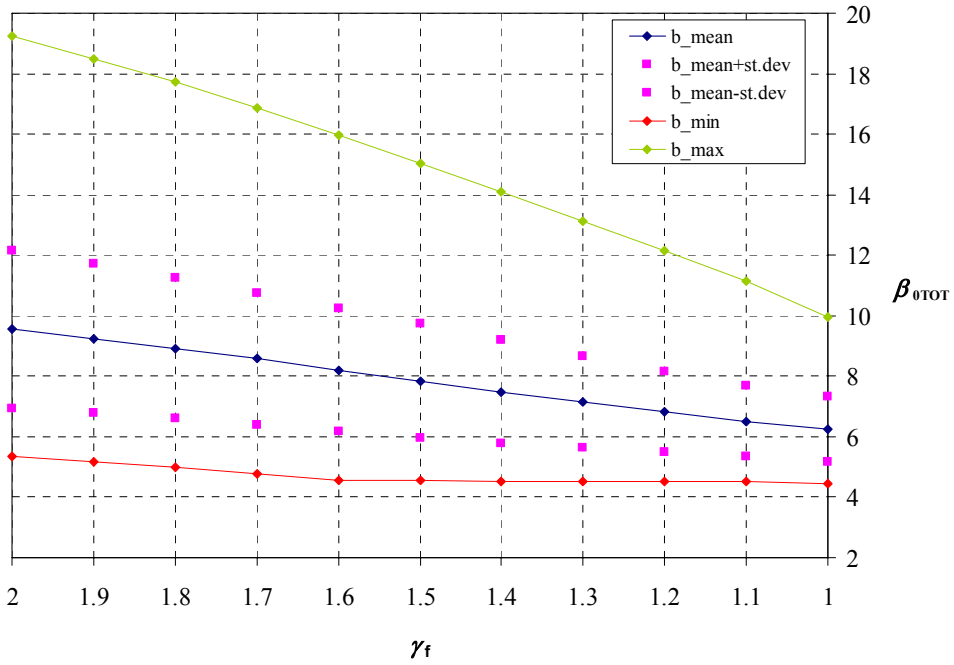

Figure 21 - Estreme values of β_{0TOT} vs γ_f [BEAMS]

3.4.16 Reliability Index of Slabs

Following the procedure explained in the previous paragraphs, the reliability index has been initially computed for each of the 180 design cases related to slabs, by varying the ratios M_L/M_D and ρ_f/ρ_{fb}. The partial safety factor for FRP reinforcement suggested in the CNR-DT203, γ_f=1.5, has been considered initially.

From the diagram reported in Figure 22 it can be noticed that the same remarks derived for beams may be summarized here: two edge zones of low, steady values of β corresponding to under-reinforced (ρ_f/ρ_{fb}<0.5) and over-reinforced sections (ρ_f/ρ_{fb}>2.5); a central zone with the maximum values of β corresponding to the balanced failing sections, where the materials are best exploited and then with the highest structural reliability values; and two transition zones with β variable going from under- or over-reinforced sections to balanced failing sections.

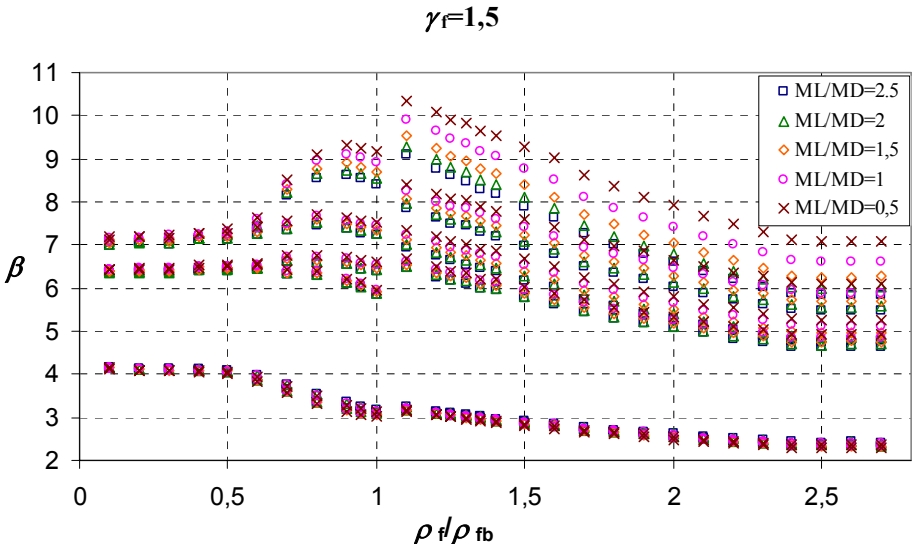

Figure 22 - Trend of β vs ρ_f/ρ_{fb} and M_L/M_D (γ_f=1.5; SLABS)

3.4.17 Reliability Index of Slabs Depending on γ_f, Regardless of M_L/M_D

The dependence of the reliability index on γ_f for the 180 design cases (slabs) has been assessed for the five ratios M_L/M_D (900 design cases overall); the mean value of β, β_0, was plotted in function of γ_f, as shown in Figure 23.

With respect to the corresponding values derived for beams (Figure 15), a general decrease of the reliability index values can be observed, although the different design spaces make such comparison vain. The two trends of the two modes of failure do not show any intersection point, and identify values of $\beta_0 > \beta_{min} = 5$ for $\gamma_f > 1.1$ when sections fail by FRP breaking, and for $\gamma_f > 1.4$ when sections fail by concrete crushing. Therefore, the value $\gamma_f = 1.1$ considered as an optimum value for beams design cases, does not match a satisfactory reliability level when referred to slabs design cases. The value $\gamma_f = 1.5$ proposed by the CNR-DT 203/2006 is enough reliable for the design cases investigated.

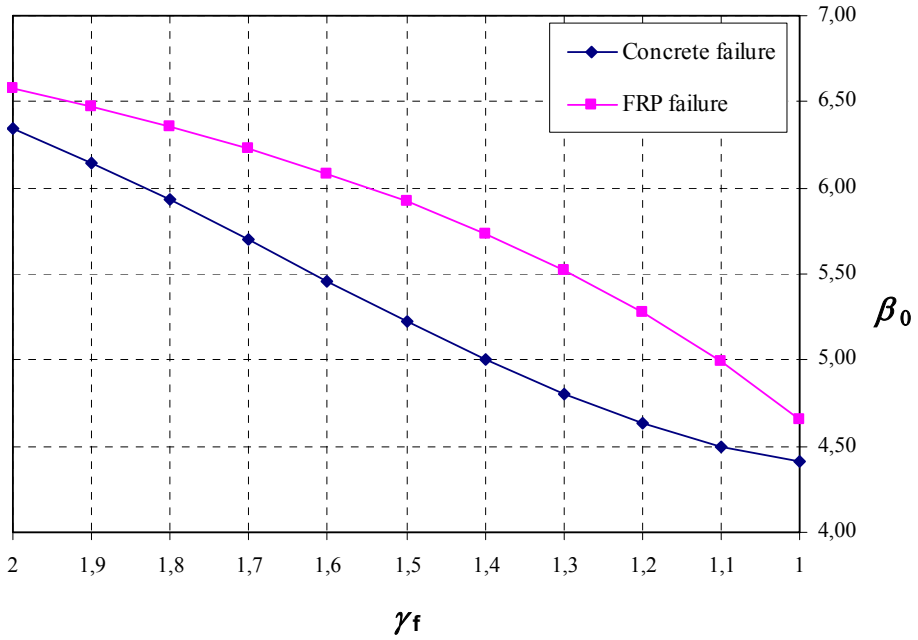

Figure 23 - β_0 vs γ_f for all M_L/M_D Ratios and all ρ_f/ρ_{fb} [SLABS]

3.4.18 Reliability Index of Slabs Accounting for *P*, *M* and *F*

The material properties, fabrication and analytical method influences have been assessed for the selected slabs design cases by applying the concepts already applied for beams, thus giving the diagram of Figure 24. As for beams, with respect to the trend of Figure 23, the trend of the two curves did not change from a qualitative standpoint, although a reduction in the reliability level is achieved.

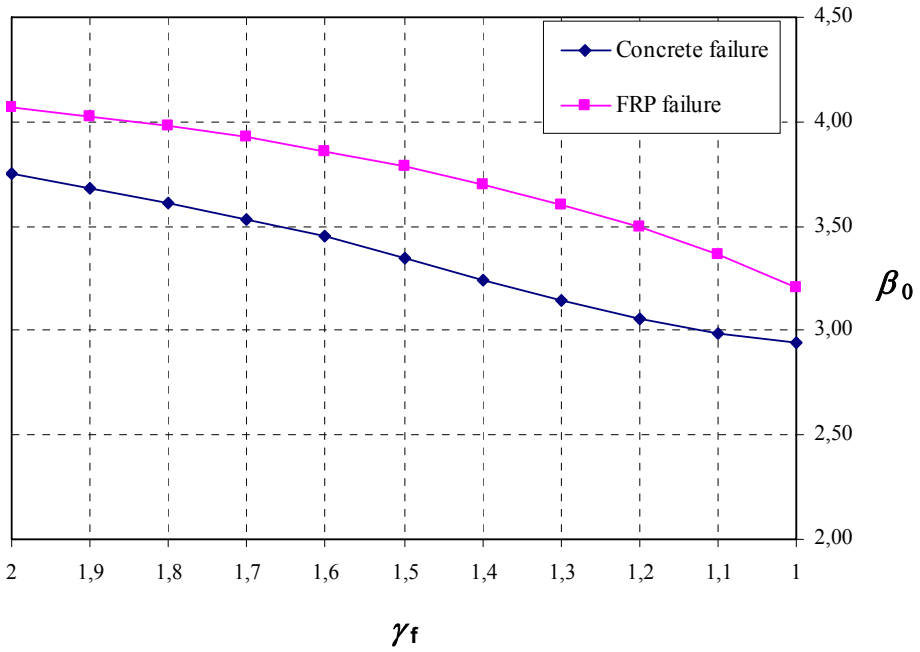

Figure 24 - β_0 vs γ_f Accounting for *P*, *M* and *F* Factors [SLABS]

3.5 CONCLUSIVE REMARKS

A reliability-based calibration of partial safety factors has been applied to assess the reliability levels of the ultimate limit state (ULS) flexural design suggested by the Italian guidelines CNR-DT 203/2006.

240 FRP-RC beams and 180 FRP-RC slabs have been designed to cover a wide design space considering an appropriate set of random design variables (cross-sectional dimensions, concrete strengths and FRP reinforcement ratios) used to develop resistance models for FRP-RC members. Monte-Carlo simulations have been performed to determine the variability in material properties and fabrication processes; whereas experimental data reported in the literature have been used to quantify the variability related to the analysis method. A structural reliability analysis has been conducted based on the established resistance models and load models obtained from literature. The reliability index, β, calculated using FORM for all FRP-RC beams and slabs for five ratios of live load to dead load moments, has been assessed in different hypotheses, namely depending on ρ_f/ρ_{fb}, M_L/M_D, γ_f, and on the uncertainty effects due to material properties (M), fabrication process (F) and analysis method (P); the following conclusions can be drawn:

1. The research work carried out is strictly dependent on the specific design cases taken into account; although a wide range of design cases has been covered and statistical properties available in literature have been assigned to design variables. More thorough and refined results will be attained with the research growth in the field of composites.
2. Regardless of member type (beams or slabs) and specific design considered, five different zones can be identified, depending on ρ_f/ρ_{fb}: two edge zones of low, steady values of β corresponding to under-reinforced ($\rho_f/\rho_{fb}<0.5$) and over-reinforced sections ($\rho_f/\rho_{fb}>2.5$); a central zone with the maximum values of β corresponding to the balanced failing sections, where the materials are best exploited and then with the highest structural reliability values; and two transition zones with β variable going from under- or over-reinforced sections to balanced failing sections.
3. For the 1200 design cases related to beam-type members (240 design cases by 5 ratios M_L/M_D) the value of γ_f to be preferred is $\gamma_f = 1.1$, as it slightly reduces the GFRP reinforcement strength and together it corresponds to a satisfactory level of safety of the member ($\beta_0 = 6.4 > \beta_{min} = 5$ at ULS). Nevertheless, it can be also observed that points with $\gamma_f = 1.5$ (current value proposed in the CNR-DT 203/2006) correspond to a good level of safety ($\beta_0 \geq 7.5$), although the limitation on the strength of FRP reinforcement can be considered too penalizing and cost-ineffective. Similar conclusions are derived if considering a different classification of results, depending on the design values of materials strengths rather than on the corresponding characteristic values;
4. With respect to the values derived for beams, a general decrease of the reliability can be observed when accounting for the 900 slabs design cases in correspondence of the same values of γ_f. The value $\gamma_f = 1.1$ considered as an optimum value for beams, does not match a satisfactory reliability level when referred to slabs. The value $\gamma_f = 1.5$ proposed by the CNR-DT 203/2006 is enough reliable for the slabs design cases investigated.

5. When accounting for M, F and P, regardless of the design space selected, the trend of the reliability index vs γ_f is similar to that obtained without the contribution of the three factors; yet a general reduction in the reliability level is observed.
6. This study focuses exclusively on the flexural behavior of GFRP-RC beams and slabs and assumes that the other modes of failure such as shear failure and bond failure do not control the design. Similar kinds of research should be conducted for other modes of failure; likewise, it would be worth to extend this research study to other types of reinforcement (i.e. CFRP and AFRP).

Chapter IV
SERVICEABILITY FLEXURAL BEHAVIOR

4.1 INTRODUCTION

In this chapter the approaches followed in the CNR-DT 203/2006 for the flexural design of FRP RC elements at serviceability limit states are presented; in particular, the deflection control of FRP RC members depending on the bond between FRP reinforcement and concrete is investigated.

4.2 SERVICEABILITY LIMIT STATES

The present paragraph deals with the most frequent serviceability limit states, and particularly those relating to:

1. Stress limitation;
2. Cracking control;
3. Deflection control.

1. The stress in the FRP reinforcement at SLS under the quasi-permanent load shall satisfy the limitation $\sigma_f \leq f_{fd}$, f_{fd} being the FRP design stress at SLS computed by setting $\gamma_f = 1$, whereas the stress in the concrete shall be limited according to the current building codes (D.M.LL.PP. 09/01/1996 or Eurocode 2, 2004).
2. At SLS, crack width shall be checked in order to guarantee a proper use of the structure as well as to protect the FRP reinforcement, such that under no circumstances crack width of FRP reinforced structures shall be higher than 0.5 mm. Since experimental tests on FRP reinforced members (with the exception of smooth bars) showed the suitability of the relationships provided by the EC2 for computation of both distance between cracks and concrete stiffening, the following equation can be used:

$$w_k = \beta \cdot s_{rm} \cdot \varepsilon_{fm}, \tag{4.1}$$

where w_k is the characteristic crack width, in mm; β is a coefficient relating average crack width to the characteristic value; s_{rm} is the final average distance between cracks, in mm; and ε_{fm} is the average strain accounting for tension stiffening, shrinkage, etc.

3. Deflection computation for FRP reinforced members can be performed by integration of the curvature diagram. Such diagram can be computed with non-linear analyses by taking into account both cracking and tension stiffening of concrete. Alternatively, simplified analyses are possible, similar to those used for traditional RC members. Experimental tests have shown that the model proposed by Eurocode 2 (EC2) when using traditional RC members can be deemed suitable for FRP RC elements too. Therefore, the following EC2 equation to compute the deflection *f* can be considered:

$$f = f_1 \cdot \beta_1 \cdot \beta_2 \cdot \left(\frac{M_{cr}}{M_{max}}\right)^m + f_2 \cdot \left[1 - \beta_1 \cdot \beta_2 \cdot \left(\frac{M_{cr}}{M_{max}}\right)^m\right] \tag{4.2}$$

where:

- f_1 is the deflection of the uncracked section;
- f_2 is the deflection of the transformed cracked section;
- $\beta_1 = 0.5$ is a non-dimensional coefficient accounting for bond properties of FRP bars;
- β_2 is a non-dimensional coefficient accounting for the duration of loading (1.0 for short time loads, 0.5 for long time or cyclic loads);
- M_{max} is the maximum moment acting on the examined element;
- M_{cr} is the cracking moment calculated at the same cross section of M_{max};
- *m* is a bond coefficient that CNR-DT 203 prescribes "*to be set equal to 2, unless specific bond characterization of FRP bars for the investigation of deflection is carried out by the manufacturer, by following the procedure to determine a different*

value of m reported in Appendix E", where the procedure to be used to determine the FRP bar-concrete adherence through appropriate tests in order to accurately evaluate deflections is described.

Here deflections can be calculated using the following formula:

$$f = f_1 \cdot \left(\frac{M_{cr}}{M_{max}} \right)^m + f_2 \cdot \left[1 - \left(\frac{M_{cr}}{M_{max}} \right)^m \right], \qquad (4.3)$$

with the quantities already having been defined.

On the basis of a population of at least five elements of concrete reinforced with FRP bars, that shall be subjected to four-points bending test, deflections and crack width are measured for fixed load values, ensuring that for a single test there is a number of at least five acquisitions over time interval between 20% and 60% of the ultimate load, P_{ult}.

The same load values are used to calculate the theoretical deflections starting from Equation 7.1.

The exponent *m* is determined on the basis of the comparison between the analytical and experimental results, using an appropriate statistical analysis, i.e. one based on the maximum likelihood method.

Upon determining this value, the experimental values of deflections for the tested specimens are then compared with the corresponding theoretical values, computed according to Equation (4.2) and assuming the *m* value obtained for the previously mentioned procedure assigned to it as well as to the coefficients β_1 e β_2 the unitary value.

4.3 BOND

The modulus of elasticity of glass and aramid FRP bars is about one-fifth that of steel. Even though carbon FRP bars have a higher modulus of elasticity than glass FRP bars, their stiffness is about two-thirds that of steel reinforcing bars. Lower stiffness causes larger deflections and crack widths for FRP reinforced members which can affect serviceability (Toutanji and Saafi, 2000). Since an important role is

played by bond between FRP bar and concrete, the bond behavior of FRP reinforced specimens is of interest in this investigation.

Two main mechanisms can be identified as transferring forces from the deformed FRP reinforcement to surrounding concrete:

- Chemical adhesion between the bar and the concrete;
- Frictional forces due to the roughness of the interface and the relative slip between the reinforcing bar and the surrounding concrete;
- Mechanical interlock between FRP deformed bar and concrete.

As a deformed bar slips with respect to the concrete along its length, chemical adhesion is lost while friction and bearing forces are mobilized. Because the forces interact with each other, it is difficult to quantify their contribution to the overall bond behavior.

4.3.1 Bond Tests

The bond behavior of FRP reinforced specimens is investigated using mainly four types of tests, namely pullout, beam-end, beam anchorage, and splice tests (Figure 1); a test method representing the direct measurement of bond stresses in actual reinforced concrete members does not exists due to the difficulty in reproducing the behavior of actual structural members in a laboratory environment.

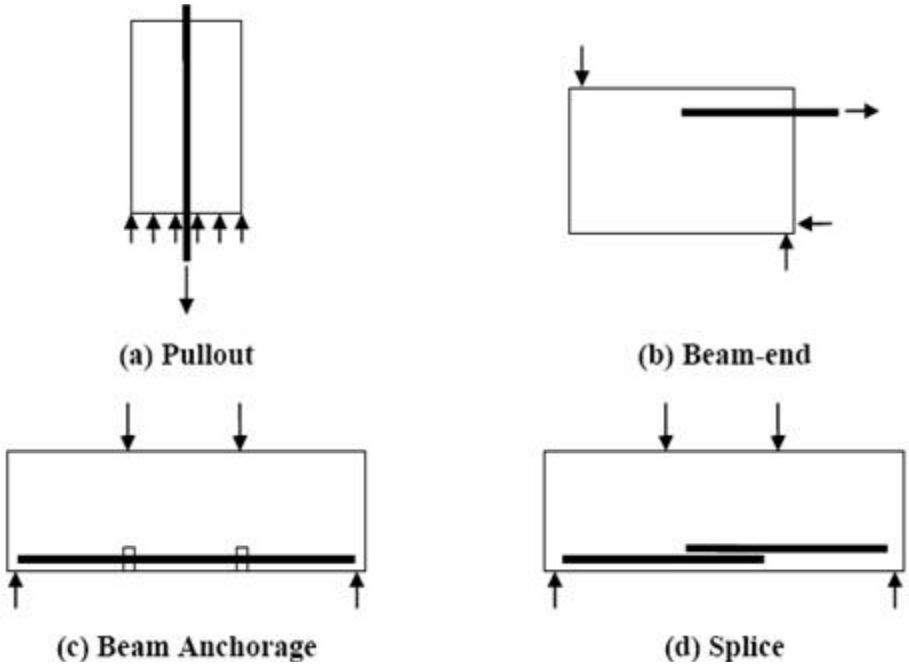

Figure 1 - Types of Test Methods

The pullout test is widely used because it is easy and inexpensive to fabricate and the test procedure is simple. Although pullout tests do not reflect the state of stresses in reinforced concrete structures, they are very useful in evaluating the load-slip relationship of reinforcing bars.

The beam-end test is also fairly inexpensive; nonetheless, evaluation of the data becomes complicated because both flexural and anchorage bond stresses are present around the reinforcing bar.

Beam anchorage and splice tests (the so-called four point bending tests) are designed to measure development and splice strengths in full-size flexural members. These tests are considered to be most realistic for representing actual beam behavior because the flexural stresses are not affected by the loading configuration. In addition, specimens allow random distribution of flexural cracking. Therefore, comparison can be made regarding overall structural performance. In this study only the beam anchorage tested specimens were taken into consideration for the calibration of bond coefficient.

4.3.2 Types of Failure

Three main types of failures can be generally identified in bond tests: bar failure, bar pullout, and concrete splitting. Among them, bar pullout and concrete splitting are desired failure types for investigating bond strength, since failure of the bar indicates that the bar had sufficient development length and the limits of bond strength have not been tested.

As the bar slips inside the concrete, surface adhesion is lost and force is transferred primarily through friction between the concrete and the reinforcement and the bearing forces acting on the deformations. The forces on the surface of the bar are balanced by compressive and shear stresses on the surrounding concrete surface.

Splitting failure occurs if the concrete cover and spacing of the bars are small enough for a splitting plane to develop.

4.3.3 Factors Affecting Bond

Bond between reinforcement and concrete is affected by many factors. The major factors influencing the bond behavior of FRP reinforced concrete are as follows (Pay, 2005):

- *Concrete cover and bar spacing*; an increase of concrete cover and bar spacing enhances the bond capacity, although this aspect is less prominent for larger diameter bars.
- *Concrete compressive strength*. The effect of concrete strength is not fully understood for FRP reinforced specimens, since there is only limited data available for FRP bar reinforced specimens. Nanni et al. (1995) investigated the effect of concrete strength on bond behavior using pullout specimens and found that concrete strength does not have any influence on pullout failures. However Malvar (1994) found that, for splitting failures, an increase in concrete strength results in an increase in bond strength.
- *Development length*; an increase in the development length of a reinforcing bar will increase the total bond force transferred between the concrete and the reinforcement; as for steel, when the bonded length increases, the effectiveness of the bonded length decreases, thus the relative gain with

increase in development length reduces. Further study is needed to quantify this effect.

- *Transverse reinforcement*; the presence of transverse reinforcement in the development region prevents the progression of splitting cracks; therefore, the bond force required to cause failure of the bar increases (Orangun et al., 1977, Tepfers, 1982, and Darwin et al., 1996 a, b). As the bond strength increases with an increase in transverse reinforcement, eventually the failure mode changes from splitting to pullout. Additional transverse reinforcement above that required to cause a pullout failure is unlikely to increase the anchorage capacity of the section (Orangun et al., 1977).
- *Bar size*; the bar size has a direct influence on the bond strength of FRP reinforced beams. As the bar size increases for a given development and splice length, the total bond force developed by the bar increases. However, the rate of increase in the bond force is lower than the increase in bar area. Consequently, bond stresses are lower for larger diameter bars.
- *Surface deformation of the reinforcement*; the force transfer between FRP bars and concrete is mainly due to chemical adhesion and friction between the concrete and the reinforcement; bearing of concrete on the surface deformation is minimal. Makinati et al. (1993), Malvar (1994), and Nanni et al. (1995) studied the effect of surface deformation on the bond strength of FRP reinforced specimens through pullout tests, concluding that the surface deformation of the bar has an influence on the bond strength.

4.4 CALIBRATION OF BOND COEFFICIENT "*m*"

A calibration analysis was conducted in compliance with the aforementioned procedure given in appendix E of CNR-DT 203/2006 in order to determine an optimum value for "*m*", based on a large experimental database available in literature, made of FRP RC elements subjected to four-points bending (beam anchorage) tests. The exponent "*m*" was determined on the basis of the comparison between analytical and experimental results, using the statistical analysis reported hereafter. This could be achieved thank to the work carried out by Dr. Sommese (Sommese, 2007) at the Dept. of Struct. Eng. of University of Naples "Federico II",

with the assistance of the work group made by Dr. Prota and the writer, and the supervision of prof. Manfredi.

4.4.1 Test Specimens and Variables

The experimental program consisted of sixty-seven concrete beam and slab specimens reinforced with continuous FRP bars, tested as reported in literature (Benmokrane et al., 1996, Alsayed, 1998, Masmoudi et al., 1998, Theriault and Benmokrane, 1998, Alsayed et al., 2000, Pecce et al, 2000, Toutanji and Deng, 2003, Yost et al., 2003, El Salakawy and Benmokrane, 2004, Al Sunna et al., 2006, Laoubi et al., 2006, Rafi et al, 2006). Figure 2 shows cross the section and the test setup layout:

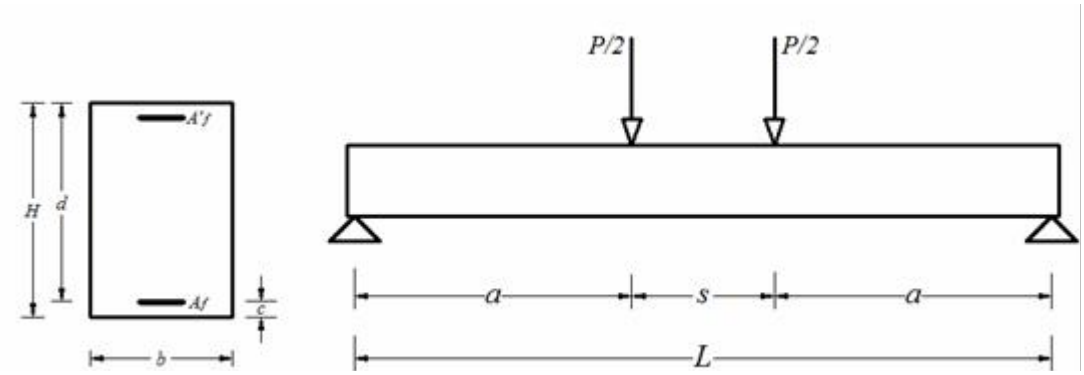

Figure 2 - Cross Section and Test Setup Layout

The cross section width, *b*, ranged between 12 and 100 cm; the height, *H*, ranged between 18 and 55 cm; the length, *L*, varied between 150 and 340 cm; the distance between the support and the applied load, *a*, ranged between 50 and 145 cm; the constant moment zone, *s*, varied between 10 and 100 cm.

In Table 1 all the geometric data are reported:

Table 1 - Geometric Data Considered

Author	b (cm)	H (cm)	c (cm)	d (cm)	L (cm)	a (cm)	s (cm)
Pecce et.al. (2000)	50	18	2,6	14	340	120	100
	50	18	2,6	14	340	120	100
	50	18	2,6	14	340	120	100
Toutanji & Deng (2003)	18	30	1,8	26	280	120	40
	18	30	1,8	26	280	120	40
	18	30	4,5	24	280	120	40
Theriault & Benmokrane (1998)	13	18	2,0	14	150	50,0	50
	13	18	2,0	14	150	50,0	50
	13	18	2,0	14	150	50,0	50
	13	18	2,0	14	150	50,0	50
	13	18	2,0	14	150	50,0	50
	13	18	2,0	14	150	50,0	50
	13	18	2,0	14	150	50,0	50
	13	18	2,0	14	150	50,0	50
El-Salakawy & Benmokrane (2004)	100	20	2,5	17	250	100	50
	100	20	2,5	17	250	100	50
	100	20	2,5	17	250	100	50
	100	20	2,2	17	250	100	50
	100	20	2,0	16	250	100	50
	100	20	2,2	17	250	100	50
	100	20	2,0	16	250	100	50
	100	20	2,2	17	250	100	50
Laoubi et al. (2006)	13	18	2,0	14	150	50,0	50
	13	18	2,0	14	150	50,0	50
	13	18	2,0	14	150	50,0	50
	13	18	2,0	14	150	50,0	50
	13	18	2,0	14	150	50,0	50
	13	18	2,0	14	150	50,0	50
	13	18	2,0	14	150	50,0	50
	13	18	2,0	14	150	50,0	50
	13	18	2,0	14	150	50,0	50
Al-Sunna et al. (2006)	15	25	2,5	21	230	76	76
	15	25	2,5	21	230	76	76
	15	25	2,5	20	230	76	76

Author	b (cm)	H (cm)	c (cm)	d (cm)	L (cm)	a (cm)	s (cm)
Benmokrane et al. (1996)	20	30	3,0	25	330	115	100
	20	30	3,0	25	330	115	100
	20	55	3,0	50	330	115	100
Alsayed (1998)	20	21	3,5	15	270	130	10
	20	26	3,5	21	270	130	10
	20	25	3,5	19	270	130	10
Masmoudi et al. (1998)	20	30	3,0	25	300	125	50
	20	30	3,0	25	300	125	50
	20	30	3,0	25	300	125	50
	20	30	4,5	23	300	125	50
	20	30	4,5	23	300	125	50
	20	30	4,5	23	300	125	50
	20	30	4,5	23	300	125	50
Rafi et al. (2006)	12	20	2,0	16	175	67,5	40
	12	20	2,0	16	175	67,5	40
Yost et.al. (2003)	22	28	5,0	22	229	107	15
	22	28	5,0	22	229	107	15
	25	28	5,1	22	229	107	15
	22	28	5,1	22	229	107	15
	25	18	3,8	14	305	145	15
	30	18	3,8	13	305	145	15
	24	18	3,8	13	305	145	15
	20	18	3,8	13	305	145	15
	15	28	5,0	22	229	107	15
	16	28	5,1	22	229	107	15
	20	28	5,1	22	229	107	15
	25	18	3,8	13	305	145	15
	19	18	3,8	13	305	145	15
	15	18	3,8	13	305	145	15
	17	18	3,8	13	305	145	15
Alsayed et al (2000)	20	21	3,5	15	270	125	20
	20	26	3,5	21	270	125	20

As for the concrete used for casting the specimens, the mean compressive strength, f_c, ranged between 30 and 97 MPa; the mean tensile strength for flexure, $f_{ct,fl}$, ranged between 2.9 and 5.2 MPa; and the compressive modulus of elasticity, E_c, ranged between 23 and 46 GPa; in particular for E_c also the corresponding theoretical values were computed (ranging between 23 and 41 GPa), using the following relationship that depends on f_c (ACI 318, 1996):

$$E_{c,the} = 4263 \cdot \sqrt{f_c} \qquad (4.4)$$

Table 2 reports the main characteristics of concrete considered in the referenced works (E_{ct}= tensile modulus of elasticity of concrete):

Table 2 - Concrete Characteristics

Author	f_c MPa	$E_{c,exp}$ GPa	$E_{c,the}$ GPa	$f_{ct,fl}$ Mpa
Pecce et.al. (2000)	30	23	23	2,9
	30	23	23	2,9
	30	23	23	2,9
Toutanji & Deng (2003)	35	35	25	3,1
	35	35	25	3,1
	35	35	25	3,1
Theriault & Benmokrane (1998)	53	31	31	3,8
	53	31	31	3,8
	57	32	32	3,9
	97	42	42	5,2
	46	29	28	3,6
	53	31	31	3,8
	93	41	41	5,1
	93	41	41	5,1
El-Salakawy & Benmokrane (2004)	40	30	26	3,3
	40	30	26	3,3
	40	30	26	3,3
	40	30	26	3,3
	40	30	26	3,3
	40	30	26	3,3
	40	30	26	3,3
Laoubi et. al. (2006)	40	30	26	3,3
	40	30	26	3,3
	40	30	26	3,3
	40	30	26	3,3
	40	30	26	3,3
	40	30	26	3,3
	40	30	26	3,3
	40	30	26	3,3
	40	30	26	3,3
Al-Sunna et.al. (2006)	38	26	26	3,2
	38	26	26	3,2
	38	26	26	3,2

Author	f_c MPa	$E_{c,exp}$ GPa	$E_{c,the}$ GPa	$f_{ct,fl}$ Mpa
Benmokrane et al. (1996)	79	45	38	4,7
	31	23	23	2,9
	31	23	23	2,9
Alsayed (1998)	31	26	23	2,9
	31	26	23	2,9
	41	30	27	3,3
Masmoudi et al. (1998)	52	33	30	3,8
	52	33	30	3,8
	52	33	30	3,8
	45	30	28	3,5
	45	30	28	3,5
	45	30	28	3,5
	45	30	28	3,5
Rafi et al. (2006)	42	27	27	3,4
	41	27	27	3,4
Yost et.al. (2003)	36	39	25	3,1
	36	39	25	3,1
	36	39	25	3,1
	36	39	25	3,1
	40	43	27	3,3
	40	43	27	3,3
	40	43	27	3,3
	40	43	27	3,3
	79	46	38	4,7
	79	46	38	4,7
	79	46	38	4,7
	79	45	38	4,7
	79	45	38	4,7
	79	45	38	4,7
	43	33	27	3,4
Alsayed et al. (2000)	43	33	27	3,4
	43	33	27	3,4

The FRP reinforcement included glass (62 specimens) and carbon bars (5 specimens) with different sizes and surface deformations. The bars tensile strength, f_{fu}, varied from 507 to 3912 MPa; the modulus of elasticity, E_f, varied from 36 to 136 GPa; and

the diameter of bars in tension, ϕ, ranged between 9 and 22 mm; the main characteristics of FRP reinforcement are reported in Table 3 (ϕ' and A_f' are related to compression reinforcement, ϕ_ω is related to shear reinforcement).

Table 3 -FRP Reinforcement Characteristics

Author	*Bar Type*	*Ø* *(mm)*	*Ø'* *(mm)*	*Af* *(cm²)*	*A'f* *(cm²)*	*Ø$_w$* *(mm)*	*f_{fu}* *(MPa)*	*E_f* *(GPa)*
Pecce et al. (2000)	GFRP (deformed)	12,7	12,7	8,86	2,53	8	644	42,0
	GFRP (deformed)	12,7	12,7	5,06	2,53	8	644	42,0
	GFRP (deformed)	12,7	12,7	8,86	2,53	8	644	42,0
Toutanji & Deng (2003)	GFRP (rods)	12,7	12,7	2,53	2,53	8	597	40,0
	GFRP (rods)	12,7	12,7	3,80	2,53	8	597	40,0
	GFRP (rods)	12,7	12,7	5,06	2,53	8	597	40,0
Theriault & Benmokrane (1998)	GFRP (deformed)	12,3	6,00	2,38	0,57	6	552	38,0
	GFRP (deformed)	12,3	6,00	2,38	0,57	6	552	38,0
	GFRP (deformed)	12,3	6,00	2,38	0,57	6	552	38,0
	GFRP (deformed)	12,3	6,00	2,38	0,57	6	552	38,0
	GFRP (deformed)	12,3	6,00	4,75	0,57	6	552	38,0
	GFRP (deformed)	12,3	6,00	4,75	0,57	6	552	38,0
	GFRP (deformed)	12,3	6,00	4,75	0,57	6	552	38,0
	GFRP (deformed)	12,3	6,00	4,75	0,57	6	552	38,0
El-Salakawy & Benmokrane (2004)	CFRP (sand-coated)	9,50	12,7	6,38	16,5	0	2991	114
	CFRP (sand-coated)	9,50	12,7	12,8	16,5	0	2991	114
	CFRP (sand-coated)	9,50	12,7	19,1	16,5	0	2991	114
	GFRP (sand-coated)	15,9	12,7	13,9	16,5	0	597	40,0
	GFRP (sand-coated)	22,2	12,7	27,1	16,5	0	597	40,0
	GFRP (sand-coated)	15,9	12,7	27,8	16,5	0	597	40,0
	GFRP (sand-coated)	22,2	12,7	38,7	16,5	0	597	40,0
	GFRP (sand-coated)	15,9	12,7	41,7	16,5	0	597	40,0
Laoubi et al. (2006)	GFRP (sand-coated)	9,54	10,0	1,43	1,57	10	507	36,0
	GFRP (sand-coated)	9,54	10,0	1,43	1,57	10	507	36,0
	GFRP (sand-coated)	9,54	10,0	1,43	1,57	10	507	36,0
	GFRP (sand-coated)	9,54	10,0	1,43	1,57	10	507	36,0
	GFRP (sand-coated)	9,54	10,0	1,43	1,57	10	507	36,0
	GFRP (sand-coated)	9,54	10,0	1,43	1,57	10	507	36,0
	GFRP (sand-coated)	9,54	10,0	1,43	1,57	10	507	36,0
	GFRP (sand-coated)	9,54	10,0	1,43	1,57	10	507	36,0
	GFRP (sand-coated)	9,54	10,0	1,43	1,57	10	507	36000
Al-Sunna et al.(2006)	GFRP (sand-helicoidal)	9,53	6,00	1,43	0,57	8	662	42,8
	GFRP (sand-helicoidal)	12,7	6,00	2,53	0,57	8	635	41,6
	GFRP (sand-helicoidal)	19,1	6,00	11,4	0,57	8	643	42,0
Benmokrane et al. (1996)	GFRP (sand-helicoidal)	19,1	6,00	5,73	0,57	6	717	45,0
	GFRP (sand-helicoidal)	19,1	6,00	5,73	0,57	6	717	45,0
	GFRP (sand-helicoidal)	19,1	6,00	5,73	0,57	6	717	45,0
Alsayed (1998)	GFRP (spiral-winding)	19,0	6,25	11,3	0,31	8	644	42,0
	GFRP (spiral-winding)	12,7	6,25	5,06	0,31	8	644	42,0
	GFRP (spiral-winding)	19,0	6,25	11,3	0,31	8	644	42,0
Masmoudi et al. (1998)	GFRP (deformed-rod)	14,9	10,0	3,49	1,57	10	552	38,0
	FRP (deformed-rod)	14,9	10,0	3,49	1,57	10	552	38,0
	FRP (deformed-rod)	14,9	10,0	5,23	1,57	10	552	38,0
	FRP (deformed-rod)	14,9	10,0	6,97	1,57	10	552	38,0
	FRP (deformed-rod)	14,9	10,0	6,97	1,57	10	552	38,0
	FRP (deformed-rod)	14,9	10,0	10,5	1,57	10	552	38,0
	FRP (deformed-rod)	14,9	10,0	10,5	1,57	10	552	38,0
Rafi et al.(2006)	CFRP (Leadline)	9,50	8,00	1,42	1,00	6	3912	136

	CFRP (Leadline)	9,50	8,00	1,42	1,00	6	3912	1360
Yost et al. (2003)	*GFRP (sand-helicoidal)*	19,1	0,00	5,73	0,00	0	604	40,3
	GFRP (sand-helicoidal)	19,1	0,00	8,59	0,00	0	604	40,3
	GFRP (sand-helicoidal)	22,2	0,00	11,6	0,00	0	604	40,3
	GFRP (sand-helicoidal)	22,2	0,00	11,6	0,00	0	604	40,3
	GFRP (sand-helicoidal)	12,7	0,00	2,53	0,00	0	604	40,3
	GFRP (sand-helicoidal)	15,9	0,00	3,97	0,00	0	604	40,3
	GFRP (sand-helicoidal)	15,9	0,00	3,97	0,00	0	604	40,3
	GFRP (sand-helicoidal)	15,9	0,00	3,97	0,00	0	604	40,3
	GFRP (sand-helicoidal)	19,1	0,00	5,73	0,00	0	604	40,3
	GFRP (sand-helicoidal)	22,2	0,00	7,74	0,00	0	604	40,3
	GFRP (sand-helicoidal)	22,2	0,00	11,6	0,00	0	604	40,3
	GFRP (sand-helicoidal)	15,9	0,00	3,97	0,00	0	604	40,3
	GFRP (sand-helicoidal)	15,9	0,00	3,97	0,00	0	604	40,3
	GFRP (sand-helicoidal)	15,9	0,00	3,97	0,00	0	604	40,3
	GFRP (sand-helicoidal)	19,1	0,00	5,73	0,00	0	604	40,3
Alsayed et al. (2000)	*GFRP*	19,0	6,25	11,3	0,31	8	677	43,4
	GFRP	12,7	6,25	5,06	0,31	8	677	43,4

4.4.2 Cracking Moment

In order to calibrate the bond coefficient "*m*" in formula (4.3), three different cases were analyzed, namely:

1. $M_{cr,exp}$, & $E_{c,exp}$;
2. $M_{cr,the}$, & $E_{c,exp}$;
3. $M_{cr,exp}$, & $E_{c,the}$,

where $M_{cr,exp}$ and $M_{cr,the}$ are the experimental and the theoretical value of the cracking moment, respectively. The definition of the cracking moment is important since it influences the evaluation of deflection for FRP reinforced members (Pecce et al., 2001); since $M_{cr,the}$ depends on the concrete strength in tension, that is a very uncertain parameter and usually can not be directly measured, but computed depending on the strength in compression, the introduction of the experimental value of the cracking moment M_{cr} allows to examine the model efficiency disregarding the influence of the uncertainties due to $M_{cr,the}$ (1st case); nevertheless, evaluating $M_{cr,the}$ is significant for the model application (2nd case); similarly, the significance of $E_{c,the}$ instead of $E_{c,exp}$ in the model application was taken into account (3rd case).

Table 4 reports the values of the ultimate load, P_{ult}, the moment of inertia of both the un-cracked (I_1) and cracked section (I_1), and of $M_{cr,exp}$ and $M_{cr,the}$ relating all specimens considered:

Table 4 - Applied Load, Moment of Inertia and Cracking Moment of Specimens

Author	P_{ult} KN	I_1 cm^4	I_2 cm^4	$M_{cr,exp}$ KNm	$M_{cr,the}$ KNm
Pecce et al. (2000)	98	18850	2535	7,6	10
	54	18545	1548	4,2	9,9
	98	18850	2535	6,0	10
Toutanji & Deng (2003)	100	28419	1796	12	10
	108	28711	2612	13	10
	118	28592	2706	11	10
Theriault & Benmokrane (1998)	87	4493	506	3,2	3,3
	80	4493	506	3,2	3,3
	78	4488	489	3,3	3,4
	90	4453	385	3,4	4,4
	89	4663	979	3,5	3,2
	84	4639	917	4,1	3,4
	114	4568	724	3,9	4,4
	118	4568	724	3,9	4,4
El-Salakawy & Benmokrane (2004)	280	48016	5628	23,	27
	334	49787	10355	24	28
	380	51501	14600	24	30
	226	47290	4411	23	27
	284	48515	7886	23	28
	326	48647	8173	23	28
	326	49595	10722	23	29
	336	49971	11573	23	29
Laoubi et al. (2006)	55	4432	303	2,8	2,8
	55	4432	303	2,6	2,8
	55	4432	303	2,8	2,8
	53	4432	303	2,7	2,8
	52	4432	303	2,7	2,8
	58	4432	303	3,0	2,8
	54	4432	303	2,8	2,8
	54	4432	303	2,8	2,8
	52	4432	303	2,7	2,8
Al-Sunna et al. (2006)	52	13683	891	4,0	6,1
	80	13864	1443	5,7	6,2
	120	15252	5048	7,2	7,0

Author	P_{ult} KN	I_1 cm^4	I_2 cm^4	$M_{cr,exp}$ KNm	$M_{cr,the}$ KNm
Benmokrane et al. (1996)	133	32191	4019	8,5	12
	140	32191	4019	10	12
	316	196236	16873	37	42
Alsayed (1997)	59	11440	2886	5,2	5,7
	77	20942	2763	6,5	8,2
	90	19198	4236	5,8	9,1
Masmoudi et al. (1998)	92	31555	2168	10	13
	95	31555	2168	10	13
	104	31878	3135	14	13
	121	32010	3871	10	13
	115	32010	3871	14	13
	136	32549	5493	10	13
	137	32549	5493	14	13
Rafi et al. (2006)	88	6024	1428	2,4	3,5
	86	6030	1440	2,4	3,5
Yost et al. (2003)	86	31305	2402	8,5	12
	100	31632	3471	8,0	12
	111	35258	4512	8,0	13
	111	31910	4445	8,5	12
	35	9144	395	4,9	5,7
	44	11006	591	5,4	6,9
	44	8726	579	4,5	5,5
	44	7372	570	3,8	4,6
	89	20911	2023	9,2	12
	89	22813	2643	7,9	13
	89	28260	3863	10	16
	53	9183	566	6,4	8,0
	44	6938	549	5,1	6,1
	44	5548	537	3,8	4,9
	53	6523	741	4,5	5,8
Alsayed & Almusallam (1995)	50	11555	3210	3,1	5,7
	80	21060	3109	6,3	8,2

4.4.3 Calibration Analysis

For each of the three cases reported in § 4.4.2, the calibration of the exponent *"m"* was carried out by computing the standard (e_1) and the mean error (e_2):

$$e_1 = \sqrt{\frac{\sum_{i=1}^{n}\left(\frac{f_{the} - f_{test}}{f_{test}}\right)_i^2}{n}}; \tag{4.5}$$

$$e_2 = \frac{\sum_{i=1}^{n}\left(\frac{f_{the} - f_{test}}{f_{test}}\right)_i}{n}, \tag{4.6}$$

where f_{the} and f_{test} are the theoretical and the experimental value of the deflection, respectively; *i* is the generic test, and *n* is the number of considered points; e_1 can be considered as a measure of the reliability of equation, whereas e_2 is a measure of the safe level of the model (e_2>0: the model is safe). The errors have been calculated in a load range which could be significant of serviceability conditions, namely 20 to 65% of ultimate load, P_{ult}; with load steps of 5%, 10 different deflection values in correspondence of as many load values were measured for each test.

Following a summary of the calibration analysis performed is reported:

- Compute the theoretical deflection corresponding to a percentage value α of the applied load (20%<α<65%):

$$f_{the}^{\alpha} = \alpha f_1 \cdot \alpha\gamma + \alpha f_2 \cdot (1 - \alpha\gamma) = \alpha\left[f_1 \cdot \gamma + f_2 \cdot (1 - \alpha \cdot \gamma)\right], \tag{4.7}$$

where:

αf_1 is the deflection of the uncracked section:

$$\alpha f_1 = \frac{0,5 \cdot \alpha P_{ult} \cdot L^3}{24 \cdot E_c \cdot I_1}; \tag{4.8}$$

αf_2 is the deflection of the transformed cracked section:

$$\alpha f_2 = \frac{0,5 \cdot \alpha P_{ult} \cdot L^3}{24 \cdot E_c \cdot I_2}; \tag{4.9}$$

and where:

$$\gamma = \left(\frac{M_{cr}}{\alpha M_{\max}} \right)^m , \tag{4.10}$$

in which $\alpha M_{\max} = 0,5 \cdot \alpha P_{ult} \cdot a$.

- Measure the corresponding experimental deflection, f_{test}^{α}, on the plots available in literature (67 out of 180 specimens could be selected);
- Compute $e_1 = \sqrt{\sum_{i=1}^{n} \left(\frac{f_{the}^{\alpha i} - f_{test}^{\alpha i}}{f_{test}^{\alpha i}} \right)_i^2 \Big/ n}$ and $e_2 = \sum_{i=1}^{n} \left(\frac{f_{the}^{\alpha} - f_{test}^{\alpha i}}{f_{test}^{\alpha i}} \right)_i \Big/ n$.

By varying the bond coefficient *m* the minimum value of e_1 (with e_2>0) was found for each of the three cases analyzed.

1. $M_{cr,exp}$ & $E_{c,exp}$

Table 5 reports the values of theoretical deflections computed for each load step when setting $M_{cr}=M_{cr,exp}$ and $E_c=E_{c,exp}$, according to equation (4.3), and the corresponding experimental values measured.

The evaluation of e_1 was carried out ignoring singular points (see "Discarded" yellow cells in Table 5), that is when the theoretical value is different by more than 100% with respect to the experimental value ($(f_{the} - f_{exp}) > 2 \cdot f_{exp}$).

Table 5 - Theoretical and Experimental Deflections ($M_{cr,exp}$, $E_{c,exp}$)

Author	f_{the} (cm)										f_{exp} (cm)									
	20%	25%	30%	35%	40%	45%	50%	55%	60%	65%	20%	25%	30%	35%	40%	45%	50%	55%	60%	65%
Pecce et al. (2000)	1,1	1,7	2,3	3,0	3,6	4,3	4,9	5,6	6,2	6,9	1,3	2,0	2,5	3,2	4,0	4,4	5,0	5,6	6,5	7,0
	0,9	1,4	2,0	2,6	3,2	3,8	4,3	4,9	5,5	6,1	1,3	1,8	2,4	3,1	3,5	4,1	4,7	5,3	5,8	6,6
	1,4	2,0	2,6	3,3	4,0	4,6	5,3	5,9	6,6	7,3	1,8	2,4	3,0	3,5	4,5	4,7	5,7	6,2	6,8	7,3
Toutanji & Deng (2003)	0,0	0,4	0,7	1,0	1,4	1,7	2,0	2,4	2,7	3,1	0,1	0,5	0,9	1,2	1,8	2,2	2,6	3,1	3,4	3,9
	0,0	0,3	0,5	0,8	1,0	1,3	1,5	1,8	2,1	2,3	0,1	0,3	0,7	1,1	1,5	1,8	2,1	2,5	2,9	3,4
	0,2	0,5	0,7	1,0	1,3	1,6	1,8	2,1	2,4	2,7	0,3	0,5	0,7	0,9	1,4	1,6	1,9	2,3	2,6	2,9
Theriault & Benmokrane (1998)	0,2	0,4	0,6	0,7	0,9	1,1	1,3	1,5	1,7	1,9	0,4	0,5	0,6	0,8	0,9	1,2	1,3	1,4	1,5	1,7
	Discard	0,3	0,5	0,6	0,8	1,0	1,1	1,3	1,5	1,7	0,7	0,8	0,9	1,1	1,2	1,3	1,4	1,5	1,6	1,7
	0,1	0,3	0,4	0,6	0,8	0,9	1,1	1,3	1,4	1,6	0,2	0,3	0,4	0,6	0,8	1,0	1,3	1,4	1,6	1,7
	0,2	0,4	0,5	0,7	0,9	1,1	1,3	1,5	1,7	1,8	0,2	0,4	0,5	0,7	1,0	1,3	1,4	1,6	1,7	1,8
	0,1	0,2	0,3	0,4	0,5	0,68	0,7	0,8	1,0	1,1	0,1	0,2	0,3	0,4	0,6	0,8	0,9	1,0	1,1	1,2
	0,0	0,1	0,2	0,3	0,4	0,5	0,6	0,7	0,8	0,9	0,1	0,3	0,3	0,5	0,7	0,9	1,2	1,4	1,6	1,7
	0,2	0,3	0,4	0,5	0,7	0,8	0,9	1,1	1,2	1,3	0,2	0,3	0,4	0,5	0,7	0,8	0,9	1,1	1,3	1,5
	Discard	0,3	0,4	0,6	0,7	0,8	1,0	1,1	1,2	1,4	0,8	0,9	1,0	1,1	1,2	1,3	1,4	1,5	1,7	1,8
El-Salakawy & Benmokrane (2004)	0,2	0,5	0,7	1,0	1,2	1,5	1,8	2,0	2,3	2,5	0,3	0,6	1,0	1,3	1,6	1,9	2,3	2,6	3,1	3,4
	0,2	0,4	0,6	0,7	0,9	1,1	1,2	1,4	1,6	1,7	0,4	0,6	1,0	1,2	1,3	1,5	1,7	2,0	2,2	2,4
	0,2	0,4	0,5	0,7	0,8	0,9	1,1	1,2	1,3	1,5	0,4	0,7	0,8	1,0	1,1	1,2	1,4	1,4	1,5	1,8
	Discard	0,3	0,5	0,8	1,1	1,3	1,6	1,8	2,1	2,4	0,3	0,5	0,6	0,8	1,2	1,4	1,7	2,1	2,4	2,8
	0,2	0,4	0,6	0,7	0,9	1,1	1,3	1,5	1,7	1,9	0,3	0,6	0,7	1,2	1,3	1,5	1,8	2,1	2,4	2,7
	0,3	0,5	0,7	0,9	1,1	1,3	1,5	1,7	1,9	2,2	0,5	0,7	1,1	1,3	1,6	1,9	2,4	2,6	2,8	2,9
	0,2	0,4	0,5	0,7	0,9	1,0	1,2	1,3	1,5	1,7	0,4	0,6	0,8	1,0	1,3	1,4	1,7	1,8	2,0	2,1
	0,2	0,4	0,5	0,7	0,8	1,0	1,1	1,3	1,4	1,6	0,4	0,6	0,8	0,9	1,2	1,4	1,7	1,8	1,9	2,2
Laoubi et al. (2006)	Discard	0,2	0,4	0,6	0,8	1,0	1,2	1,4	1,6	1,8	0,2	0,3	0,4	0,5	0,6	0,7	0,9	1,2	1,4	1,6
	0,0	0,2	0,4	0,6	0,8	1,0	1,2	1,4	1,6	1,8	0,2	0,2	0,4	0,5	0,7	0,9	1,1	1,3	1,4	1,6
	Discard	0,2	0,4	0,6	0,8	1,0	1,2	1,4	1,6	1,8	0,1	0,3	0,4	0,5	0,8	1,0	1,2	1,4	1,5	1,6
	Discard	0,2	0,4	0,6	0,8	1,0	1,2	1,4	1,5	1,7	0,2	0,3	0,3	0,5	0,6	0,8	1,1	1,2	1,4	1,6
	Discard	0,2	0,4	0,5	0,7	0,9	1,1	1,3	1,5	1,7	0,4	0,5	0,5	0,6	0,8	0,9	1,1	1,2	1,4	1,6
	Discard	0,2	0,4	0,6	0,8	1,0	1,3	1,5	1,7	1,9	0,2	0,2	0,3	0,6	0,8	1,0	1,2	1,4	1,7	1,9
	Discard	0,2	0,4	0,6	0,8	1,0	1,2	1,4	1,6	1,8	0,1	0,3	0,5	0,8	0,9	1,1	1,3	1,6	1,7	1,9
	Discard	0,2	0,4	0,6	0,8	1,0	1,2	1,4	1,6	1,8	0,2	0,3	0,3	0,5	0,7	0,8	1,0	1,3	1,4	1,7
	Discard	0,2	0,3	0,5	0,7	0,9	1,1	1,3	1,5	1,7	0,3	0,3	0,4	0,5	0,7	0,8	1,0	1,2	1,3	1,5
Al-Sunna et al. (2006)	Discard	0,3	0,5	0,8	1,1	1,3	1,6	1,9	2,1	2,4	0,2	0,2	0,4	1,2	1,4	1,5	1,7	2,0	2,3	2,4
	0,1	0,4	0,6	0,9	1,1	1,4	1,6	1,9	2,1	2,4	0,2	0,5	1,0	1,2	1,4	1,5	1,8	1,9	2,1	2,3
	0,2	0,3	0,4	0,5	0,6	0,5	0,8	0,9	1,0	1,2	0,3	0,4	0,5	0,7	0,8	0,9	1,0	1,1	1,3	1,4
Benmokrane et al. (1996)	0,7	1,0	1,4	1,7	2,1	2,2	2,8	3,2	3,6	3,9	0,5	0,7	1,0	1,3	1,8	2,2	2,6	2,8	3,2	3,5
	0,6	0,9	1,3	1,7	2,1	2,9	2,8	3,2	3,6	4,0	0,5	0,9	1,3	1,5	1,9	2,2	2,6	3,0	3,5	3,7
	Discard	0,2	0,4	0,6	0,8	1,0	1,2	1,4	1,6	1,8	0,3	0,5	0,8	1,0	1,2	1,3	1,6	1,8	2,1	2,3
Alsayed	0,3	0,4	0,6	0,7	0,9	1,0	1,2	1,3	1,5	1,6	0,5	0,8	1,1	1,2	1,3	1,5	1,7	1,8	2,1	2,4

(1997)	0,3	0,5	0,7	0,9	1,1	1,3	1,5	1,7	2,0	2,2	0,4	0,7	0,9	1,2	1,4	1,6	2,0	2,4	2,6	2,9
	0,3	0,4	0,6	0,7	0,8	1,0	1,1	1,3	1,4	1,5	0,7	0,8	1,0	1,3	1,4	1,5	1,7	1,9	2,1	2,3
Masmoudi et al. (1998)	0,2	0,5	0,9	1,2	1,6	1,9	2,3	2,6	3,0	3,3	0,2	0,4	0,7	1,1	1,4	2,0	2,4	2,7	3,2	3,5
	0,3	0,6	0,9	1,3	1,7	2,0	2,4	2,7	3,1	3,4	0,2	0,4	1,0	1,2	1,6	2,0	2,6	2,8	3,3	3,7
	Discard	0,2	0,5	0,8	1,0	1,3	1,5	1,8	2,1	2,4	0,2	0,3	0,5	0,7	1,4	1,7	2,0	2,4	2,7	2,9
	0,4	0,7	1,0	1,2	1,5	1,8	2,1	2,4	2,6	2,9	0,4	0,7	1,0	1,4	1,7	2,0	2,3	2,7	3,0	3,4
	0,1	0,4	0,6	0,9	1,1	1,4	1,7	1,9	2,2	2,5	0,3	0,4	0,7	1,0	1,3	1,7	2,0	2,4	2,7	3,0
	0,4	0,6	0,8	1,1	1,3	1,5	1,7	1,9	2,2	2,4	0,4	0,5	0,9	1,1	1,4	1,8	2,0	2,2	2,3	2,6
	0,2	0,5	0,7	0,9	1,1	1,3	1,6	1,8	2,0	2,2	0,4	0,6	0,8	1,0	1,5	1,7	1,9	2,0	2,2	2,4
Rafi et al. (2006)	0,3	0,4	0,5	0,6	0,8	0,9	1,0	1,1	1,3	1,4	0,3	0,5	0,6	0,8	1,0	1,2	1,4	1,5	1,6	1,7
	0,3	0,4	0,5	0,6	0,7	0,9	1,0	1,1	1,2	1,3	0,2	0,6	0,6	0,7	1,0	1,2	1,3	1,4	1,5	1,7
Yost et al. (2003)	***Discard***	***Discard***	0,2	0,3	0,4	0,5	0,6	0,8	0,9	1,0	0,0	0,1	0,3	0,3	0,5	0,7	0,8	0,9	1,0	1,2
	Discard	0,1	0,2	0,3	0,4	0,5	0,6	0,7	0,7	0,8	0,1	0,3	0,4	0,5	0,6	0,7	0,8	0,9	1,0	1,1
	Discard	0,1	0,2	0,3	0,4	0,4	0,5	0,6	0,7	0,7	0,1	0,1	0,3	0,4	0,4	0,5	0,5	0,7	0,7	0,9
	0,1	0,1	0,2	0,3	0,4	0,4	0,5	0,6	0,7	0,7	0,1	0,2	0,2	0,3	0,4	0,5	0,5	0,7	0,8	0,9
	0,2	0,7	1,3	1,8	2,4	3,0	3,6	4,2	4,7	5,3	0,6	0,7	0,7	1,9	1,9	3,1	3,1	3,2	4,6	4,6
	Discard	0,8	1,3	1,8	2,2	2,7	3,2	3,7	4,2	4,7	0,0	1,5	1,6	1,9	2,0	2,8	2,8	3,7	3,7	4,8
	0,6	1,1	1,6	2,1	2,6	3,1	3,6	4,1	4,6	5,1	0,7	1,8	1,8	2,8	2,8	4,1	4,1	4,6	4,6	6,0
	0,8	1,3	1,8	2,4	2,9	3,4	3,9	4,4	4,9	5,4	0,5	1,7	1,7	2,4	2,5	3,7	3,7	4,4	4,5	6,1
	0,0	0,1	0,2	0,3	0,4	0,6	0,7	0,8	0,9	1,0	0,1	0,1	0,2	0,3	0,5	0,6	0,7	0,8	0,9	1,3
	0,0	0,1	0,2	0,3	0,4	0,5	0,6	0,6	0,7	0,8	0,1	0,2	0,3	0,3	0,5	0,5	0,6	0,7	0,8	0,9
	0,0	0,0	0,1	0,1	0,2	0,3	0,3	0,4	0,4	0,5	0,1	0,1	0,2	0,2	0,3	0,4	0,4	0,5	0,5	0,6
	Discard	1,0	1,6	2,1	2,7	3,3	3,9	4,5	5,1	5,7	0,1	0,9	1,9	1,9	2,8	2,8	4,1	5,3	5,4	6,5
	0,5	0,9	1,4	1,9	2,4	2,9	3,4	3,9	4,5	5,0	0,6	1,7	1,8	2,8	2,8	4,1	4,2	5,1	5,6	6,4
	0,9	1,4	1,9	2,4	2,9	3,4	4,0	4,5	5,0	5,5	0,6	1,4	1,4	2,8	2,9	3,7	3,8	4,8	5,1	6,6
	0,8	1,2	1,7	2,1	2,6	3,0	3,5	3,9	4,4	4,8	0,4	1,0	1,5	1,6	3,0	3,1	3,8	4,3	4,4	5,1
Alsayed & Almusallam (1995)	0,3	0,4	0,5	0,7	0,8	0,9	1,1	1,2	1,3	1,5	0,5	0,7	0,8	1,0	1,1	1,3	1,5	1,7	1,8	1,9
	0,3	0,5	0,8	1,0	1,2	1,4	1,6	1,8	2,0	2,2	0,5	0,8	0,9	1,3	1,5	1,8	2,1	2,4	2,8	3,0

Therefore, for each specimen tested e_1 and e_2 were computed, as reported in Table 6:

Table 6 - Standard Error (e_1) & Mean Error (e_2) [$M_{cr,exp}$, $E_{c,exp}$]

Author	*Standard Error (e_1)*	*Mean Error (e_2)*
Pecce et al. (2000)	0,072	-0,052
	0,138	-0,116
	0,100	-0,076
Toutanji & Deng (2003)	0,189	-0,186
	0,232	-0,199
	0,087	0,018
Theriault & Benmokrane (1998)	0,149	0,024
	0,291	-0,226
	0,080	0,021
	0,100	0,036
	0,216	0,068
	0,336	-0,308
	0,078	0,030
	0,368	-0,346
El-Salakawy & Benmokrane (2004)	0,196	-0,189
	0,270	-0,266
	0,218	-0,203
	0,110	-0,060
	0,252	-0,244
	0,273	-0,270
	0,247	-0,245
	0,258	-0,256
Laoubi et al. (2006)	0,311	0,236
	0,283	0,169
	0,110	0,065
	0,245	0,206
	0,214	-0,046
	0,273	0,175
	0,102	-0,088
	0,232	0,173
	0,164	0,104
Al-Sunna et al. (2006)	0,277	0,043
	0,169	-0,114
	0,152	-0,149

Author	*Standard Error (e_1)*	*Mean Error (e_2)*
Benmokrane et al. (1996)	0,357	0,301
	0,114	0,101
	0,303	-0,288
Alsayed (1997)	0,406	0,161
	0,265	-0,262
	0,209	-0,205
Masmoudi et al. (1998)	0,342	-0,334
	0,198	-0,193
	0,363	-0,358
	0,237	0,133
	0,261	0,115
	0,178	-0,114
	0,091	-0,051
Rafi et al. (2006)	0,172	-0,141
	0,147	0,016
Yost et al. (2003)	0,160	-0,140
	0,183	-0,105
	0,248	-0,094
	0,117	-0,052
	0,252	-0,247
	0,170	0,012
	0,389	0,143
	0,394	0,133
	0,181	-0,022
	0,173	-0,137
	0,259	0,087
	0,177	0,056
	0,082	0,022
	0,211	-0,144
	0,124	-0,004
Alsayed & Almusallam (1995)	0,236	-0,225
	0,196	0,051

Average e_1	*Average e_2*
0,212	**-0,062**

The bond coefficient corresponding to the minimum value e_1=0.212 is m=0.872. As for e_2, since the value derived is nearly zero, it can be concluded that the analytical model is sufficiently reliable.

A different evaluation was performed deriving m for each load step of every single test, after setting $f_{\exp} = f_{the}$, so that $f_{\exp} = f_1 \cdot \gamma + f_2 \cdot (1-\gamma)$. Therefore γ was derived:

$$\gamma = \frac{f_{\exp} - f_2}{f_1 - f_2}, \tag{4.11}$$

from which:

$$m = \log_{\frac{M_{cr}}{M_{\max}}} \left(\frac{f_{\exp} - f_2}{f_1 - f_2} \right). \tag{4.12}$$

Hence the following quantities were plotted as shown in Figure 3:

$$\left[\left(\frac{M_{cr,\exp}}{M_a} \right)^{m=\text{var}}, \left(\frac{M_{cr,\exp}}{M_a} \right) \right]; \left[\left(\frac{M_{cr,\exp}}{M_a} \right)^{0.872}, \left(\frac{M_{cr,\exp}}{M_a} \right) \right]; \left[\left(\frac{M_{cr,\exp}}{M_a} \right)^{2}, \left(\frac{M_{cr,\exp}}{M_a} \right) \right]$$

($M_a = \alpha M_{\max}$).

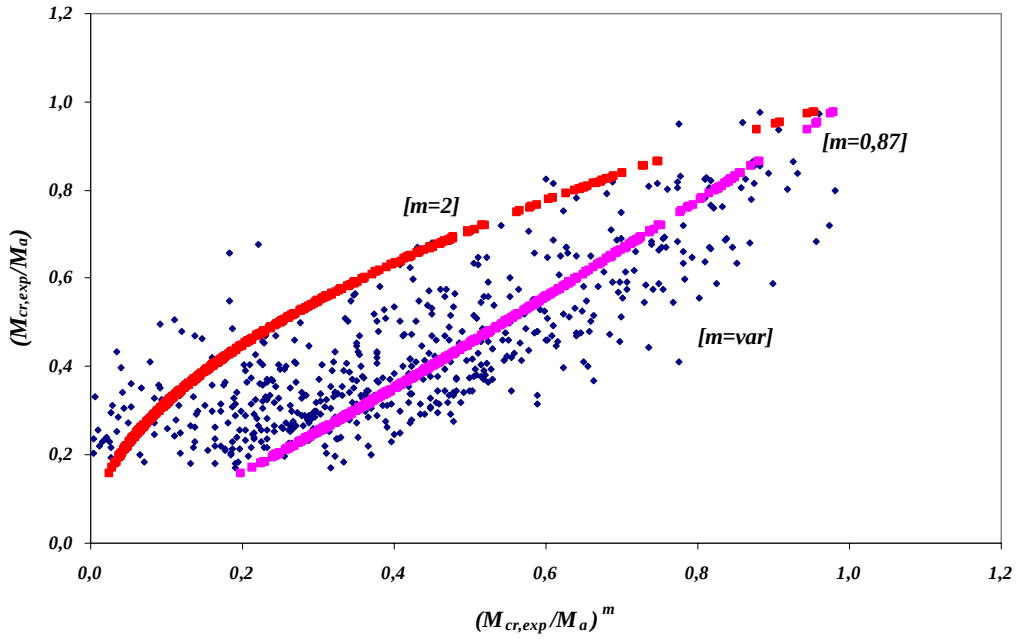

Figure 3 - $(M_{cr}/M_a)^m$ vs (M_{cr}/M_a) $[M_{cr,exp};E_{c,exp}]$

It can be noticed that magenta points, corresponding to $\left(M_{cr,\exp}/M_a\right)^{0.872}$, approximate blue points with $\left(M_{cr,\exp}/M_a\right)^{m=\text{var}}$ better than red points corresponding to $\left(M_{cr,\exp}/M_a\right)^2$; thus, m=0.872 is suggested in replacement of m=2 in equation (4.3).

2. $M_{cr,the}$ & $E_{c,exp}$

The significance of model was evaluated in the second case computing theoretical deflections for each load step after setting $M_{cr}=M_{cr,the}$ and $E_c=E_{c,exp}$, according to equation (4.3), and comparing the results with the corresponding experimental values measured. The same procedure already explained for the first case was followed, computing e_1 and e_2 for each specimen tested, as reported in Table 7:

Table 7 - Standard Error (e_1) & Mean Error (e_2) [$M_{cr,the}$, $E_{c,exp}$]

Author	*Standard Error (e_1)*	*Mean Error (e_2)*
Pecce et al. (2000)	0,274	-0,244
	0,810	-0,732
	0,358	-0,326
Toutanji & Deng (2003)	0,594	0,128
	0,679	0,172
	0,227	0,145
Thèriault & Benmokrane (1998)	0,147	-0,030
	0,320	-0,267
	0,081	-0,049
	0,266	-0,227
	0,271	0,090
	0,321	-0,229
	0,125	-0,092
	0,429	-0,410
El-Salakawy & Benmokrane (2004)	0,333	-0,328
	0,348	-0,344
	0,289	-0,273
	0,274	-0,244
	0,375	-0,368
	0,372	-0,369
	0,348	-0,341
	0,353	-0,348
Laoubi et al. (2006)	0,276	0,202
	0,254	0,033
	0,170	-0,010
	0,166	0,108
	0,225	-0,109
	0,342	0,145
	0,127	-0,118
	0,198	0,135
	0,136	0,023
Al-Sunna et al. (2006)	0,745	-0,622
	0,283	-0,234
	0,168	-0,165

Author	*Standard Error (e_1)*	*Mean Error (e_2)*
Benmokrane et al. (1996)	0,070	0,000
	0,068	-0,040
	0,423	-0,402
Alsayed (1997)	0,367	-0,359
	0,324	-0,319
	0,471	-0,463
Masmoudi et al. (1998)	0,527	-0,381
	0,481	-0,371
	0,197	-0,142
	0,247	-0,243
	0,138	-0,104
	0,172	-0,159
	0,155	-0,142
Rafi et al. (2006)	0,251	-0,237
	0,272	-0,230
Yost et al. (2003)	0,314	-0,309
	0,407	-0,397
	0,272	-0,260
	0,143	-0,128
	0,396	-0,088
	0,286	-0,191
	0,263	-0,236
	0,168	-0,006
	0,518	-0,336
	0,623	-0,482
	0,997	-0,772
	0,232	-0,210
	0,339	-0,325
	0,148	-0,101
	0,221	0,001
Alsayed & Almusallam(1995)	0,451	-0,440
	0,360	-0,354

Average e_1	*Average e_2*
0,318	**-0,205**

The bond coefficient corresponding to the minimum value e_1=0.318 is m=0.790. With respect to case 1) it can be observed that the average standard error e_1 in case 2) is higher, and that the average mean error, e_2, is considerably lower than zero, confirming that considering the analytical value of M_{cr} instead of the corresponding experimental value decreases the model reliability.

As for case 1), the following quantities were plotted as shown in Figure 4:

$$\left[\left(\frac{M_{cr,the}}{M_a}\right)^{m=\text{var}},\left(\frac{M_{cr,the}}{M_a}\right)\right];\left[\left(\frac{M_{cr,the}}{M_a}\right)^{0.790},\left(\frac{M_{cr,the}}{M_a}\right)\right];\left[\left(\frac{M_{cr,the}}{M_a}\right)^{2},\left(\frac{M_{cr,the}}{M_a}\right)\right]$$

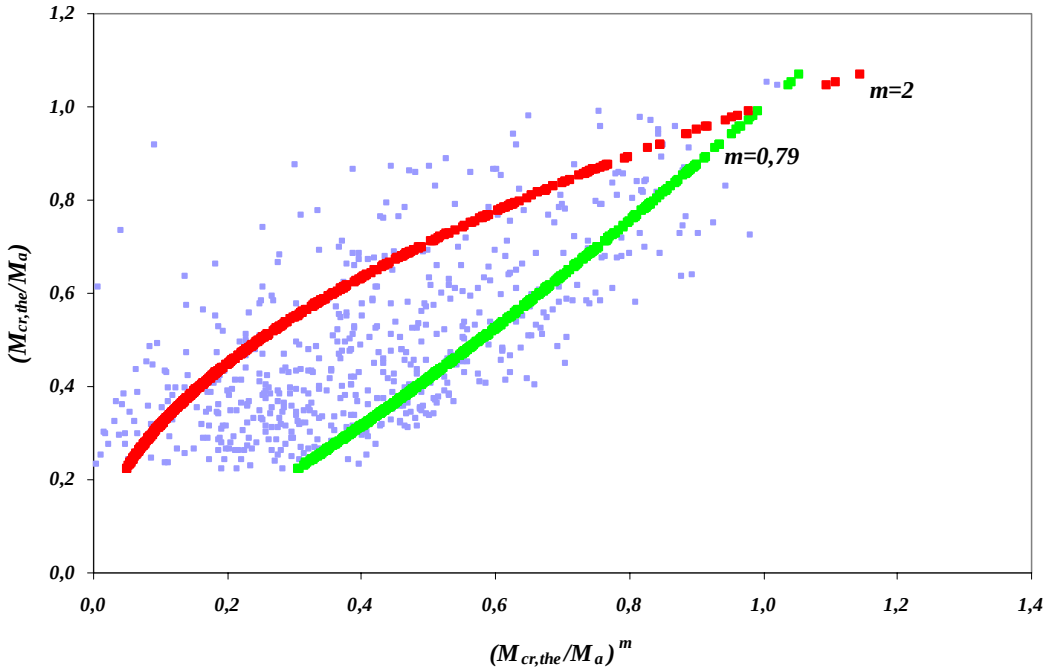

Figure 4 - $(M_{cr}/M_a)^m$ vs (M_{cr}/M_a) $[M_{cr,the};E_{c,exp}]$

None of the two lines (m=2 and m=0.79) approximates the points with m=var. properly, confirming that the red line is not enough reliable and that considering $M_{cr,the}$ instead of $M_{cr,exp}$ implies an accuracy reduction of the model proposed.

3. $M_{cr,exp}$ & $E_{c,the}$

The significance of considering $E_{c,the}$ instead of $E_{c,exp}$ in the model application was taken into account in case 3). The theoretical deflections were computed for each load step after setting $M_{cr}=M_{cr,exp}$ and $E_c=E_{c,the}$, according to equation (4.3), and comparing the results with the corresponding experimental deflections already measured.

The same procedure already explained for the first two cases was followed, computing e_1 and e_2 for each specimen tested, as reported in Table 8:

Table 8 - Standard Error (e_1) & Mean Error (e_2) [$M_{cr,exp}$, $E_{c,the}$]

Author	*Standard Error (e_1)*	*Mean Error (e_2)*
Pecce et al. (2000)	0,144	-0,133
	0,214	-0,199
	0,165	-0,150
Toutanji & Deng (2003)	0,230	-0,191
	0,276	-0,182
	0,095	-0,006
Theriault & Benmokrane (1998)	0,155	-0,071
	0,344	-0,298
	0,100	-0,076
	0,103	-0,067
	0,194	-0,013
	0,381	-0,358
	0,085	-0,056
	0,416	-0,399
El-Salakawy & Benmokrane (2004)	0,251	-0,245
	0,304	-0,301
	0,242	-0,230
	0,157	-0,135
	0,293	-0,286
	0,314	-0,311
	0,281	-0,279
	0,288	-0,288
Laoubi et al. (2006)	0,218	0,124
	0,202	0,069
	0,083	-0,031
	0,151	0,097
	0,233	-0,144
	0,201	0,070
	0,176	-0,170
	0,151	0,068
	0,111	0,005
Al-Sunna et al. (2006)	0,251	-0,072
	0,229	-0,198
	0,201	-0,199

Author	*Standard Error (e_1)*	*Mean Error (e_2)*
Benmokrane et al. (1996)	0,289	0,230
	0,066	0,040
	0,350	-0,340
Alsayed (1997)	0,362	-0,355
	0,248	-0,245
	0,388	-0,384
Masmoudi et al. (1998)	0,177	0,027
	0,212	0,011
	0,227	-0,188
	0,143	-0,127
	0,220	-0,206
	0,142	-0,054
	0,211	-0,200
Rafi et al. (2006)	0,210	-0,162
	0,258	-0,152
Yost et al. (2003)	0,342	0,315
	0,094	0,057
	0,360	0,352
	0,788	0,610
	0,622	0,484
	0,477	0,396
	0,286	0,240
	0,495	0,470
	0,231	0,156
	0,148	0,121
	0,155	-0,051
	0,139	0,058
	0,190	-0,172
	0,235	0,134
	0,465	0,255
Alsayed & Almusallam(1995)	0,310	-0,308
	0,274	-0,272

Average e_1	*Average e_2*
0,248	**-0,059**

The bond coefficient corresponding to the minimum value e_1=0.248 is m=0.720.

Case 3) can be considered intermediate between cases 1) and 2), its average standard error e_1 being higher than e_1 of case 1), but lower than e_1 of case 3), yet quite reliable as it resulted for case 1).

As for case 1) and 2), the following quantities were plotted as shown in Figure 5:

$$\left[\left(\frac{M_{cr,\exp}}{M_a}\right)^{m=\text{var}},\left(\frac{M_{cr,\exp}}{M_a}\right)\right];\left[\left(\frac{M_{cr,\exp}}{M_a}\right)^{0.72},\left(\frac{M_{cr,\exp}}{M_a}\right)\right];\left[\left(\frac{M_{cr,\exp}}{M_a}\right)^{2},\left(\frac{M_{cr,\exp}}{M_a}\right)\right]$$

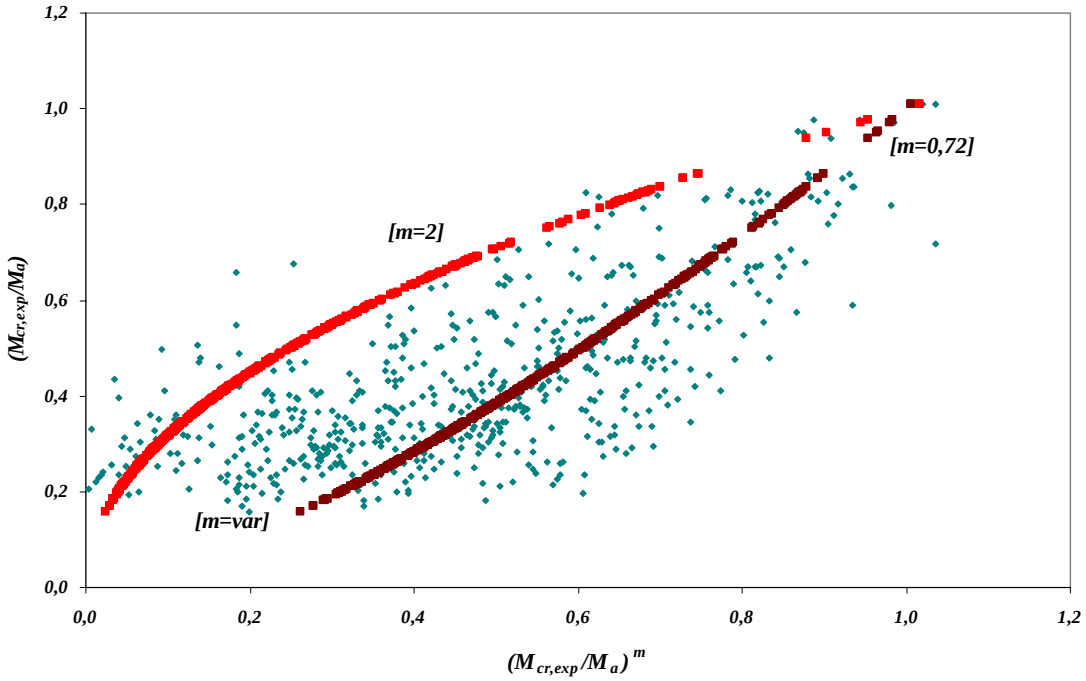

Figure 5 - $(M_{cr}/M_a)^m$ vs (M_{cr}/M_a) $[M_{cr,exp};E_{c,the}]$

Figure 5 confirms the results reported in Table 8: the brown line corresponding to m=0.79 approximates the points with m=var. better than line with m=2, confirming that the red line is not enough reliable.

4.5 CONCLUSIVE REMARKS

Figure 6 shows the three lines obtained for the three values of m derived, compared to the red line relating m=2:

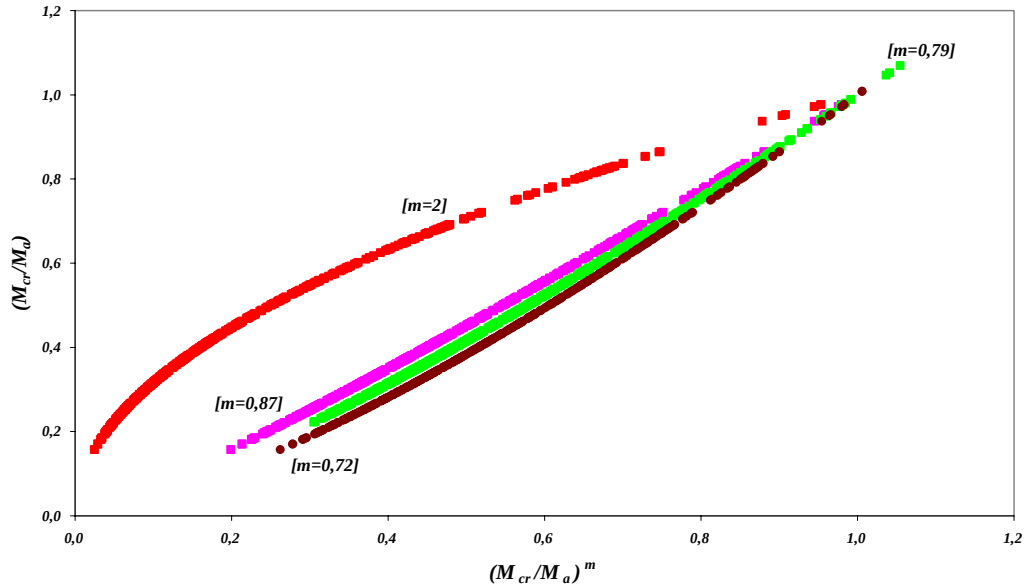

Figure 6 - Comparison of Results

It can be observed that the three lines corresponding to the three cases considered are very close and have concave trend, being m<1, converse to the trend of *m*=2 line. From the comparison of the four lines with respect to the points obtained setting *m*=var., it can be concluded that the bond coefficient *m*=2 in equation (4.3) should be replaced by a value lower than unity.

As for the three cases analyzed, Table 9 shows a summary of the results obtained:

Table 9 - Summary of Results

Case:	e_1	e_2	***m***
1) $M_{cr,exp}$; $E_{c,exp}$	0,212	-0,062	0,87
2) $M_{cr,the}$; $E_{c,exp}$	0,318	-0,205	0,79
3) $M_{cr,exp}$; $E_{c,the}$	0,248	-0,059	0,72

The first value m_1=0.87 corresponds to the minimum value of the average standard error e_1 with a sufficient level of safety ($e_2 \approx 0$): this confirms that considering the experimental values of the cracking moment and of the modulus of elasticity of concrete instead of the theoretical values brings to more reliable predictions. Therefore the value *m*=0.87 to use as bond coefficient when computing deflections of FRP RC elements in equation (4.3) of CNR-DT 203/2006 is the one proposed.

Of the two other cases considered, case 3) where the theoretical value of E_c replaced the experimental value, resulted to give better predictions than case 2), where the theoretical value of M_{cr} was used instead of the corresponding experimental value. The investigation of available data collected allowed concluding that computing the cracking moment (rather than accounting for its experimental value) penalizes the reliability and the safety of deflection calculations more than considering $E_{c,the}$ instead of $E_{c,exp}$.

Nevertheless, the values of m derived in case 2) and in case 3) do not differ from the value of case 1) considerably, with a maximum variation of 17% of m_3 with respect to m_1. Hence, considering the theoretical aforementioned values rather than the corresponding experimental quantities does not penalize the reliability of results considerably.

Chapter V
SHEAR ULTIMATE BEHAVIOR

5.1 INTRODUCTION

The present chapter focuses on the assessment of Eurocode-like design equations for the evaluation of the shear strength of FRP RC members, as proposed by the CNR-DT 203 (2006). Both the concrete and the FRP stirrups contributions to shear are taken into account: the new equations derived with reference to Eurocode equations for shear of steel RC members are verified through comparison with the equations given by ACI, CSA and JSCE guidelines, considering a large database of members with and without shear reinforcement failed in shear.

5.2 LITERATURE REVIEW

Most of the current design provisions which have been developed for the design of FRP-reinforced concrete members follow the approach of conventional reinforced concrete design methods, using the well-known $V_c + V_s$ format to compute the shear resistance of RC members, although the specific manners in which they derive the contribution of concrete V_c may differ considerably, whereas the steel contribution V_s is determined similarly.

For steel-RC members, the Joint ASCE-ACI Committee 445 (ASCE-ACI, 1998) assessed that the quantity V_c can be considered as a combination of five mechanisms activated after the formation of diagonal cracks:

1. shear stresses in uncracked compressed concrete;
2. aggregate interlock;
3. dowel action of the longitudinal reinforcing bars;
4. arch action; and
5. residual tensile stresses transmitted directly across the cracks.

All of these mechanisms provided by conventional steel RC elements are expected to be affected when using FRP reinforcement due to larger strains that are generally mobilized in the latter. They are discussed in turn in the following.

The contribution of the uncracked concrete in RC members depends mainly on the concrete strength, $f_c^{'}$, and on the depth of the uncracked zone, which is function of the longitudinal reinforcement properties. In steel RC elements the neutral axis depth decreases rapidly during yielding, thus reducing the area of concrete in compression, whereas in FRP RC members the area of concrete under compression is considerably smaller than that developed in similar steel RC sections already at relatively low load levels. As the strain in the bars increases, however, the compression area does not decrease further as is the case for steel (Zhao et al., 1997a, 1997b).

The aggregate mechanical interlock allows the shear transfer across a crack in the tensile zone; its magnitude is estimated to range between 33% and 50% of the shear capacity of uncracked concrete (Taylor, 1970), although these percentages reduce when the crack width increases (Walraven, 1981); the aggregate interlock is function of:

- the crack roughness, which depends on the maximum aggregate size;
- the crack width, which depends on the reinforcement stiffness; and
- the concrete strength.

Higher strain values and a smaller reinforcement ratio required to sustain a given load in FRP with respect to steel, together with a lower stiffness, reduce the total stiffness of the element and thus larger deflections and wider cracks are attained; a smaller amount of shear force is therefore expected to be carried by aggregate interlock in FRP reinforced members.

The dowel action refers to the shear force resisting transverse displacement between two parts of a structural element split by a crack that is bridged by the reinforcement; therefore dowel contribution strongly depends on the transverse stiffness and strength of the reinforcement (Razaqpur and Isgor, 2006). Experimental tests carried out by Tottori and Wakui (1993) show that the dowel capacity of members using FRP reinforcement is about 70% of those using reinforcing steel; it has been suggested (Kotsovos and Pavlovic, 1999) that the load carried by dowel action of the reinforcement across a crack is negligible in steel-reinforced elements; with FRP reinforcement, which has a low transverse stiffness and strength, an even smaller load will be carried by dowel action (Kanematsu et al., 1993). Hence, when FRP

reinforcement is used as flexural reinforcement the dowel contribution can be neglected (Kanakubo and Shindo, 1997).

The arch action occurs in the uncracked concrete near the end of elements where the shear span to depth ratio (a/d ratio) is less than 2.5 (ASCE-ACI, 1998). The shift in the resistance mechanism from the so-called beam action to the arch action can substantially increase the shear resistance of a member because shear resistance by arch action is dependent on the effective compressive strength rather than the shear strength of concrete and on the strength and proper anchorage of the longitudinal reinforcement. With proper anchorage, the FRP reinforcement can resist high tensile forces and can serve as tie for the arch; therefore, the arch mechanism may substantially contribute to the shear resistance of FRP-reinforced members (Razaqpur and Isgor, 2006).

The residual tension in cracked concrete has been found to be present for crack widths smaller than 0.15 mm (ASCE-ACI, 1998); since generally wider cracks are observed in FRP RC members, this contribution to the shear resistance can be neglected.

Therefore, it is critical that an accurate assessment of concrete contribution to the shear strength of members reinforced with FRP bars as flexural reinforcement, V_c, is performed.

Test results have shown that the shear strength of FRP RC beams is significantly lower than that predicted using equations developed for steel reinforcement (Goodspeed et al., 1990; Yost, 1993); therefore, it is definitely recognized that existing shear strength equations related to steel-RC members should be modified to be suitable for FRP-RC members, accounting for the different mechanical properties of FRP compared to steel reinforcement.

This is the approach taken herein to extend the equation given by Eurocode 2 (1992) for the shear capacity of steel RC members to the case of FRP RC members. A modified formula accounting for the concrete contribution to shear capacity of FRP RC elements has been derived; this expression has been included in the lately issued guidelines of the Italian Research Council CNR-DT 203 (2006).

The equation reported by Eurocode 2 (1992) accounting for the concrete contribution to shear was taken into account rather than that proposed in the last version of Eurocode 2 (2004), being the 1992 equation included in several national codes and widely used by designers, therefore the Eurocode 2 (1992) approach was deemed more suitable to let professionals becoming accustomed to the new design guidelines.

As for the shear reinforcement, its role can be summarized as follows (Stratford and Burgoyne, 2003):

- enabling the transfer of tensile actions across inclined shear cracks;
- confining the compression-zone concrete, thus increasing the shear-capacity;
- enclosing the flexural reinforcement, thus preventing dowel-splitting of the concrete and promoting the dowel-rupture of FRP reinforcement.

The contribution of the shear reinforcement to the shear capacity depends on the maximum stress that the reinforcement can attain. In the case of steel reinforcement it is assumed that steel overcomes the yielding strain and then the maximum stress (yielding stress) can be evaluated without exact assessment of the maximum strain; in the case of FRP transverse reinforcement, which is linear elastic up to failure, it is important to define the maximum strain in order to assess the stress in FRP transverse reinforcement. Furthermore, FRP reinforcement needs large strains to develop its full tensile strength, but in the bent zones such strength cannot be attained due to its anisotropic properties: the strength reduction is attributed to the residual stress concentration, hence minimum values for the bend radius are recommended by all the existing provisions. Increasing tendency of shear force carried by shear reinforcement after diagonal cracks seems to be predictable by the truss analogy (Tottori and Wakui, 1993) as shown in the equations reported by the main design provisions; however, technical question marks exist over its applicability (Stratford and Burgoyne, 2002). The same approach has been adopted herein to derive an equation accounting for the contribution of the FRP shear reinforcement to shear capacity of FRP RC elements; this expression has also been included in the CNR-DT 203 (2006).

5.3 REVIEW OF CURRENT DESIGN PROVISIONS

The present paragraph deals with the most frequent serviceability limit states, and particularly those relating to:

Findings from experimental investigations on concrete members longitudinally reinforced with carbon (C) and glass (G) FRP bars and with no shear reinforcement show that the shear strength reduction experienced by such elements when compared to those reinforced with the same amount of steel reinforcement is mainly due to the lower modulus of elasticity. Such investigations also reveal that the axial stiffness of the reinforcing bars is a key parameter when evaluating the concrete shear strength of flexural members reinforced with FRP bars. Most of the current international design provisions developed methods to compute V_c that are based on these findings.

As for the shear reinforcement, the main code proposals for FRP reinforcement assume an effective stirrup strain for use in the truss analogy (Guadagnini et al., 1999). The original intention of the "allowable strain" concept (Clarke and O' Regan, 1995) was to limit the stirrup strain so that the crack width at failure was similar to that in steel-reinforced concrete, thus allowing the full "concrete contribution" to be developed (Stratford and Burgoyne, 2003).

This section summarizes the design equations to compute both V_c and V_f as recommended by the American Concrete Institute (ACI 440.1R-06, 2006), by the Canadian Standard Association (CAN/CSA-S806_02, 2002), and by the Japanese Society of Civil Engineers (JSCE, 1997).

5.3.1 ACI 440.1R-06 Design Guidelines

The ACI 440.1R bases the design of cross sections subject to shear on the same approach used by the ACI 318-02 (ACI 318, 2002): $\phi V_n \geq V_u$, where ϕ is the strength safety factor, V_u is the factored shear force at the section considered, and V_n is the nominal shear strength, computed as the sum of the shear resistance provided by concrete, V_c, and the FRP shear reinforcement, V_f.

As for the computation of V_c, a new design method was proposed by Tureyen and Frosh (2002) and adopted by the ACI 440.1R-06 (2006); according to this method V_c can be evaluated as follows:

$$V_c = \frac{2}{5} k \sqrt{f_c'} b_w d \,, \tag{5.1}$$

where $k = \sqrt{2\rho_f n_f + (\rho_f n_f)^2} - \rho_f n_f$, ρ_f being the flexural FRP reinforcement ratio, and $n_f = E_f / E_c$, where E_f and E_c are the modulus of elasticity of FRP reinforcement and concrete, respectively; f'_c is the specified compressive strength of concrete; b_w is the web width; and d is the distance from the compression fiber to the centroid of the main tensile reinforcement.

Eq. (5.1) accounts for the axial stiffness of the FRP reinforcement through the neutral axis depth, $c = kd$, which is a function of the reinforcement ratio, ρ_f, and the modular ratio, n_f. This equation has been shown to provide a reasonable factor of safety for FRP reinforced specimens across the range of reinforcement ratios and concrete strengths tested to-date (Tureyen and Frosch, 2003). Eq. (5.1) may be rewritten in the following way:

$$V_c = \frac{12}{5} k \frac{1}{6} \sqrt{f_c'} b_w d \,. \tag{5.2}$$

This form of the equation indicates that eq. (5.1) is simply the ACI 318 (2002) shear equation for steel reinforcement, modified by the factor $12/5k$ which accounts for the axial stiffness of the FRP reinforcement (ACI 440.1R-06, 2006).

The ACI 318, 2002 method used to calculate the shear contribution of steel stirrups is applied also when using FRP as shear reinforcement. The shear resistance provided by FRP stirrups perpendicular to the axis of the member, V_f, is derived as follows:

$$V_f = \frac{A_{fv} f_{fv} d}{s}, \tag{5.3}$$

where A_{fv} is the amount of FRP shear reinforcement within stirrups spacing s, f_{fv} is the tensile strength of FRP for shear design, taken as the smallest of the design tensile strength f_{fd}, the stress corresponding to $0.004E_f$, or the strength of the bent portion of the FRP stirrups f_{fb}, computed as:

$$f_{fb} = \left(0,05\frac{r_b}{d_b} + 0,30 \right) f_{fd}, \quad (5.4)$$

where r_b and d_b are the internal radius and the equivalent diameter of bent bar, respectively.

As it is for equation given for V_f in ACI 318 (2002), eq. (5.3) is based on a modified truss analogy. The truss analogy assumes that the total shear is carried by the shear reinforcement. Yet, according to findings on both non-prestressed and prestressed members it is now recognized that the shear reinforcement needs to be designed to carry only the shear exceeding that which causes inclined cracking, provided that the diagonal members in the truss are assumed to be inclined at 45 deg (ACI 318R-02, 2002).

5.3.2 CAN/CSA-S806_02 Design Guidelines

The traditional $V_c + V_f$ philosophy is also used by the Canadian Standard Association (CSA S806-02, 2002). Two cases are identified therein:

- members longitudinally reinforced with FRP using steel stirrups; and
- members with longitudinal and transverse FRP reinforcement.

Only the latter case will be discussed herein. The CSA S806-02 gives the following expression to compute V_c, for sections having either the minimum amount of transverse reinforcement required or $d < 300mm$:

$$V_c = 0.035\lambda\phi_c \left(f_c' \rho_f E_f \frac{V}{M} d \right)^{\frac{1}{3}} b_w d, \quad (5.5)$$

where λ accounts for concrete density (set equal to 1 herein); ϕ_c is the resistance factor for concrete; V and M are the factored shear force and moment at the section

of interest, such that $\frac{V}{M}d \le 1.0$; moreover, V_c needs not be taken as less than $0.1\lambda\phi_c\sqrt{f_c'}b_w d$ nor shall it exceed $0.2\lambda\phi_c\sqrt{f_c'}b_w d$.

The computation of V_c slightly differs from the approach followed by the Canadian guidelines for steel, CSA A23.3-94 (1994), where:

$$V_{c,s} = 0.2\lambda\phi_c\sqrt{f_c'}b_w d\ . \tag{5.6}$$

Thus, according to the Canadian approach, the contribution of concrete to the shear resistance when using steel is an upper bound for V_c.

For sections with $d > 300mm$ and with no transverse shear reinforcement or less than the minimum amount required, V_c is calculated using:

$$V_c = \left(\frac{130}{1000+d}\right)\lambda\phi_c\sqrt{f_c'}b_w d \ge 0.08\,\lambda\phi_c\sqrt{f_c'}b_w d\ . \tag{5.7}$$

The latter equation is derived from the corresponding formula given for steel reinforced sections multiplied by 0.5; this coefficient replaces the term $\sqrt{E_f/E_s}$ (E_s being the modulus of elasticity of the steel reinforcement), when considering $E_f = 50$ GPa and $E_s = 200$ GPa. Therefore, eq. (5.7) represents the lower bound for concrete contribution to the shear strength of FRP reinforced concrete members regardless of the type of reinforcing bars (El-Sayed et al., 2006).

For members with FRP flexural and shear reinforcement, the value of V_f shall be calculated as:

$$V_f = \frac{0.4\phi_f A_{fv} f_{fu} d}{s}, \tag{5.8}$$

where ϕ_f is the resistance factor for FRP reinforcement equal to 0.75, and f_{fu} is the characteristic strength of FRP shear reinforcement.

5.3.3 JSCE Design Guidelines

According to the Japan Society of Civil Engineers recommendations for design and construction of concrete structures using continuous fiber reinforcing materials (JSCE, 1997), the design shear capacity of FRP RC elements can be computed adopting the same principles as for the design of steel RC, using the equation $V_{ud} = V_{c,f} + V_f$, where:

$$V_{c,f} = \beta_d \beta_p \beta_n f_{vcd} b_w d / \gamma_b , \tag{5.9}$$

where:

$\beta_d = \sqrt[4]{1/d} \le 1.5$; $\beta_p = \sqrt[3]{100 \rho_f E_f / E_s} \le 1.5$; $\beta_n = 1$ in this study where no axial forces are taken into account; $f_{vcd} = 0.2\sqrt[3]{f_c^{'}/\gamma_c} \le 0.72 N/mm^2$, γ_c being the concrete safety factor, set equal to 1.3 when $f_c^{'} < 50 N/mm^2$, if not $\gamma_c = 1.5$; γ_b is a member factor generally set equal to 1.3 at the ULS.

The design shear capacity given by shear reinforcement shall be computed as:

$$V_f = \frac{A_{fv} E_{fw} \varepsilon_{fw}}{s} z \Big/ \gamma_b \tag{5.10}$$

where E_{fw} is the modulus of elasticity of shear reinforcement, $z = d/1.15$, γ_b is the member factor generally set equal to 1.15 at the ULS, and ε_{fw} is the design value of shear reinforcement strain in ULS, obtained from:

$$\sqrt{\left(\frac{h}{0.3}\right)^{-1/10} \frac{f_c^{'}}{\gamma_c} \frac{\rho_f E_f}{\rho_{fw} E_{fw}}} \cdot 10^{-4} , \tag{5.11}$$

where h is the member depth, ρ_{fw} is the reinforcement ratio of shear reinforcement ($\rho_{fw} = A_{fv}/b_w s$).

When $E_{fw}\varepsilon_{fw}$ is greater than f_{fbd}, defined as the design value for the strength of the stirrup bent portion (equal to $f_{fbd} = f_{fb}/\gamma_{mfb}$, f_{fb} being defined in eq. (5.4) and γ_{mfb} generally set as 1.3), f_{fbd} is substituted for $E_{fw}\varepsilon_{fw}$.

Eq. (5.10) is equivalent to the corresponding Japanese equation for steel RC after taking into account the different nature of the reinforcement by substituting the yield stress of steel with the product $E_{fw}\varepsilon_{fw}$.

5.3.4 Italian Guidelines

In compliance with the Eurocode 2 approach (Eurocode 2, 1992), the CNR-DT 203 (2006) distinguishes two different cases for shear, namely for members not requiring and requiring shear reinforcement.

In the former case, at ULS the design shear strength of a member reinforced with longitudinal FRP reinforcement can be evaluated as the minimum of the design shear resistance provided by concrete, $V_{Rd,ct}$, and the design value of the maximum shear force which can be sustained by the member before crushing of the compression strut, $V_{Rd,max}$.

As for the derivation of $V_{Rd,ct}$, the new formula presented is a modified version of the Eurocode 2 shear equation recommended for conventional steel RC members, which is (disregarding the axial forces term):

$$V_{Rd,c} = \tau_{Rd} k_d \left(1.2 + 40\rho_s\right) b_w d\,, \tag{5.12}$$

where $V_{Rd,c}$ is the design shear resistance provided by concrete when longitudinal steel reinforcement is used; τ_{Rd} is the design shear stress per unit area, defined as $0.25 f_{ctk0.05}/\gamma_c$, $f_{ctk0.05}$ being the characteristic tensile strength of concrete (5% fractile); γ_c is the strength safety factor for concrete (γ_c = 1.6); k_d is a factor taken equal to 1 in members where more than 50 % of the bottom reinforcement is interrupted; if not, it will be $k_d = (1.6 - d) \geq 1$ (with d in meters); ρ_s is the geometrical percentage of longitudinal reinforcement and cannot exceed the value 0.02.

A calibration has been conducted by the CNR DT 203 Task Group in order to modify eq. (5.12) and extend it to FRP RC members; the following expression for $V_{\mathrm{Rd,ct}}$ has been proposed:

$$V_{\mathrm{Rd,ct}} = 1.3\left(\frac{E_{\mathrm{f}}}{E_{\mathrm{s}}}\right)^{1/2} V_{\mathrm{Rd,c}}, \tag{5.13}$$

where ρ_{f} replaces ρ_{s} and can not be less than 0.01 nor exceed 0.02; moreover the limitation $1.3\cdot\left(E_{\mathrm{f}}/E_{\mathrm{s}}\right)^{1/2} \le 1$ shall be satisfied; the coefficient 1.3 was determined after the comparison with experimental data reported in the following section.

The rationale behind the above formula was based on the objective of developing a reliable and simple equation having a structure which practitioners are familiar with. Once a full comprehension will be reached about how much the different mechanisms change their contribution compared to the case of steel reinforcement, then it will be appropriate to propose an updated equation in which weighted safety factors are specifically applied to each term of equation (5.12). The assessment analysis of eq. (5.13) is reported in the following section.

When considering members requiring shear reinforcement, the ultimate design shear strength of a member reinforced with longitudinal FRP reinforcement and FRP stirrups can be evaluated as the minimum between $V_{\mathrm{Rd,ct}} + V_{\mathrm{Rd,f}}$ and $V_{\mathrm{Rd,max}}$, where $V_{\mathrm{Rd,ct}}$ and $V_{\mathrm{Rd,max}}$ are the same quantities introduced before, and $V_{\mathrm{Rd,f}}$ is the contribution of FRP stirrups, computed in compliance with the truss analogy as:

$$V_{\mathrm{Rd,f}} = \frac{A_{\mathrm{fv}}\, f_{\mathrm{fr}}\, d}{s}, \tag{5.14}$$

where f_{fr} is the so-called reduced tensile strength of FRP for shear design, defined as $f_{\mathrm{fd}}/\gamma_{\mathrm{f},\Phi}$, f_{fd} being the design tensile strength of FRP reinforcement, computed dividing the characteristic value by the strength safety factor for FRP ($\gamma_{\mathrm{f}} = 1.5$), and $\gamma_{\mathrm{f},\Phi}$ being the partial factor which further reduces the design tensile strength of FRP reinforcement to account for the bending effect; $\gamma_{\mathrm{f},\Phi}$ shall be set equal to:

- 2 when no specific experimental tests are performed, provided that the bend radius is not less than six times the equivalent diameter, d_b;
- the ratio of the straight FRP bar strength to the bent FRP portion design strength, in all other cases.

Similarly to ACI eq. (5.3), CSA eq. (5.8), and JSCE eq. (5.10), eq. (5.14) depends on the amount of FRP shear reinforcement, on the distance from the compression fiber to the centroid of the main tensile reinforcement, on the stirrups spacing and on the design tensile strength of the FRP shear reinforcement. A comparison of the four formulations is reported hereafter.

5.4 COMPARISON BETWEEN EXPERIMENTAL RESULTS AND CODES PREDICTIONS

5.4.1 Members Without Shear Reinforcement

In order to verify equation (5.13), a database composed of test results related to 88 tested beams and one way slabs without FRP stirrups (Nagasaka et al., 1993, Tottori and Wakui, 1993, Nakamura & Higai, 1995, Zhao et al., 1995, Vijay et al., 1996, Mizukawa et al., 1997, Duranovic et al., 1997, Swamy & Aburawi, 1997, Deitz et al., 1999, Yost et al., 2001, Alkhajardi et al., 2001, Tureyen & Frosh, 2002, Tariq & Newhook, 2003, Lubell et al., 2004, Razaqpur et al., 2004, El-Sayed et al., 2005, El-Sayed et al., 2006) was used for comparisons, as given in Table 1; test results where premature failure occurred were disregarded (Michaluk et al., 1998).

Six specimens were reinforced with aramid FRP bars, 32 specimens reinforced with carbon FRP, and 50 specimens reinforced using glass FRP bars. All specimens failed in shear. The concrete compressive strength, f_c', ranged between 22.7 and 50.0 MPa (specimens with $f_c' > 50\text{MPa}$ were neglected not being typical of FRP RC members). The reinforcement ratio of tensile FRP bars, ρ_f, ranged between 0.0025 and 0.03; however, since CNR-DT 203 prescribes a minimum ρ_f equal to 0.01 for members that do not require shear reinforcement, experimental points below this threshold (dashed line in Figure 1 and Figure 2) were not considered for the sake of

the comparison. The effective depth, d, ranged between 150 and 970 mm, and the shear span to depth ratio, a/d, ranged between 1.78 and 6.50.

Table 1 - Database for FRP RC Members Without Shear Reinforcement

Reference	f'_c [MPa]	b_w [mm]	d [mm]	ρ_f	E_f [GPa]	*Type*	V_{exp} [kN]
Nagasaka et al. '93	34,1	250	265	0,019	56	AFRP	**113**
	22,9	250	265	0,019	56	AFRP	**83**
Tottori and Wakui '93	44,6	200	325	0,007	137	CFRP	**98**
	44,5	200	325	0,007	137	CFRP	**123**
	45,0	200	325	0,007	137	CFRP	**118**
	46,9	200	325	0,009	192	CFRP	**147**
	46,9	200	325	0,009	192	CFRP	**93**
	46,9	200	325	0,009	192	CFRP	**78**
	46,9	200	325	0,009	58	CFRP	**152**
	46,9	200	325	0,009	58	CFRP	**62**
	46,9	200	325	0,009	58	CFRP	**47**
Nakamura & Higai '95	22,7	300	150	0,013	29	GFRP	**33**
	27,8	300	150	0,018	29	GFRP	**36**
Zhao et al '95	34,3	150	250	0,015	105	CFRP	**45**
	34,3	150	250	0,030	105	CFRP	**46**
	34,3	150	250	0,023	105	CFRP	**41**
Vijay et al. '96	44,8	150	265	0,014	54	GFRP	**45**
	31	150	265	0,006	54	GFRP	**45**
Mizukawa et al. '97	34,7	200	260	0,013	130	CFRP	**62**
Duranovic et al. '97	38,1	150	210	0,013	45	AFRP	**26**
	32,9	150	210	0,013	45	AFRP	**22**
Swamy & Aburawi '97	34,0	254	222	0,016	34	GFRP	**39**
Deitz et al. '99	28,6	305	158	0,007	40	GFRP	**27**
	30,1	305	158	0,007	40	GFRP	**28**
	27	305	158	0,007	40	GFRP	**29**
	28,2	305	158	0,007	40	GFRP	**29**
	30,8	305	158	0,007	40	GFRP	**28**
Yost et al. '01	36,3	229	225	0,011	40	GFRP	**39**
	36,3	229	225	0,011	40	GFRP	**39**
	36,3	229	225	0,011	40	GFRP	**37**
	36,3	178	225	0,014	40	GFRP	**28**
	36,3	178	225	0,014	40	GFRP	**35**
	36,3	178	225	0,014	40	GFRP	**32**
	36,3	229	225	0,017	40	GFRP	**40**
	36,3	229	225	0,017	40	GFRP	**49**
	36,3	229	225	0,017	40	GFRP	**45**
	36,3	279	225	0,018	40	GFRP	**44**
	36,3	279	225	0,018	40	GFRP	**46**
	36,3	279	225	0,018	40	GFRP	**46**
	36,3	254	224	0,021	40	GFRP	**38**
	36,3	254	224	0,021	40	GFRP	**51**
	36,3	254	224	0,021	40	GFRP	**47**
	36,3	229	224	0,023	40	GFRP	**44**
	36,3	229	224	0,023	40	GFRP	**42**
	36,3	229	224	0,023	40	GFRP	**41**

Reference	f'_c [MPa]	b_w [mm]	d [mm]	ρ_f	E_f [GPa]	*Type*	V_{exp} [kN]
Alkhajardi et al. '01	24,1	178	279	0,023	40	GFRP	**53**
	24,1	178	287	0,008	40	GFRP	**36**
	24,1	178	287	0,013	40	GFRP	**40**
Tureyen & Frosh '02	39,7	457	360	0,010	41	GFRP	**108**
	39,9	457	360	0,010	38	GFRP	**95**
	40,3	457	360	0,010	47	AFRP	**115**
	42,3	457	360	0,019	41	GFRP	**137**
	42,5	457	360	0,019	38	GFRP	**153**
	42,6	457	360	0,019	47	AFRP	**177**
Tariq & Newhook '03	37,3	160	346	0,007	42	GFRP	**55**
	37,3	160	346	0,007	42	GFRP	**64**
	43,2	160	346	0,011	42	GFRP	**43**
	43,2	160	346	0,011	42	GFRP	**46**
	34,1	160	325	0,015	42	GFRP	**49**
	34,1	160	325	0,015	42	GFRP	**45**
	37,3	130	310	0,007	120	CFRP	**49**
	37,3	130	310	0,007	120	CFRP	**46**
	43,2	130	310	0,011	120	CFRP	**48**
	43,2	130	310	0,011	120	CFRP	**53**
	34,1	130	310	0,015	120	CFRP	**56**
	34,1	130	310	0,015	120	CFRP	**58**
Lubell et al. '04	40,0	450	970	0,005	40	GFRP	**136**
Razaqpur et al. '04	40,5	200	225	0,003	145	CFRP	**36**
	49,0	200	225	0,005	145	CFRP	**47**
	40,5	200	225	0,006	145	CFRP	**47**
	40,5	200	225	0,009	145	CFRP	**43**
	40,5	200	225	0,005	145	CFRP	**96**
	40,5	200	225	0,005	145	CFRP	**47**
	40,5	200	225	0,005	145	CFRP	**38**
El-Sayed et al. '05	40,0	1000	165	0,004	114	CFRP	**140**
	40,0	1000	165	0,008	114	CFRP	**167**
	40,0	1000	161	0,012	114	CFRP	**190**
	40,0	1000	162	0,009	40	GFRP	**113**
	40,0	1000	159	0,017	40	GFRP	**142**
	40,0	1000	162	0,017	40	GFRP	**163**
	40,0	1000	159	0,024	40	GFRP	**163**
	40,0	1000	154	0,026	40	GFRP	**168**
El-Sayed et al. '06	50,0	250	326	0,009	130	CFRP	**78**
	50,0	250	326	0,009	40	GFRP	**71**
	44,6	250	326	0,012	130	CFRP	**104**
	44,6	250	326	0,012	40	GFRP	**60**
	43,6	250	326	0,017	130	CFRP	**125**
	43,6	250	326	0,017	40	GFRP	**78**

The predictions from equation (5.13) were compared with the values derived using equations (5.1), (5.7) and (5.9). Table 2 reports the mean, the standard deviation and the coefficient of variation relating the ratio of the shear resistance attained experimentally, V_{exp}, to the corresponding analytical value derived according to each of the four considered guidelines, V_{pred}, both with and without safety factors. It can be seen that the CNR-DT 203 equation has the least mean values of both V_{exp}/V_{pred} (i.e., 1.05, w/o safety factor) and coefficient of variation (i.e., 29 %).

Table 2 - Comparison of Eq. (5.13) with Major Design Provisions

	V_{exp} / V_{pred}							
	CNR DT 203		*ACI 440.1R*		*CSA S806*		*JSCE*	
	w/o Saf. Fact.	w/ Saf. Fact.	w/o Saf. Fact.	w/ Saf. Fact.	w/o Saf. Fact.	w/ Saf. Fact.	w/o Saf. Fact.	w/ Saf. Fact.
Mean	**1,05**	**1,69**	**2,02**	**2,69**	**1,50**	**2,51**	**1,51**	**2,14**
St. Dev.	**0,31**	**0,49**	**0,61**	**0,82**	**0,51**	**0,86**	**0,48**	**0,68**
Coeff. of Var.	**29%**		**30%**		**34%**		**32%**	

Figure 1 shows that the trend line of CNR-DT 203 equation is similar to that of CSA S-802 equation, regarded together with the Japanese equation as the most reliable. For the CNR-DT 203 equation when considering the material safety factors all the values V_{exp}/V_{pred} remained greater than unity $\left(\left(V_{exp}/V_{pred}\right)_{ave} = 1.69\right)$, as shown in Figure 2; therefore eq. (5.13) can be deemed adequately conservative as well. Hence, the equation (5.13) is found to be reliable for predicting the concrete contribution to the shear capacity of FRP RC members.

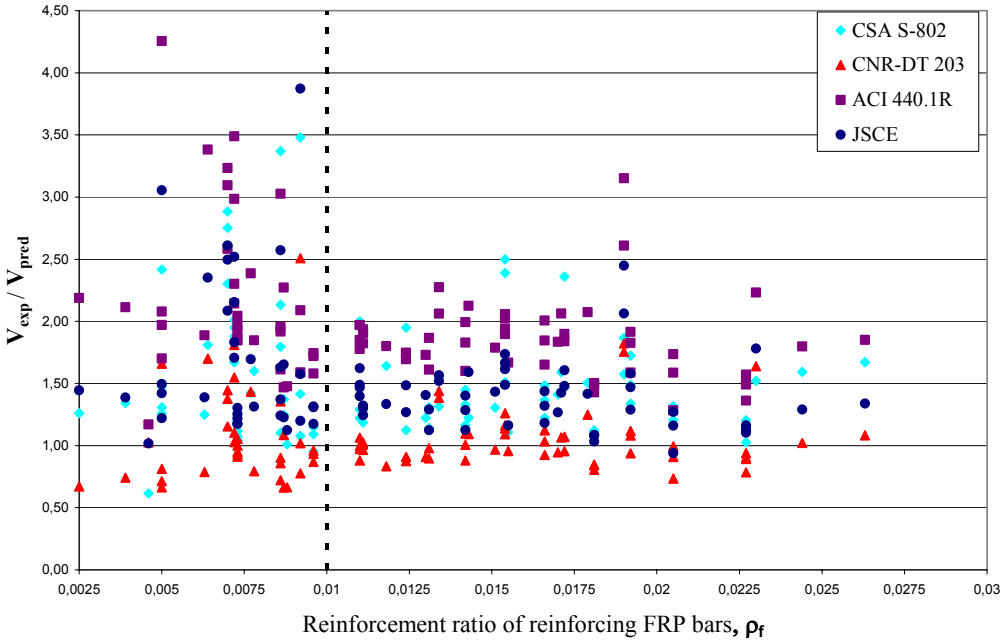

Figure 1 - Comparison of Eq. (5.13) with Major Design Provisions (w/o Saf. Factors)

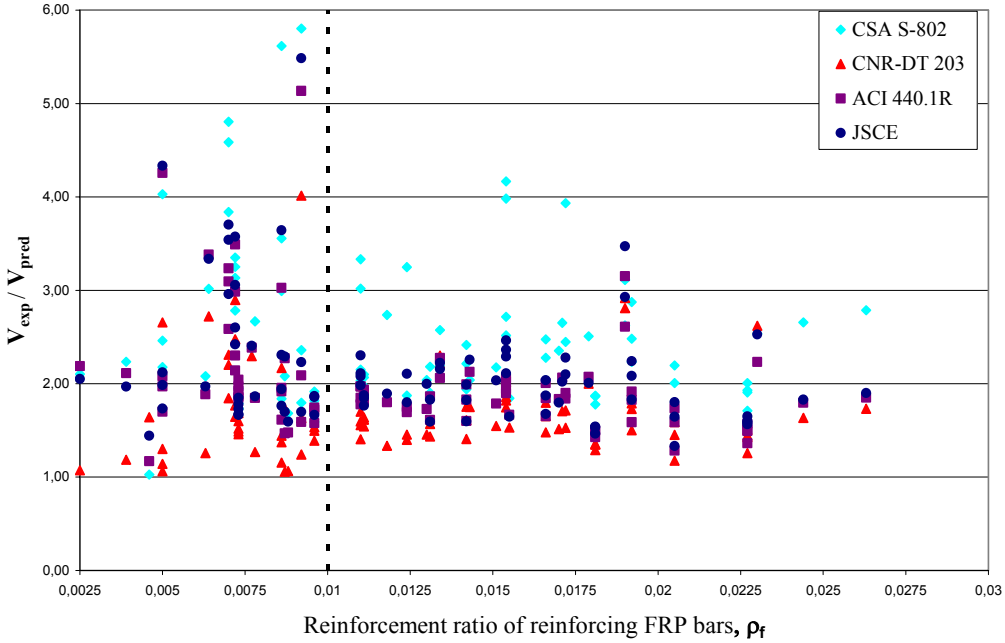

Figure 2 - Comparison of Eq. (5.13) with Major Design Provisions (w/ Saf. Factors)

5.4.2 Members With Shear Reinforcement

In order to verify equation (5.14), a database composed of test results related to 85 tested beams reinforced with FRP stirrups and failed in shear (shear tension, shear compression or flexural shear failure) was collected from experimental programs carried out by Nagasaka et al. (1993), Tottori and Wakui (1993), Maruyama & Zhao (1994, 1996), Nakamura & Higai (1995), Zhao et al. (1995), Vijay et al. (1996), Duranovic et al. (1997), Shehata et al. (1999), Alsayed et al. (1997), and Whitehead & Ibell (2005), as given in Table 3; such database was the basis for comparison of eq. (5.14) with equations (5.3), (5.8) and (5.10), although results reported by Whitehead & Ibell (2005) were not considered for comparison since all specimens had $f_c^{'} > 50\text{MPa}$. Only specimens with both longitudinal and transverse FRP reinforcement were investigated. None of the tested specimens was disregarded depending on the shape of stirrups: specimens having closed loops or helical shaped stirrups made either of bars or square rods were used for comparisons; in some of the beams having helical stirrups the helixes were placed only along the top of beam, in such cases the depth of the helixes rather than the effective depth was used in calculations. Moreover, for beams with circular helixes, according to the relevant researchers the assumption of considering an effective diameter reduced by 30% with

respect to the nominal diameter value was made in order to account for the reduced tie action. In cases where no specifications on the internal radius of stirrups bend, r_b, were provided in the literature source, the minimum value $r_b = 3d_b$ suggested by Ehsani et al. (1995) was considered.

21 specimens were reinforced with aramid FRP stirrups, 37 specimens had carbon FRP stirrups, 23 specimens were reinforced using glass FRP stirrups, and 4 specimens had hybrid (carbon and glass) FRP stirrups. The ultimate tensile strength of FRP shear reinforcement, f_{fu} (corresponding to the characteristic value in both JSCE and CNR-DT 203) ranged between 400 and 2040 MPa (environmental factors assigned by both ACI 440.1R-06, 2006 and CNR-DT 203, 2006 accounting for durability issues in the FRP reinforcement were set equal to the unity); A_{fv} ranged between 9 and 346 mm^2; ρ_{fw} ranged between 0.04 and 1.50 %; d ranged between 100 and 750 mm, and s ranged between 20 and 200 mm. It is underlined that specimens tested by Nagasaka et al. (1993) had a considerably high amount of shear FRP reinforcement (ρ_{fw} =0.5% in 6 specimens, 1.0% in 10 specimens and 1.5% in 8 specimens).

Table 3 - Database for FRP RC Members With Shear Reinforcement

Reference	Geometric data			Concrete	Longitudinal reinforcement			Shear reinforcement			V_{exp}
	b	*d*	*a/d*	f'_c	*Type*	ρ_l	E_l	*Type*	ρ_{fw}	E_f	
	[mm]	[mm]		[MPa]		[%]	[GPa]		[%]	[GPa]	[kN]
Tottori & Wakui '93	200	325	3,2	44,4	CFRP	0,70	137	GFRP	0,15	40	**103**
	200	325	3,2	44,7	CFRP	0,70	137	GFRP	0,15	40	**106**
	200	325	3,2	44,9	CFRP	0,70	137	AFRP	0,07	69	**85**
	200	325	2,2	44,6	CFRP	0,70	137	CFRP	0,07	110	**162**
	200	325	3,2	44,8	CFRP	0,70	137	CFRP	0,07	110	**83**
	200	325	4,3	44,6	CFRP	0,70	137	CFRP	0,07	110	**74**
	200	325	3,2	45,0	CFRP	0,70	137	CFRP	0,04	144	**98**
	200	325	3,2	44,7	CFRP	0,70	140	CFRP	0,06	137	**108**
	200	325	3,2	44,7	CFRP	0,70	140	CFRP	0,10	137	**157**
	200	325	3,2	39,4	CFRP	0,70	140	AFRP	0,12	58	**103**
	200	325	3,2	39,4	AFRP	0,92	58	AFRP	0,09	58	**83**
	200	325	3,2	39,4	AFRP	0,92	58	AFRP	0,13	58	**98**
	200	325	3,2	39,4	AFRP	0,92	58	AFRP	0,23	58	**132**
	200	325	3,2	39,4	AFRP	0,92	58	AFRP	0,12	58	**107**
	200	325	3,2	39,4	AFRP	0,92	58	AFRP	0,12	58	**78**
	200	325	3,2	39,4	AFRP	0,92	58	CFRP	0,04	137	**86**
	150	250	2,5	35,5	CFRP	0,55	94	CFRP	0,12	94	**58**
	150	250	2,5	37,6	CFRP	0,55	94	CFRP	0,24	94	**82**
	150	250	2,5	34,3	CFRP	1,05	94	CFRP	0,12	94	**71**
	150	250	2,5	34,2	CFRP	2,11	94	CFRP	0,12	94	**81**
	300	500	2,5	31,9	CFRP	0,53	94	CFRP	0,06	94	**160**
	150	260	3,1	42,2	AFRP	3,08	63	AFRP	0,13	53	**60**
Nagasaka et al. '93	250	253	1,2	29,5	AFRP	1,90	56	CFRP	0,50	115	**251**
	250	253	1,2	34,7	AFRP	1,90	56	CFRP	1,00	115	**317**
	250	253	1,2	33,5	AFRP	1,90	56	CFRP	1,50	115	**366**
	250	253	1,8	29,5	AFRP	1,90	56	CFRP	0,50	115	**208**
	250	253	1,8	29,5	AFRP	1,90	56	CFRP	1,00	115	**282**
	250	253	1,8	29,5	AFRP	1,90	56	CFRP	1,50	115	**288**
	250	253	2,4	33,5	AFRP	1,90	56	CFRP	0,50	115	**162**
	250	253	2,4	33,5	AFRP	1,90	56	CFRP	1,00	115	**234**
	250	253	1,8	34,1	AFRP	1,90	56	AFRP	0,50	62	**205**
	250	253	1,8	35,4	AFRP	1,90	56	AFRP	1,00	62	**277**
	250	253	1,8	34,1	AFRP	1,90	56	HFRP	0,50	45	**173**
	250	253	1,8	34,1	AFRP	1,90	56	HFRP	1,00	45	**248**
	250	253	1,8	35,4	AFRP	1,90	56	GFRP	0,50	47	**179**
	250	253	1,8	36,7	AFRP	1,90	56	GFRP	1,00	47	**233**
	250	253	1,8	24,0	AFRP	1,90	56	CFRP	1,00	115	**211**
	250	253	1,8	23,0	AFRP	1,90	56	CFRP	1,50	115	**226**
	250	253	2,4	24,8	AFRP	1,90	56	CFRP	1,00	115	**186**
	250	253	2,4	23,4	AFRP	1,90	56	CFRP	1,50	115	**195**
	250	253	1,8	23,0	AFRP	1,90	56	AFRP	1,00	62	**194**
	250	253	1,8	23,0	AFRP	1,90	56	AFRP	1,50	62	**207**
	250	253	1,8	24,0	AFRP	1,90	56	HFRP	1,00	45	**194**
	250	253	1,8	24,0	AFRP	1,90	56	HFRP	1,50	45	**216**
	250	253	1,8	40,3	AFRP	1,90	56	CFRP	1,50	115	**298**
	250	253	2,4	40,0	AFRP	1,90	56	CFRP	1,50	115	**231**
Vijay et al. '96	150	265	1,9	44,8	AFRP	1,43	54	AFRP	0,93	54	**127**
	150	265	1,9	44,8	AFRP	1,43	54	AFRP	0,62	54	**115**
	150	265	1,9	31,0	AFRP	0,64	54	AFRP	0,93	54	**123**
	150	265	1,9	31,0	AFRP	0,64	54	AFRP	0,62	54	**123**
Maruyama & Zhao '94	150	250	2,5	36,2	CFRP	0,55	94	CFRP	0,12	94	**59**
	150	250	2,5	38,3	CFRP	0,55	94	CFRP	0,24	94	**84**
	150	250	2,5	35,0	CFRP	1,05	94	CFRP	0,12	94	**73**
	150	250	2,5	33,1	CFRP	1,10	94	CFRP	0,24	94	**89**
	150	250	2,5	31,3	CFRP	1,39	94	CFRP	0,24	94	**95**
	150	250	2,5	30,5	CFRP	2,11	94	CFRP	0,24	94	**120**
	150	250	2,5	30,5	CFRP	2,11	94	CFRP	0,18	94	**86**
	150	250	2,5	31,3	CFRP	2,11	94	CFRP	0,15	94	**75**
	150	250	2,5	34,9	CFRP	2,11	94	CFRP	0,12	94	**83**
Nakamura & Higai '95	200	250	3,0	35,4	GFRP	1,61	29	GFRP	0,35	31	**83**
	200	250	3,0	33,4	GFRP	1,61	29	GFRP	0,35	31	**100**
	200	250	3,0	35,2	GFRP	1,61	29	GFRP	0,18	31	**56**
	200	250	3,0	35,2	GFRP	1,61	29	GFRP	0,18	31	**66**
Zhao et al. '95	150	250	3,0	34,3	CFRP	3,02	105	GFRP	0,42	39	**113**
	150	250	3,0	34,3	CFRP	3,02	105	CFRP	0,42	100	**126**
	150	250	3,0	34,3	CFRP	2,27	105	GFRP	0,42	39	**116**
	150	250	2,0	34,3	CFRP	1,51	105	GFRP	0,42	39	**123**
	150	250	4,0	34,3	CFRP	1,51	105	GFRP	0,42	39	**73**
Maruyama & Zhao '96	150	250	2,5	34,0	CFRP	1,07	100	GFRP	0,43	30	**110**
	150	250	2,5	34,0	CFRP	1,07	100	GFRP	0,43	30	**107**
	150	250	2,5	34,0	CFRP	1,07	100	GFRP	0,43	30	**148**
	150	250	2,5	34,0	CFRP	1,07	100	GFRP	0,43	30	**131**
	300	500	2,5	29,5	CFRP	1,07	100	GFRP	0,86	30	**370**
	450	750	2,5	29,5	CFRP	1,07	100	GFRP	1,28	30	**590**
Alsayed et al. '97	200	310	3,2	29,5	GFRP	1,37	36	GFRP	0,21	42	**69**
	200	309	2,4	29,6	GFRP	1,28	43	GFRP	0,40	42	**109**
Duranovic et al. '97	150	230	3,3	33,0	GFRP	1,31	45	GFRP	0,35	45	**49**
	150	230	2,2	33,0	GFRP	1,31	45	GFRP	0,35	45	**67**
Shehata et al. '00	135	470	3,2	50,0	CFRP	1,25	137	CFRP	0,29	137	**305**
	135	470	3,2	50,0	CFRP	1,25	137	GFRP	1,07	41	**305**
Whitehead & Ibell '05	110	100	3,1	55,61	AFRP	0,32	60	AFRP	0,40	60	**45**
	110	200	3,1	63,91	AFRP	0,32	60	AFRP	0,19	60	**51**
	110	100	3,1	55,61	AFRP	0,32	60	AFRP	0,40	60	**53**
	110	100	3,1	58,1	AFRP	0,32	60	AFRP	0,80	60	**55**
	110	200	3,1	58,1	AFRP	0,32	60	AFRP	0,29	60	**60**

(*) Single leg area

The predictions from equation (5.14) were compared with the values derived using equations (5.3), (5.8), and (5.10). Table 2 reports the ratio of the shear resistance attained experimentally, V_{exp}, to the corresponding analytical values derived according to each of the four considered guidelines, V_{pred} (both V_{exp} and V_{pred} are meant to be the total strength of the tested specimens).

Table 4 - Comparison of Eq. (5.14) with Major Design Provisions

	V_{exp} / V_{pred}							
	CNR DT 203		***ACI 440.1R***		***CSA S806***		***JSCE***	
	w/o Saf. Fact.	**w/** Saf. Fact.	**w/o** Saf. Fact.	**w/** Saf. Fact.	**w/o** Saf. Fact.	**w/** Saf. Fact.	**w/o** Saf. Fact.	**w/** Saf. Fact.
Mean	**0,83**	**1,28**	**1,63**	**2,18**	**1,08**	**1,58**	**2,66**	**3,68**
St. Dev.	**0,27**	**0,42**	**0,69**	**0,92**	**0,39**	**0,60**	**1,13**	**1,57**
Coeff. of Var.	**32%**	**33%**	**42%**	**42%**	**36%**	**38%**	**43%**	**43%**

The CNR-DT 203 equation proves to give the least $\left(V_{exp}/V_{pred}\right)_{ave}$ both with and without safety factors, i.e. 0.83 and 1.28, respectively, and the least coefficients of

variation, i.e. 32 % and 33%, respectively (see Table 5; two different values of coefficient of variation were derived for equations where two different material factors are present, namely concrete and FRP safety factors); Figure 3 shows the calculated ultimate shear strength based on the four equations (each with all safety factors set equal to 1) versus that measured:

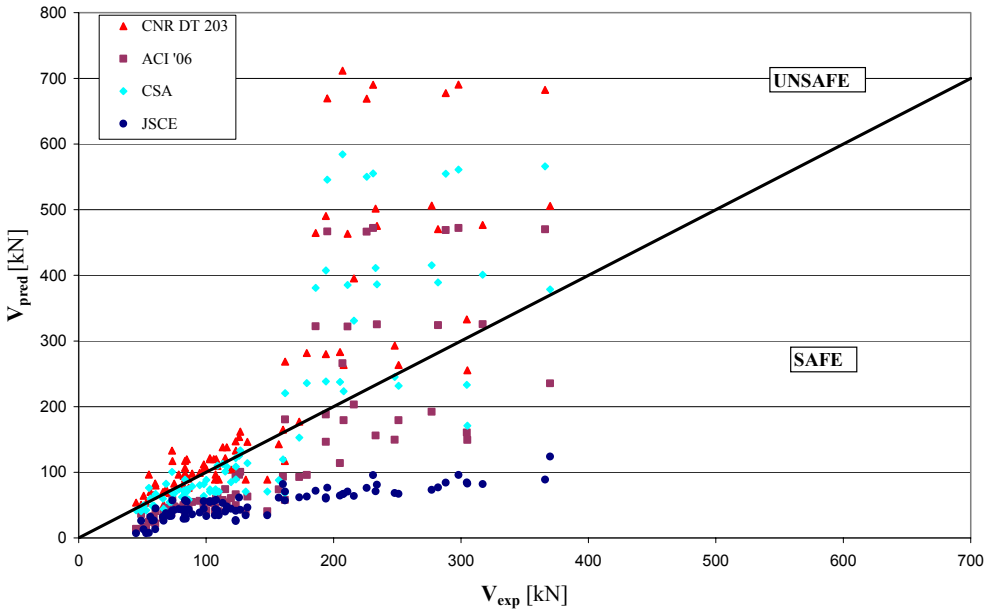

Figure 3 - Comparison of Eq. (5.14) with Major Design Provisions (w/o Saf. Factors)

The comparison between experimental results and predictions given by CNR-DT 203, ACI 440.1R-06 and CSA S-802 equations points out that there are some very un-conservative results which are related to the test data by Nagasaka et al. (1993) (see upper portion of Figure 3). The authors believe that this discrepancy could be due to the fact that only part of the high percentage of shear reinforcement is effectively contributing to the shear capacity of the members.

In such cases V_{exp}/V_{pred} was found to be lower than unity even when considering safety factors for all the equations except for the JSCE equation (which conversely seems rather conservative); again, this is particularly occurring for the experimental results reported by Nagasaka et al. (1993). This aspect is better investigated hereafter.

5.4.3 Influence of Bent Strength of Stirrups and Shear Reinforcement Ratio

The available literature data found in the first stage for the bend strength of FRP induced the CNR DT 203 Task Group to set an upper bound value of $\gamma_{f,\Phi} = f_{fd}/f_{fb} = 2$. Later more data were retrieved (Nagasaka et al., 1993, Nakamura and Higai, 1995, Vijay et al., 1996, Shehata et al., 1999), and then it is now possible to investigate the influence of the strength reduction of stirrups due to the bend based on a wider number of data.

For 32 out of 85 shear tested beams the ratio f_{fd}/f_{fb} was provided by the relevant authors; 26 extra values were reported by Shehata et al. (1999) from tests carried out to specifically study the bend effect on the strength of FRP stirrups. In Figure 4 the overall 58 values f_{fd}/f_{fb} versus E_f are depicted, showing the great scattering of results; similar outcomes are attained when considering d_b in lieu of E_f (see Figure 5).

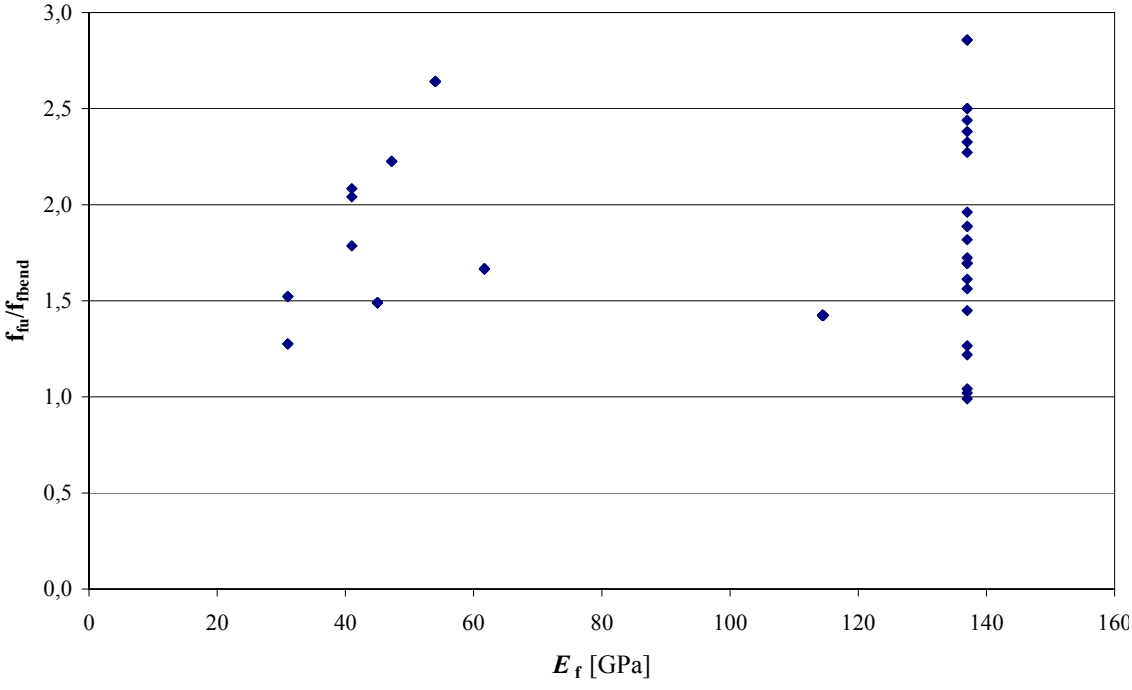

Figure 4 - Straight to Bend Strength Ratio vs Modulus of Elasticity of FRP Bars

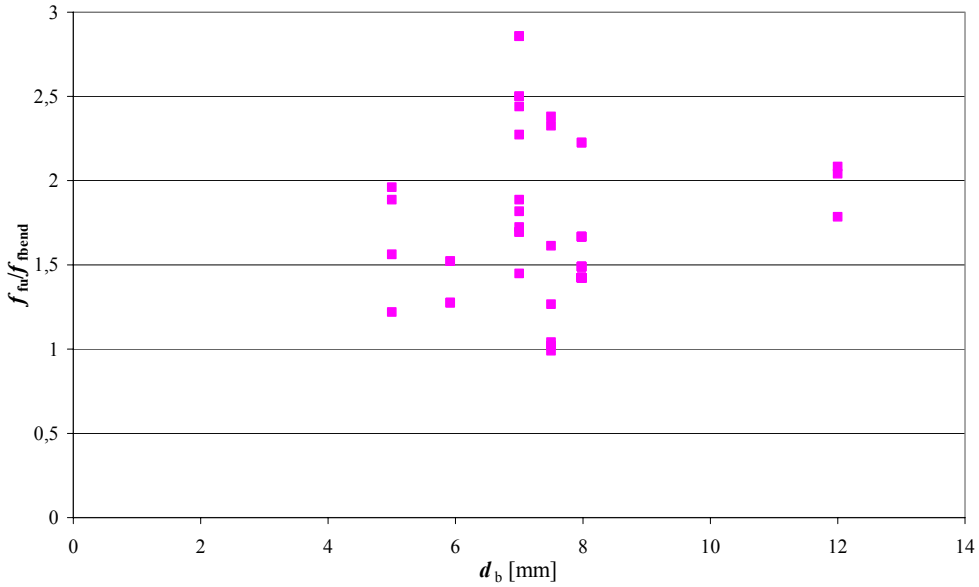

Figure 5 - Straight to Bend Strength Ratio vs Diameter of FRP Bars

Equation (5.14) modified by replacing $\gamma_{f,\Phi} = 2$ with the experimental value of f_{fd}/f_{fb} can be considered:

$$V_f = \frac{A_{fv} f_{fd} d}{s} \frac{f_{fb}}{f_{fd}} \qquad (5.15)$$

The 32 shear tested specimens where f_{fd}/f_{fb} was available were used for comparison of eq. (5.15) with CNR DT 203 eq. (5.14) and ACI eq. (5.3) (only the American equation was considered as reference for comparison with the Italian equation because it has a slightly different approach, limited predominantly by the maximum strain rather than by the strength of stirrup bent portion). Table 5 reports the mean, the standard deviation and the coefficient of variation of V_{exp}/V_{pred} relating each of the three equations, both with and without safety factors; Figure 6 shows the trend of V_{exp} versus V_{pred}, derived with the three equations.

Table 5 - Comparison of Eq. (5.14) with Eq. (5.15) and Eq. (5.3)

	V_{exp}/V_{pred}								
	CNR DT 203						*ACI 440.1R*		
	$\gamma_{f,\Phi} = 2$			$\gamma_{f,\Phi} = f_{fd}/f_{fb}$					
	w/o Saf. Fact.	w/ Saf. Fact.		w/o Saf. Fact.	w/ Saf. Fact.		w/o Saf. Fact.	w/ Saf. Fact.	
			ρ_{max}=1%			ρ_{max}=1%			ρ_{max}=1%
Mean	**0,64**	**0,97**	**1,03**	**0,56**	**0,85**	**0,89**	**1,22**	**1,62**	**1,71**
St. Dev.	**0,23**	**0,36**	**0,31**	**0,28**	**0,44**	**0,40**	**0,55**	**0,74**	**0,66**
Coeff. of Var.	**37%**	**37%**	**30%**	**51%**	**52%**	**44%**	**46%**	**46%**	**39%**

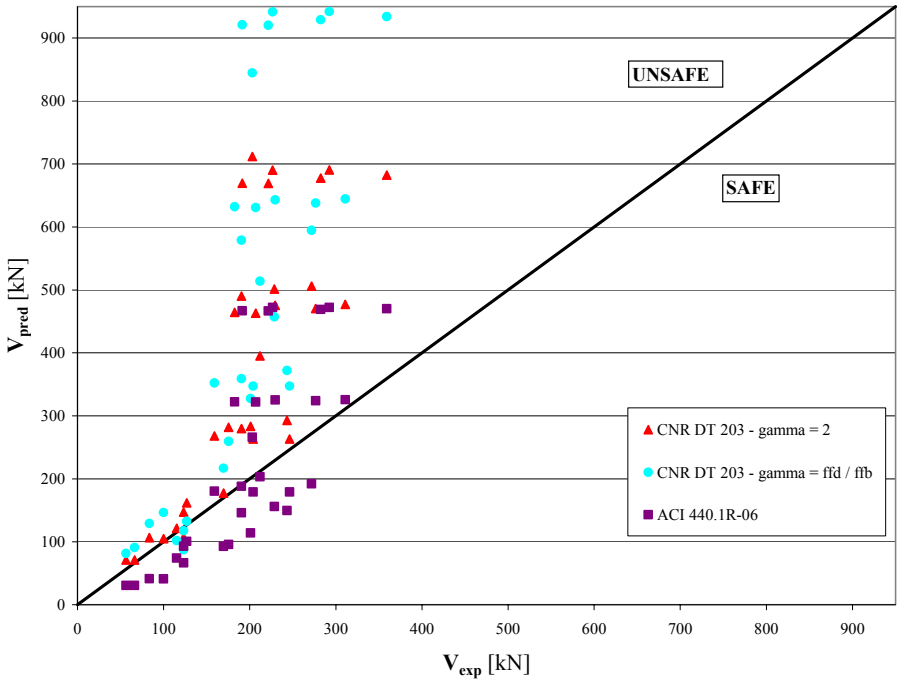

Figure 6 - Comparison of Eq. (5.15) with Eq. (5.3) and Eq. (5.14)

The results show that eq. (5.3), where the minimum value for f_{fv} always corresponded to $0.004E_f$ (the value 0.004 is justified as the strain that prevents degradation of aggregate interlock and corresponding concrete shear, Priestley et al. (1996), gives better predictions than equations (5.14) and (5.15); besides, better outcomes are derived for eq. (5.14) than eq. (5.15), which greatly overestimates the shear capacity when f_{fd}/f_{fb} is lower than 1.8 (that is when the bend strength of the bar approaches that of the straight portion) and gives more scattered predictions, as expected; similarly to what was observed for Figure 3, also the most un-conservative predictions in Figure 6 are related to the experiments conducted by Nagasaka et al. (1993).

Therefore, it can be concluded that the strength of stirrups bent portion seems not to be a significant factor affecting the FRP stirrups contribution to shear; this result becomes more evident when the bend strength of stirrup approaches that of the straight portion and justifies the larger inaccuracy of some analytical results (Nagasaka et al., 1993). Such conclusion is in agreement with the results of shear tests carried out by Nagasaka et al. (1993), where the average stress of FRP stirrups

across a critical crack obtained from the strain gage readings was measured to be only half of the breaking strength of bent portions. According to the findings of Nagasaka et al. (1993), the values reported in Table 6 are suggested as limit strains, $\varepsilon_{f,lim}$, depending on the type of stirrup fiber:

Table 6 - Proposed Values for the Limit Strain of FRP Stirrups

type of fiber	$\varepsilon_{f,lim}$
CFRP	0.0035
AFRP	0.0070
GFRP	0.0085

such values were used in replacement of 0.004 given by ACI 440.1R-06 (2006) in eq. (5.3), while in equation (14) f_{fr} was replaced by $\varepsilon_{f,lim} \cdot E_f$, thus yielding to equation (5.16):

$$V_f = \frac{A_{fv}\, \varepsilon_{f,lim} E_f\, d}{s} \qquad (5.16)$$

Table 7 shows that the two modified equations seem to give better predictions than corresponding equations (5.3) and (5.16) (the comparison was based on the total group of shear tested beams, i.e. 85 experimental results).

Table 7 - Influence of Limit Strain of FRP Stirrups on CNR DT 203 and ACI 440.1R Equations

	V_{exp} / V_{pred}							
	CNR DT 203				***ACI 440.1R***			
	$\gamma_{f,\Phi} = 2$		$\varepsilon_{f,lim} * E_f$		$0.004 * E_f$		$\varepsilon_{f,lim} * E_f$	
	w/o Saf. Fact.	**w/** Saf. Fact.	**w/o** Saf. Fact.	**w/** Saf. Fact.	**w/o** Saf. Fact.	**w/** Saf. Fact.	**w/o** Saf. Fact.	**w/** Saf. Fact.
Mean	**0,83**	**1,28**	**1,03**	**1,60**	**1,63**	**2,18**	**1,43**	**1,90**
St. Dev.	**0,27**	**0,42**	**0,31**	**0,48**	**0,69**	**0,92**	**0,52**	**0,70**
Coeff. of Var.	**32%**	**33%**	**30%**	**30%**	**42%**	**42%**	**37%**	**37%**

In addition, Nagasaka et al. (1993) pointed out that for stirrup ratios ρ_{fw} over 1 % the increase rate of shear capacity greatly reduces; if this remark is accounted for in eq. (5.3) and eq. (5.14) by limiting ρ_{fw} to 1%, better predictions are attained for the referred equations in terms of both mean and coefficient of variation (see Table 5).

5.5 CONCLUSIVE REMARKS

The paper presents an assessment of Eurocode-like design equations for predicting the shear strength of FRP RC members, which have been included in the lately issued CNR-DT 203 2006 guidelines of the Italian Research Council. The new expressions for the concrete and FRP stirrups contributions to the shear strength of FRP RC members have been compared with the corresponding American, Canadian and Japanese provisions using a large experimental database. The following conclusions can be drawn:

1. The equation proposed by the CNR DT 203 accounting for the concrete contribution to the shear strength, V_c, gives accurate predictions and can be conservatively used by practitioners.
2. For shear reinforced members, the strength of stirrups bent portion seems not to be a significant factor affecting the FRP stirrups contribution to shear; this is confirmed by experimental results where the effective strain measured in the stirrups across critical cracks governed the shear failure, namely 0.0035 for CFRP stirrups, 0.007 for AFRP stirrups and 0.0085 for GFRP stirrups. Moreover, in many shear tested members when the bend strength of stirrup approaches that of the straight portion the shear capacity did not increase as expected.
3. The equation proposed by the CNR DT 203 accounting for the stirrups contribution to the shear strength seems to give rather good results; nevertheless, the $\gamma_{f,\Phi}$ factor accounting for bending effects of stirrups should be replaced by a term accounting for the limit strain not governed by rupture of bent portion.
4. Increasing the stirrup ratio ρ_{fw} over 1 % seems not to increase the shear capacity; when setting $\rho_{fw,max} = 1\%$ more reliable predictions are attained.

Chapter VI
TEST METHODS FOR THE CHARACTERIZATION OF FRP BARS

6.1. INTRODUCTION

In its final part the CNR-DT 203/2006 devotes 5 appendixes to specific topics that are paramount to lead practitioners and manufacturers in the use of FRP bars and grids; these appendixes are:

A. *Manufacturing techniques of FRP bars and grids*, that basically reports the main characteristics of resins and the manufacturing processes of FRP bars;
B. *Test methods for characterizing FRP bars*, for determining the geometric and mechanical properties of FRP bars, as proposed by the ACI Committee 440 in the document entitled "Guide Test Methods for Fiber-Reinforced Polymers (FRPs) for Reinforcing or Strengthening Concrete Structures" (2004);
C. On *technical data sheet for FRP bars*, that the manufacturer shall write reporting the statistical values needed for the evaluation of the characteristic strengths (e.g. sample mean, standard deviation, population, percentile, confidence interval);
D. On *selection and testing of FRP bars: tasks and responsibilities of professionals* (namely manufacturers, designers, contractors/subcontractors, construction managers, test laboratories and inspectors);
E. *Calculating deflections and crack widths for flexural elements of concrete reinforced with FRP bars*; this section describes the procedure to be used by the manufacturer to determine through appropriate tests the FRP bar-concrete bond in order to accurately evaluate deflections and crack widths.

This chapter particularly focuses on the investigation of mechanical characteristics and geometrical properties of large-scale GFRP bars according to the Appendix B of the CNR-DT 203/2006 (and to ACI 440.3R-04). Furthermore, ad-hoc test set-up procedures to facilitate the testing of such large-scale bars are presented. The information gathered throughout this investigation adds to the body of knowledge supporting further development of standard test methods for FRP reinforcing bars.

6.2. MECHANICAL CHARACTERIZATION OF LARGE-DIAMETER GFRP BARS

The use of GFRP bars is widely employed in a variety of civil engineering structures ranging from bridge deck applications to RC members used as ground containment. Similar applications often require GFRP bars with large diameters to be used primarily because of their low modulus of elasticity as compared to steel reinforcing bars.

Because of the anisotropic characteristics of GFRP bars, micro defects are more likely to affect the behavior of large-scale bars than the behavior of small-scale bars. As a result, load sharing between fibers is modified in large-scale bars where the stress path from the edge to the core of the reinforcing bar is somehow altered and significantly less effective as compared to both small-scale GFRP bars and steel bars. Although official test method documents such as ACI, ISO and ASTM are now available for the mechanical and geometrical characterization of FRP material, in many instances material suppliers do not provide product specifications in compliance with the aforementioned documents. Usually this omission either happens because of lack of information provided in test methods protocol or because of practical difficulties of laboratory implementation of the prescribed test methods.

6.2.1 Overview of the Existing Standard Test Methods

The existing standard test methods do not provide exhaustive recommendations for testing large-diameter FRP bars. In the following paragraphs, a brief overview of the existing recommendations is presented.

The ACI 440.3R-04 guide (2004) in Appendix A gives the recommended dimensions of test specimens and steel anchoring devices for testing FRP bars under monotonic, sustained, and cyclic tension. The outside diameter, the nominal wall thickness, and the minimum length of the anchoring steel device are given as a function of the bar diameter. Because 22 mm is the maximum GFRP bar diameter considered, the ACI guide does not provide any recommendations for larger diameters. Moreover, ACI prescribes that the total length of the specimen needs to be equal to the free length, L (where L shall be at least 40 times the bar diameter), plus two times the anchoring length, L_a. Considering a 32 mm diameter GFRP bar, the resulting free length is

calculated as L = 1280 mm; by adding the maximum values given for L_a (460 mm for a 22 mm GFRP bar), the minimum total length of the specimen should be 2200 mm. Most of the times, technical laboratories are not equipped to handle such long specimens for testing.

6.2.2 Experimental Program

6.2.2.1 Test Setup

The experimental study consisted of performing tensile tests carried out with the use of a RC hollow column, which housed the GFRP specimen and acted as a load contrast. This setup enabled the provision of a whole shield for the personnel involved in the test against the dangerous scattering of fibers, which happens because of the high loads developed during the test.

A 100-ton hydraulic jack and a 100-ton load cell were applied to the edges of the hollow column to provide and measure the required load, respectively. Steel plates were placed against the RC hollow column to better distribute the load. A picture and a sketch of the test setup used are represented in Figure 1.

An electric pump not shown in the picture was connected to the jack to apply the load. The rate of loading was such that GFRP bar failure was achieved in an average of seven minutes. Standard atmosphere laboratory conditions (23 ± 3 ˚C and 50 ± 10 % relative humidity) were measured during the performed tests.

Similarly, the ISO TC 71/SC 6 N standard (2005) in Section 6, showing test methods for tensile properties, prescribes that when using FRP bars, the free length shall be not less than 300 mm and not less than 40 times the nominal diameter, d_b, which gives the same value as obtained with the ACI guide. Regarding the anchoring length, the ISO standard underlines that the anchoring device shall have the capability to transmit only the tensile force along the longitudinal axis of the test pieces; although, ISO doesn't provide further information on specific minimum values to account for.

Finally, the ASTM D7205 standard (2006) prescribes that the free length of the specimen shall not be less than 380 mm nor less than 40 times d_b; this measurement

leads to the same derived value as the above standards. The length of the specimen in the anchors shall be sufficient for adequate anchorage.

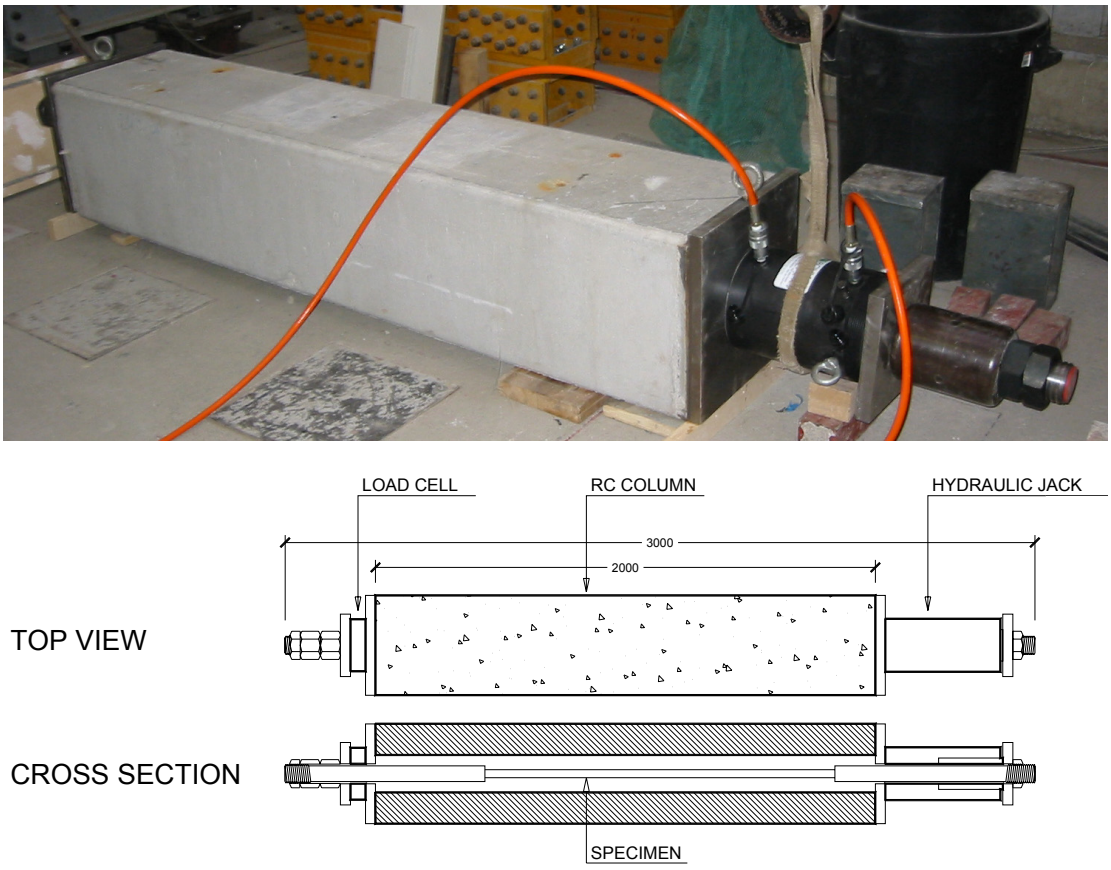

Figure 1. Test Setup

6.2.2.2 Specimen Preparation

Three-meter-long, 32-mm diameter, *Rockworm* GFRP bars manufactured by ATP were used for the experimental campaign. The bar surface was ribbed with helical-shaped polyester resin.

GFRP geometrical properties were calculated following ACI 440.3R.04 procedures for the determination of cross sectional area, equivalent diameter, and equivalent circumference.

Two anchoring-steel hollow cylinders 800 mm long were used to provide the necessary grip for the tensile test for each specimen as shown in Figure 2. The adhesive used to yield the grip between the anchoring cylinder and the bar was a two-component epoxy resin, "EPOJET" from Mapei S.p.A. Each steel hollow

cylinder was assembled with four top and four bottom screws used to align the specimen before pouring the resin.

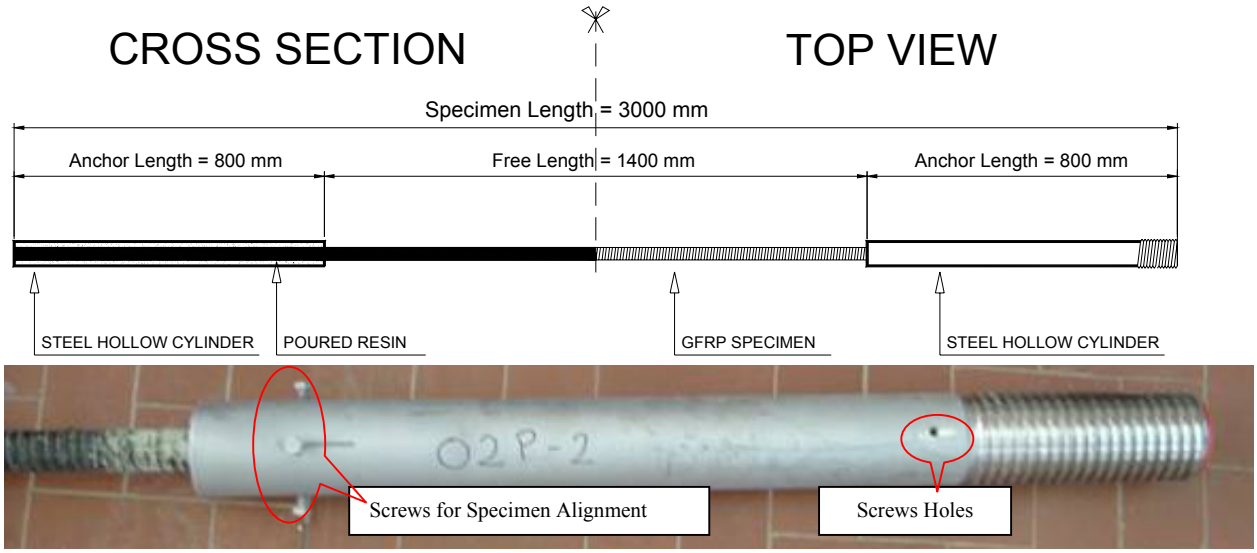

Figure 2. Sketch of the Specimen and Picture of Steel Hollow Cylinders used as Anchorage Device

Further characteristics of the anchoring-steel hollow cylinders (*e.g.,* external diameter, internal threaded pattern, and wall thickness) will be discussed later since they were gradually modified, after registering failures in the device itself, to better resist the high stresses generated during the test.

6.2.2.3 Strain Measuring Devices

The strain assessment of GFRP specimens was the most difficult aspect of the experimental campaign to deal with. The very first test was conducted on a bar just to record the failure load value with no strain measuring devices employed.

The ribbed surface of the bar did not allow attachment of the strain gages without changing the bar geometry. The possibility of gluing strain gages directly to the bar was also considered (see Figure 3a). A preliminary test run using this configuration showed that the measured strain was compatible with its expected value; however, the maximum load recorded at failure was smaller than the one obtained in the very first test because of the reduced cross section of the bar, which resulted from the necessary elimination of the protuberances for the application of the strain gages.

As a second attempt, a thin, 80-mm long, smooth layer of very deformable resin having a diameter barely larger than the bar diameter (see Figure 3b) was applied around the middle portion of the specimen in order to provide a suitable support for the strain gages. Three strain gages installed every 120 degrees were used for each test.

Skepticism that the effective strain measured by the applied strain gages could have been smaller than the strain experimented by the bar urged the implementation of a third strain measuring approach based on the use of Linear Variable Differential Transducer (LVDT) to measure the elongation of the specimen under the applied load. The LVDT was centered in the middle portion of the specimen as shown in Figure 3c; its gage length was assumed equal to the specimen length.

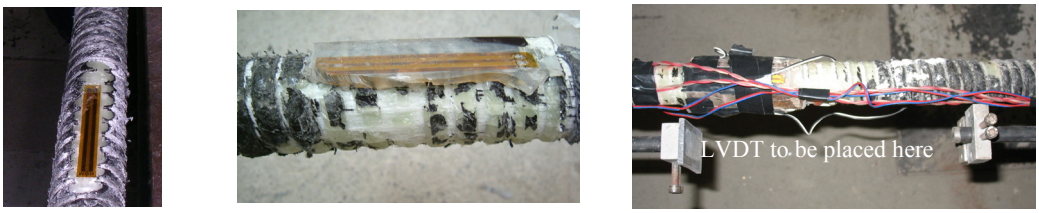

a) Strain gage glued to the bar

b) Strain gage on top of a layer of resin (at the end of the test)

c) LVDT on center portion of specimen

Figure 3. Measuring Devices to Record Strain

6.2.2.4 Tensile Tests

As briefly highlighted before, many adjustments were performed during the test phase on both the anchoring device and strain measuring system to achieve the complete success of the test. Following is a brief summary of the steps carried out to improve the efficiency of the proposed test setup:

1. As a first step, steel hollow cylinders with inner diameters of 65 mm and wall thicknesses of 10 mm were used. Two specimens were prepared using this configuration; in both instances, slip between poured resin and anchoring device occurred.
2. The inner surface of the steel hollow cylinders was threaded improving the grip to prevent the bar from slipping from the anchoring device. The performed test validated this solution, yet the test failed for the rupture of the steel hollow cylinder edge, as shown in Figure 4a.

a) Rupture of steel hollow cylinder used as anchoring device

b) Rupture of FRP bar protuberances

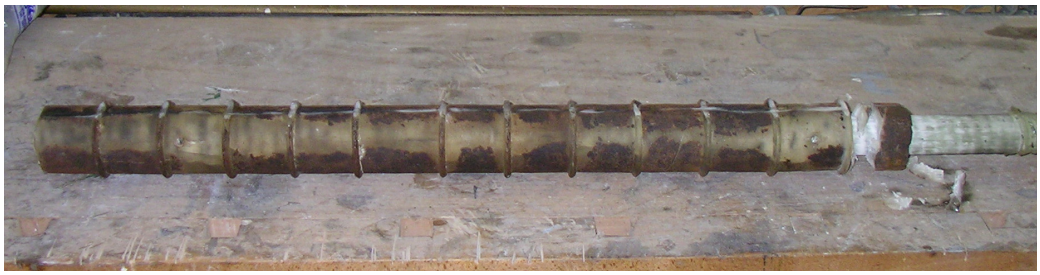

c) Circular inner threads resulting after removal of steel hollow cylinder

d) Typical broom rupture of GFRP bar

Figure 4. Several Failure Modes of the Tested Specimens

1. The steel hollow cylinder diameter was therefore enlarged to 75 mm to resist higher loads. The wall thickness was maintained at 10 mm as was the threading of the inner surface. Two tests were performed. The first had the best result, with the rupture of the bar at a load of about 80 tons. Nevertheless, the second test showed the same rupture of the steel hollow cylinder edge (see Figure 4a) as in case 2 but at a higher load (approximately 75 tons). The inspection of the rupture showed that the broken section had a

double thinning because of both inner and outer threading of the steel hollow cylinder.

2. The distance between the inner threads of the steel hollow cylinder was increased to avoid overlapping the outer thread. Five tests were performed in this phase, and they all failed because of a new event—the rupture of the bar protuberances from the bar itself (see Figure 4b) at a load ranging between 50 and 60 tons. Inspection of the specimens showed that the inner threads had been made circular by the manufacturer (Figure 4c) instead of elliptical, as required. The achieved stress on the protuberances could forego the bar core failure because of their weakness. In fact, bar protuberances are made out of mere resin and do not include any glass fiber.
3. As a last step, steel hollow cylinders with proper internal elliptical threads were delivered. Nine tests were carried out; the typical broom failure of the bar (see Figure 4d) was obtained at a load of approximately 80 tons. Further slip of the protuberances from the bar itself was observed at a load close to the one expected for the rupture of the bar. However, this specific failure is not because of inefficiency of the proposed test setup.

6.2.3 Test Results

6.2.3.1 Geometrical Properties

The cross sectional properties of the GFRP bars were determined using 5 bar specimens, approximately 200 mm long, and a graduated measuring cylinder with a gradient of 10 mL, as suggested by ACI 440.3R-04 (2004), and of sufficient height and diameter to contain the specimen. After filling the dried cylinder with water and measuring the length of each specimen 3 times (rotating the specimens by 120 degrees for each measurement), each one was immersed in the fluid to determine the volume increase.

When the volume and length of each of the 5 specimens had been determined, the cross-sectional area A was determined by dividing the specimen's volume by its length and rounding to the nearest 1 mm^2. Hence, the equivalent diameter (d_b) of each specimen was calculated by assuming the cross section to be a circle. Please

note that the cylinder gradient used was found to be inappropriate for such a test, its accuracy being not very adequate for such small volume increases. Table 1 shows the derived cross-sectional properties of the bars.

Table 1. Geometrical Properties of the GFRP Bars

Specimen	GEOMETRICAL PROPERTIES					
	Area				Diameter	Circumf.
	V_1 [ml]	V_0 [ml]	L [mm]	**A** [mm²]	$\mathbf{d_b}$ [mm]	C_b [mm]
1	915	700	257.0	837	32.6	102.5
2	910	700	258.0	814	32.2	101.1
3	910	700	258.1	814	32.2	101.1
4	912	700	257.9	822	32.4	101.6
5	912	700	258.4	820	32.3	101.5
AVERAGE				**821**	**32**	**102**

6.2.3.2 Tensile Properties

Table 2 and Table 3 report the mechanical properties of the bars brought to failure. ACI 440.3R-04 prescribes basing the test findings on test specimens that fail in the test section only (see Figure 4d). Hence, the bars which had the ribs detachment have not been taken into account, since that occurred in the anchoring section. However, this issue is one of the possible failures that this product may undergo when applied in the field; therefore, these findings should be taken into account by the standard test methods, provided that such failures are not promoted by the anchoring device itself.

Table 2. Mechanical Properties of the GFRP Bars Arrived at Failure

Specimen	Test date [-]	Bar Area [mm²]	Ultimate Load F_u [N]	Tensile Strength f_u [MPa]
1	12/5/05	**821**	**806,704**	983
2	7/6/05	**821**	**640,816**	781
3	7/6/05	**821**	**793,077**	966
4	20/6/05	**821**	**762,585**	929
5	20/6/05	**821**	**810,141**	987

Table 3. Mean Values Extracted

Average Tensile Strength [MPa]	929
Standard Deviation [MPa]	86
Guaranteed Tensile Strength [MPa]	671
Modulus of Elasticity [Gpa]	44.7
Guaranteed Ultimate Strain [-]	0.015

6.3. CONCLUSIVE REMARKS

The main objective of the performed tensile tests was to investigate the effectiveness of the proposed test setup procedures specifically designed for the mechanical characterization of large-scale (32 mm) GFRP bars to be used as internal reinforcement of concrete members.

The following conclusions can be drawn:

- Micro defects in GFRP reinforcement are more likely to affect the behavior of large-scale bars than the behavior of small-scale ones; hence, testing of the former should be supported when possible. The proposed test setup was found to be effective for this purpose.
- The tests were safe, in spite of the high loads produced, thanks to the screening provided by the RC hollow column, which effectively bore the considerable stresses and protected the bystanders from the bars' splinters.
- Excellent protection was offered by the RC hollow column against dust and micro-fiber scatterings, which is very valuable when dealing with fibrous materials.

The only drawback observed was the obstruction to the view of the bar behavior during the test execution. Therefore, a modification necessary to improve the technology proposed will consist in the use of two separated RC hollow columns joined together with structural steel in the middle part. This modification will allow observers to watch the ongoing test and to apply an extensometer or an LVDT, which can be easily removed before the bar failure. Moreover, the structural steel can be varied to fit the different lengths of specimens having different diameter.

Chapter VII
CONCLUSIONS

This study furthered the assessment of some crucial aspects that are at the basis of the Design Guidelines CNR-DT 203/2006, "*Guide for the Design and Construction of Concrete Structures Reinforced with Fiber-Reinforced Polymer Bars*", recently issued under the auspices of the National Research Council (CNR), that is the result of the effort lavished in ten years of research, applications and experience gained in Italy on FRP, validated and supported by the knowledge provided by the existing international codes relating to the design of FRP RC structures.
In particular this thesis analyzes:

- The ultimate limit states (ULS) design, both for flexure and shear;
- The serviceability limit states (SLS) flexural design, specifically the deflection control;
- Test methods for characterizing FRP bars.

Following the main conclusions relating to these aspects are summarized.

7.1 ULTIMATE FLEXURAL BEHAVIOR

A reliability-based calibration of partial safety factors has been applied to assess the reliability levels of the ULS flexural design suggested by the Italian guidelines CNR-DT 203/2006. 240 FRP-RC beams and 180 FRP-RC slabs have been designed to cover a wide design space considering an appropriate set of random design variables (cross-sectional dimensions, concrete strengths and FRP reinforcement ratios) used to develop resistance models for FRP-RC members. Monte-Carlo simulations have been performed to determine the variability in material properties and fabrication processes; whereas experimental data reported in the literature have been used to quantify the variability related to the analysis method. A structural reliability analysis has been conducted based on the established resistance models and load models obtained from literature. The reliability index, β, calculated using FORM for all FRP-RC beams and slabs for 5 ratios of live load to dead load moments (0.5 to 2.5)

and 30 values of ρ_f/ρ_{fb}, has been assessed mainly depending on γ_f and on the uncertainty effects due to material properties (M), fabrication process (F) and analysis method (P); the following conclusions can be drawn:

1. The research work carried out is strictly dependent on the specific design cases taken into account; although a wide range of design cases has been covered and statistical properties available in literature have been assigned to design variables. More thorough and refined results will be attained with the research growth in the field of composites.
2. Regardless of member type (beams or slabs) and specific design considered, five different zones can be identified, depending on ρ_f/ρ_{fb}: two edge zones of low, steady values of β corresponding to under-reinforced ($\rho_f/\rho_{fb}<0.5$) and over-reinforced sections ($\rho_f/\rho_{fb}>2.5$); a central zone with the maximum values of β corresponding to the balanced failing sections, where the materials are best exploited and then with the highest structural reliability values; and two transition zones with β variable going from under- or over-reinforced sections to balanced failing sections.
3. For the 1200 design cases related to beam-type members (240 design cases by 5 ratios M_L/M_D) the value of γ_f to be preferred is $\gamma_f = 1.1$, as it slightly reduces the GFRP reinforcement strength and together it corresponds to a satisfactory level of safety of the member ($\beta_0 = 6.4 > \beta_{min} = 5$ at ULS). Nevertheless, it can be also observed that points with $\gamma_f = 1.5$ (current value proposed in the CNR-DT 203/2006) correspond to a good level of safety ($\beta_0 \geq 7.5$), although the limitation on the strength of FRP reinforcement can be considered too penalizing and cost-ineffective. Similar conclusions are derived if considering a different classification of results, depending on the design values of materials strengths rather than on the corresponding characteristic values;
4. With respect to the values derived for beams, a general decrease of the reliability can be observed when accounting for the 900 slabs design cases in correspondence of the same values of γ_f. The value $\gamma_f = 1.1$ considered as an

optimum value for beams, does not match a satisfactory reliability level when referred to slabs. The value $\gamma_f = 1.5$ proposed by the CNR-DT 203/2006 is enough reliable for the slabs design cases investigated.

5. When accounting for *M*, *F* and *P*, regardless of the design space selected, the trend of the reliability index vs γ_f is similar to that obtained without the contribution of the three factors; yet a general reduction in the reliability level is observed.

7.2 SERVICEABILITY FLEXURAL BEHAVIOR

The approaches followed in the CNR-DT 203/2006 for the flexural design of FRP RC elements at serviceability limit states have been illustrated; in particular, the deflection control of FRP RC members depending on the bond between FRP reinforcement and concrete has been investigated.

A calibration analysis was conducted in compliance with the procedure proposed by the CNR-DT 203/2006 to determine an optimum value for the bond coefficient *m*, based on a large experimental database available in literature, made of FRP RC elements subjected to four-points bending (beam anchorage) tests. The exponent *m* was determined on the basis of the comparison between analytical and experimental results, using the statistical analysis reported hereafter. Three different cases were analyzed in order to assess the influence of considering the theoretical values of the cracking moment $M_{cr,the}$ and of the modulus of elasticity of concrete, $E_{c,the}$, rather than the corresponding experimental values ($M_{cr,exp}$ & $E_{c,exp}$). The definition of the cracking moment is important since it influences the evaluation of deflection for FRP reinforced members (Pecce et al., 2001); since $M_{cr,the}$ depends on the concrete strength in tension, that is a very uncertain parameter and usually can not be directly measured, but computed depending on the strength in compression, the introduction of the experimental value of the cracking moment M_{cr} allows to examine the model efficiency disregarding the influence of the uncertainties due to $M_{cr,the}$ (1st case: $M_{cr}=M_{cr,exp}$ & $E_c=E_{c,exp}$); nevertheless, evaluating $M_{cr,the}$ is significant for the model application (2nd case: $M_{cr}=M_{cr,the}$ & $E_c=E_{c,exp}$;); similarly, the significance of $E_{c,the}$ instead of $E_{c,exp}$ in the model application was taken into account (3rd case: $M_{cr}=M_{cr,exp}$ & $E_c=E_{c,the}$).

The analyses showed that the bond coefficient m=2 proposed by CNR-DT 203/2006 should be replaced by a value lower than unity.

Of the three values derived for the three cases investigated, the first case, where m_1=0.87, proves that considering the experimental value of the cracking moment and of the modulus of elasticity of concrete instead of the theoretical values brings to more reliable deflection predictions. Therefore the value m=0.87 is that proposed to use as bond coefficient when computing the deflections of FRP RC elements using the CNR-DT 203/2006 equation.

Of the two other cases considered, case 3) where the theoretical value of E_c replaced the experimental value, resulted to give better predictions than case 2), where the theoretical value of M_{cr} was used instead of the corresponding experimental value. The investigation of available data collected allowed concluding that computing the cracking moment (rather than accounting for its experimental value) penalizes the reliability and the safety of deflection calculations more than considering $E_{c,the}$ instead of $E_{c,exp}$.

Nevertheless, the values of m derived in case 2) and in case 3) do not differ from the value of case 1) considerably, with a maximum variation of 17% with respect to m_1. Hence, considering the theoretical aforementioned values rather than the corresponding experimental quantities does not penalize the reliability of results considerably.

7.3 SHEAR ULTIMATE BEHAVIOR

The assessment of Eurocode-like design equations for the evaluation of the shear strength of FRP RC members, as proposed by the CNR-DT 203/2006 has been carried out as well. Both the concrete and the FRP stirrups contributions to shear have been taken into account: the new equations derived with reference to Eurocode equations for shear of steel RC members have been verified through comparison with the equations given by ACI, CSA and JSCE guidelines, considering a large database of members with and without shear reinforcement failed in shear. The following conclusions can be drawn:

1. The equation proposed by the CNR DT 203 accounting for the concrete contribution to the shear strength, V_c, gives accurate predictions and can be conservatively used by practitioners.
2. For shear reinforced members, the strength of stirrups bent portion seems not to be a significant factor affecting the FRP stirrups contribution to shear; this is confirmed by experimental results where the effective strain measured in the stirrups across critical cracks governed the shear failure, namely 0.0035 for CFRP stirrups, 0.007 for AFRP stirrups and 0.0085 for GFRP stirrups. Moreover, in many shear tested members when the bend strength of stirrup approaches that of the straight portion the shear capacity did not increase as expected.
3. The equation proposed by the CNR DT 203 accounting for the stirrups contribution to the shear strength seems to give rather good results; nevertheless, the $\gamma_{f,\Phi}$ factor accounting for bending effects of stirrups should be replaced by a term accounting for the limit strain not governed by rupture of bent portion.
4. Increasing the stirrup ratio ρ_{fw} over 1 % seems not to increase the shear capacity; when setting $\rho_{fw,max} = 1\%$ more reliable predictions are attained.

7.4 TEST METHODS FOR THE CHARACTERIZATION OF FRP BARS

The investigation of the mechanical and geometrical properties of large-scale GFRP bars has been accomplished according to the indications proposed by CNR-DT 203/2006 and by ACI 440.3R-04 guidelines. Furthermore, ad-hoc test set-up procedures to facilitate the testing of such large-scale bars have been contrived, since the available standard test methods do not provide exhaustive recommendations for testing large-diameter FRP bars. The experimental study consisted of performing tensile tests carried out with the use of a RC hollow column, which housed the GFRP specimen and acted as a load contrast. The following conclusions have been drawn:

- Micro defects in GFRP reinforcement are more likely to affect the behavior of large-scale bars than the behavior of small-scale ones; hence, testing of the

former should be supported when possible. The proposed test setup was found to be effective for this purpose.

- The tests were safe, in spite of the high loads produced, thanks to the screening provided by the RC hollow column, which effectively bore the considerable stresses and protected the bystanders from the bars' splinters.
- Excellent protection was offered by the RC hollow column against dust and micro-fiber scatterings, which is very valuable when dealing with fibrous materials.

The only drawback observed was the obstruction to the view of the bar behavior during the test execution. Therefore, a modification necessary to improve the technology proposed will consist in the use of two separated RC hollow columns joined together with structural steel in the middle part. This modification will allow observers to watch the ongoing test and to apply an extensometer or an LVDT, which can be easily removed before the bar failure. Moreover, the structural steel can be varied to fit the different lengths of specimens having different diameter.

The information gathered throughout this investigation adds to the body of knowledge supporting further development of standard test methods for FRP reinforcing bars.

7.5 RECOMMENDATIONS

Further research is deemed necessary to investigate aspects related to the design of concrete structures reinforced with FRP bars, as:

- Assessing the reliability levels related to other modes of failure that might control the design of FRP RC structures, such as shear failure and bond failure. Likewise, it would be worth to extend this research study to other types of reinforcement, as CFRP and AFRP.
- Assessing the reliability of the formulation proposed by the CNR-DT 203/2006 to compute crack widths of FRP RC members, and that of the formulation computing the development length of FRP reinforcement.
- Investigating the influence of FRP bar properties on the different mechanisms contributing to the concrete strength. The outcomes of this research plan will

be used to optimize the proposed equations in order to determine safety factors with different weight depending on each mechanism.

REFERENCES

1. ACI Committee 318, "Building Code Requirements for Structural Concrete (318- 02) and Commentary (318R-02)," American Concrete Institute, Farmington Hills, 2002, Michigan, 443p;
2. American Concrete Institute (ACI), 1996, "Building code requirements for reinforced concrete and commentary, ACI 318-95, Detroit.
3. ACI 440.1R-01 (2001), "Guide for the Design and Construction of Concrete Reinforced with FRP Bars", ACI Committee 440, American Concrete Institute (ACI), Farmington Hills;
4. ACI 440.1R-03 (2003), "Guide for the Design and Construction of Concrete Reinforced with FRP Bars", ACI Committee 440, American Concrete Institute (ACI), 42 p;
5. ACI 440.1R-06 (2006), "Guide for the Design and Construction of Concrete Reinforced with FRP Bars", ACI Committee 440, American Concrete Institute (ACI);
6. ACI 440.3R-04, 2004, "Guide Test Methods for Fiber-Reinforced Polymers (FRPs) for Reinforcing or Strengthening Concrete Structures", *American Concrete Institute*, Farmington Hills, MI, USA.
7. Aiello, M., and Ombres, L., 2000, Load-Deflection Analysis of FRP Reinforced Concrete Flexural Members, Journal of Composites for Construction, Vol.4, No.4;
8. Alkhrdaji, T., Wideman, M., Belarbi, A., and Nanni, A. "Shear Strength of GFRP RC Beams and Slabs" Proceedings of the International Conference, Composites in Construction-CCC 2001, Porto/Portugal, 2001, p. 409-414.
9. Alsayed, S. H., Al-Salloum, Y. A., and Almusallam, T. H. (1997). "*Shear Design for Beams Reinforced by GFRP Bars*" Third International Symposium on Non-Metallic (FRP) Reinforcement for Concrete Structures, Sapporo, Japan, p. 285-292.

10. Alsayed, S.H., 1998, "Flexural Behaviour of Concrete Beams Reinforced with FRP Bars", Cement and Concrete Composites, No. 20, pp. 1-11;
11. Alsayed, S.H., Al-Salloum, Y.A., and Almusallam, T.H., 2000, "Performance of glass fiber reinforced plastic bars as a reinforcing material for concrete structures", Department of Civil Engineering, King Saud University, P.O. Box 800, Riyadh 11421, Saudi Arabia Composites: Part B 31, pp 555 – 567;
12. Al-Sunna, R., Pilakoutas, K., Waldron, P., Guadagnini, M, 2006, "Deflection of GFRP Reinforced Concrete Beams", Fédération Internationale du Béton Proceedings of the 2° International Congress, June 5-8, 2006, Naples, Italy;
13. ASCE-American Concrete Institute (ACI) Committee 445. "Recent approaches to shear design of structural concrete," 1998 J. Struct. Eng.;124 (12): 1375-1417;
14. ASTM D618 (2002), "Conditioning Plastics and Electrical Insulating Materials for Testing", ASTM International;
15. ASTM D7205, 2006, "Standard Test Method for Tensile Properties of Fiber Reinforced Polymer Matrix Composite Bars", American Society for Testing and Materials, Philadelphia, USA;
16. Benmokrane, B., Tighiouart, B., and Chaallal, O., 1996, "Bond Strength and Load Distribution of Composite GFRP Reinforcing Bars in Concrete", ACI Materials Journal, V. 93, No. 3, pp. 246-253;
17. Benmokrane, B., Desgagne, G., and Lackey, T., 2004, "Design, Construction and Monitoring of Four Innovative Concrete Bridge Decks Using Non-Corrosive FRP Composite Bars," 2004 Annual Conference of the Transportation Association of Canada, Québec City, Québec, Canada;
18. Bradberry, T.E., 2001, "Fiber-Reinforced-Plastic Bar Reinforced Concrete Bridge Decks," 80th Annual Transportation Research Board, Jan. 9-13, 2001, CD #01-3247, Washington, DC, USA;
19. Brown, V., and Bartholomew, C., 1996, "Long-Term Deflections of GFRP-Reinforced Concrete Beams," *Proceedings of the First International Conference on Composites in Infrastructure (ICCI-96)*, H. Saadatmanesh and M. R. Ehsani, eds., Tucson, Ariz., pp. 389-400;

20. BS EN 1990:2002, Eurocode. Basis of structural design British-Adopted European Standard , 27-Jul-2002 / 118 p.;
21. BS 8110 (1997), "Structural use of concrete, Part 1 - Code of Practice for Design and Construction", British Standards Institution (BSI), London, 132 p;
22. Chinn, J., Ferguson, P. M., and Thompson, J. N., 1955, "Lapped Splices in Reinforced Concrete Beams," Journal of the American Concrete Institute, V. 27, No. 2,
23. Clarke, J.L., and O' Regan, D. P. "Design of concrete structures reinforced with fibre composite rods" Proc., Non-Metallic (FRP) Reinforcement for Concrete Structures (FRPRCS-2), E & FN Spon, London, Great Britain, 1995, p. 646-653.
24. Clarke J. L., O'Regan D. P. and Thirugnanenedran C., 1996, "EUROCRETE Project, Modification of Design Rules to Incorporate Non-ferrous Reinforcement", EUROCRETE Project, Sir William Halcrow & Partners, London, 64 p;
25. CNR-DT 203/2006. "Guide for the Design and Construction of Concrete Structures Reinforced with Fiber-Reinforced Polymer Bars" National Research Council, Rome, Italy, 2006;
26. CSA A23.3-94. "Design of Concrete Structures for Buildings" Canadian Standards Association, Rexdale, Toronto, Ontario, 1994, 220 p;
27. CSA A23.3 (2004), "Design of Concrete Structures", Canadian Standards Association, Ontario;
28. CSA-S806-02 (2002), "Design and Construction of Building Components with Fibre-Reinforced Polymers", Canadian Standards Association, Ontario, 177 p;
29. Darwin, D., Tholen, M. L., Idun, E. K., and Zuo, J., "Splice Strength of High Relative Rib Area Reinforcing Bars," ACI Structural Journal, V. 93, No. 1, Jan.-Feb. 1996, pp. 95-107;

30. Darwin, D., Zuo, J., Tholen, M. L., and Idun, E. K., "Development Length Criteria for Conventional and High Relative Rib Area Reinforcing Bars," ACI Structural Journal, V. 93, No. 3, May-June 1996, pp. 347-359;
31. Deitz, D. H., Harik, I. E., and Gesund, H. "One-Way Slabs Reinforced with Glass Fiber Reinforced Polymer Reinforcing Bars" Proceedings of the 4th International Symposium, Fiber Reinforced Polymer Reinforcement for Reinforced Concrete Structures, MI., 1999, p. 279-286;
32. Di Sciuva, M., Lomario, D., 2003, "*A Comparison between Monte Carlo and FORMs in Calculating the Reliability of a Composite Structure*", Journal of Composite Structures, Vol. 59, pp 155-162;
33. D.M.LL.PP. 09/01/1996. 1996. "Norme tecniche per il calcolo, l'esecuzione ed il collaudo delle strutture in cemento armato, normale e precompresso e per le strutture metalliche", Rome, Italy;
34. Duranovic, N., Pilakoutas, K., and Waldron, P. "Tests on Concrete Beams Reinforced with Glass Fibre Reinforced Plastic Bars" Proceedings of the Third International Symposium on Non-Metallic (FRP) Reinforcement for Concrete Structures (FRPRCS-3), Japan Concrete Institute, Sapporo, Japan, 1997, V.2, p. 479-486;
35. Ehsani, M. R.; Saadatmanesh, H.; and Tao, S., 1995, "*Bond of Hooked Glass Fiber Reinforced Plastic (GFRP) Reinforcing Bars to Concrete*", ACI Materials Journal, V. 92, No. 4, July-Aug., p. 391-400;
36. Ellingwood B., Galambos T.V., MacGregor J.G., Cornell C.A., 1980, "*Development of a probability based load criterion for American national standard A58 building code requirements for minimum design loads in buildings and other structures*", Special Publication 577, Washington (DC, USA): US Department of Commerce, National Bureau of Standards;
37. Ellingwood, B., MacGregor, J. G., Galambos, T. V., and Cornell, C. A., 1982, "Probability-based load criteria: Load factors and load combinations." J. Struct. Div., ASCE, 108 (5), 978–997;
38. Ellingwood, B. R., 1995, Toward load and resistance factor design for fiber-reinforced polymer composite structures, Journal of structural engineering, ASCE;

39. Ellingwood, B. R., 2003, Toward Load and Resistance Factor Design for Fiber-Reinforced Polymer Composite structures, Journal of Structural Engineering, Vol. 129, No. 4, pp.449-458;
40. El-Salakawy, E. and Benmokrane, B., 2004, "Serviceability of Concrete Bridge Deck Slabs Reinforced with Fiber-Reinforced Polymer Composite Bars", ACI Structural Journal, V.101, No 5, pp. 727-736;
41. El Sayed, A.K., El-Salakawy, E.F., and Benmokrane, B. "*Shear Strength of One-Way Concrete Slabs Reinforced with FRP Composite Bars*" Journal of Composites for Construction, 2005, Vol. 9, No 2, p. 147-157;
42. El Sayed, A.K., El-Salakawy, E.F., and Benmokrane, B. (2006), "Shear Strength of Concrete Beams Reinforced with FRP Bars: Design Method" 7th International Symposium on Fiber-Reinforced Polymer (FRP) Reinforcement for Concrete Structures (FRPRCS-7), Nov. 6-9, 2005, Kansas City, Missouri, USA, SP 230-54, pp. 955-974;
43. El-Sayed, A. K., El-Salakawy, E. F., and Benmokrane, B. "*Shear Strength of FRP-Reinforced Concrete Beams without Transverse Reinforcement*" ACI Structural Journal, 2006, V. 103, No 2, p. 235-243;
44. EN 1992-1-1 Eurocode 2 "Design of concrete structures - Part 1-1: General rules and rules for buildings", 1992;
45. ENV 1991-1, 1994, Eurocode 1: Basis of design and actions on structures – Part 1: Basis of design;
46. EN 1992-1-1 Eurocode 2 "Design of concrete structures - Part 1-1: General rules and rules for buildings", 2004;
47. Fico, R. Parretti, R. Campanella, G., Nanni, A., and Manfredi, G., 2006, Mechanical Characterization of Large-Diameter GFRP bars, 2nd International fib Congress, Naples;
48. Fico, R., Prota, A., and Manfredi, G., 2007, "*Assessment of Eurocode-like Design Equations for the Shear Capacity of FRP RC Members*", Journal of Composites Part B: Engineering, Article in Press;

49. Frangopol, D. M., and Recek, S., 2003, "Reliability of fiber-reinforced composite laminates plates", Journal of Probabilistic Engineering Mechanics, Vol. 18, pp. 119-137;
50. Galambos, T. V., Ellingwood, B., MacGregor, J. G., and Cornell, C. A., 1982. "Probability-based load criteria: assessment of current design practice" *J. Struct. Div., ASCE,* 108 (5), 959–977;
51. Goodspeed, C., Schmeckpeper, E., Henry, R., Yost, J. R., and Gross, T. "Fiber reinforced plastic grids for the structural reinforcement of concrete." Proc., 1st Materials Engrg. Cong., ASCE, New York, 1990, p. 593–604;
52. Guadagnini, M., Pilakoutas, K., and Waldron, P. "Shear Design for Fibre Reinforced Polymer Reinforced Concrete Elements" Proc., 4th Int. Symp. On Fiber Reinforced Polymer Reinforcement for Reinforced Concrete Structures: Selected Presentation Proc., American Concrete Institute, Farmington Hills, Mich., 1999, p. 11-21;
53. He, Z., and Huang, Y., 2006, "Reliability assessment of flexural capacity design for FRP-reinforced concrete", Engineering Structures, *Article in Press*;
54. ISIS (2001), "Reinforcing Concrete Structures with Fibre Reinforced Polymers", Design Manual No. 3, Canadian Network of Centres of Excellence on Intelligent Sensing for Innovative Structures, Winnipeg, 158 p;
55. ISO TC 71/SC 6 N, 2005, "Non-Conventional Reinforcement of Concrete – Test Methods – Part 1: Fiber Reinforced Polymer (FRP) Bars and Grids", International Organization for Standardization, Geneva, Switzerland;
56. JSCE (1997), "Recommendation for Design and Construction of Concrete Structures Using Continuous Fiber Reinforcing Materials", Research Committee on Continuous Fiber Reinforcing Materials, Japan Society of Civil Engineers, Tokyo, 325 p;
57. Kanakubo, T., and Shindo, M. "Shear Behaviour of Fiber-Mesh Reinforced Plates," Third International Symposium on Non-Metallic (FRP) Reinforcement for Concrete Structures, Sapporo, Japan, 1997, p. 317-324;
58. Kanematsu, H., Sato, Y., Ueda, T., and Kakuta, Y. "A study on failure criteria of FRP rods subject to tensile and shear force." Proc. FIP '93 Symp.–

Modern Prestressing Techniques and their Applications, Japan Prestressed Concrete Engineering Association, Tokyo, 1993:Vol. 2, p. 743-750;

59. Kotsovos, M. D., and Pavlovic, M. N. "Ultimate Limit State Design of Concrete Structures - A New Approach", Thomas Telford, Ltd., London, 1999;
60. Kulkarni, S., 2006, "Calibration of flexural design of concrete members reinforced with FRP bars", Thesis for Master of Science in civil engineering. Graduate Faculty of the Louisiana State University and Agricultural and Mechanical College;
61. Laoubi, L., El-Salakay, E., and Benmokrane, B., 2006, "Creep and durability of sand-coated glass FRP bars in concrete elements under freeze/thaw cycling and sustained loads", Cement & Concrete Composites 28 (2006) 869–878;
62. La Tegola, A., 1998, Actions for Verification of RC Structures with FRP Bars, Journal of Composites for Construction;
63. Lubell, A.; Sherwrvod, T.;Bents, E.; and Collins, M. P. "Safe Shear Design of Large, Wide Beams", Concrete International, 2004, V. 26, No. l, p. 67-79;
64. Malvar, J. L., "Technical Report: Bond Stress Slip Characteristics of FRP Bars," Naval Facilities Engineering Service Center, Port Hueneme, CA, Feb. 1994, 45 pp;
65. Maruyama, K., and Zhao, W. J. (1994). "*Flexural and Shear Behaviour of Concrete Beams Reinforced with FRP Rods*" Corrosion and Corrosion Protection of Steel in Concrete, Swamy, R.N. (ed), University of Sheffield, UK, p. 1330-1339;
66. Maruyama, K., and Zhao, W. (1996). "*Size Effect in Shear Behavior of FRP Reinforced Concrete Beams*" Advanced Composite Materials in Bridges and Structures, Montreal, Quebec, p. 227-234;
67. Masmoudi, R., Theriault, M., and Benmokrane, B., 1998, "Flexural Behavior of Concrete Beams Reinforced with Deformed Fiber Reinforced Plastic Reinforcing Rods", ACI Structural Journal, V. 95, No. 6, pp. 665-676;
68. Meier, U., 1992, "Carbon Fiber Reinforced Polymers: Modern Materials in Bridge Engineering," *Structural Engineering International,* Journal of the

International Association for Bridge and Structural Engineering, V. 2, No. 1, pp. 7-12;

69. Michaluk, C.R., Rizkalla, S.H., Tadros, G. and Benmokrane, B. "*Flexural Behaviour of One-Way Concrete Slabs Reinforced by Fiber Reinforcing Plastic Reinforcement*", ACI Structural Journal, 1998, 95(3), p. 353-365;
70. Mizukawa, Y., Sato, Y., Ueda, T., and Kakuta, Y. "A Study on Shear Fatigue Behavior of Concrete Beams with FRP Rods" Proceedings of the Third International Symposium on Non-Metallic (FRP) Reinforcement for Concrete Structures (FRPRCS-3), Japan Concrete Institute, Sapporo, Japan, 1997, V.2, p. 309-316;
71. Monti, G., and Santini, S., 2002, "Reliability-based Calibration of Partial Safety Coefficients for Fiber-Reinforced Plastic", Journal of Composites for Construction, Vol. 6, No. 3, pp. 162-167;
72. Nagasaka, T., Fukuyama, H., and Tanigaki, M. "Shear performance of concrete beams reinforced with FRP stirrups". In ACI SP-138. Edited by A. Nanni and C. Dolan. American Concrete Institute, Detroit, Mich., 1993, p. 789–811.
73. Nakamura, H., and Higai, T., "Evaluation of Shear Strength of Concrete Beams Reinforced with FRP", Concrete Library International, Proceedings of Japan Society of Civil Engineers. No 26, 1995, p. 111-123.
74. Nanni, A., 1993, "Flexural Behavior and Design of Reinforced Concrete Using FRP Rods," *Journal of Structural Engineering*, V. 119, No. 11, pp. 3344-3359;
75. Nanni, A., Al-Zahrani, M. M., Al-Duajani, S. U., Bakis, C. E., and Boothby, T. E., "Bond of FRP Reinforcement to Concrete-Experimental Results," Non-Metallic Reinforcement (FRP) for Concrete Structures, Proceedings of the Second International Symposium, 1995, L. Taerwe, Editor, pp. 135-145;
76. Nanni, A., "Composites: Coming on Strong," *Concrete Construction*, Vol. 44, 1999;
77. Nanni, A., 2001, "Relevant Field Application of FRP Composites in Concrete Structures", *Proceedings of the International Conference Composites in*

Construction – CCC2001, J. Figueras, L. Juvandes, and R. Faria, Eds., Portugal, pp. 661-670;

78. Neocleous, K., Pilakoutas, K., and Waldron, P., 1999, "Structural reliability for fibre reinforced polymer reinforced concrete structures". Proceeding of the 4th International Symposium on Fibre Reinforced Polymers for Reinforced Concrete Structures, p. 65–74;
79. Nowak A. S., and Collins K. R., "*Reliability of Structures*", McGraw-Hill. 2000;
80. Nowak A.S., Szerszen M.M., 2003, "*Calibration of Design Code, for Buildings (ACI318): Part 1 - Statistical Models for Resistance*", Structural Journal, ACI, Vol.100, No.3, pp. 377-382;
81. Okeil, A., El-Tawil, S., and Shahawy, M., 2002, "*Flexural Reliability of Reinforced Concrete Bridge Girders Strengthened with CFRP Laminates*", Journal of Bridge Engineering, Vol.7, No. 5, pp. 290-299;
82. Okeil, A. M., El-Tawil, S., and Shahawy, M. (2001). "*Short-term tensile strength of CFRP laminates for flexural strengthening of concrete girders*" ACI Struct. J., 98(4), 470–478;
83. Orangun, C. O., Jirsa, J. O., and Breen, J. E., "A Revaluation of Test Data on Development Length and Splices," ACI Journal, Proceedings V.74, No.3, Mar. 1977, pp. 114-122;
84. Pay, A.C., 2005, Bond Behavior of Unconfined Steel and FRP Bar Splices in Concrete Beams, Purdue University, PhD Thesis;
85. Pecce M, Manfredi G, and Cosenza E, 2000, "Experimental Response and Code Models of GFRP RC Beams in Bending", Journal of Composites for Costruction, Vol. 4, No. 4, November 2000, pp. 182-190;
86. Pecce M., Manfredi G., Cosenza E., "A Probabilistic Assessment of Deflections in FRP RC Beams", Proceedings of the Fifth Conference on Non-Metallic Reinforcement for Concrete Structures, FRPRCS5, Cambridge, UK, 16-18 July 2001;

87. Pilakoutas, K., Neocleous, K., and Guadagnini, M., "Design philosophy issues of fibre reinforced polymer reinforced concrete structures". Journal of Composites for Construction, ASCE 2002;6(3):154–61;
88. Plecnik, J., and Ahmad, S. H., 1988, "Transfer of Composite Technology to Design and Construction of Bridges," *Final Report* to USDOT, Contract No. DTRS 5683-C000043;
89. Plevris, N., Triantafillou, T. C., and Veneziano, D., 1995, "Reliability of RC members strengthened with CFRP laminates", Journal of structural engineering, ASCE;
90. Priestley, M. N.; Seible, F.; and Calvi, G. M., 1996, "*Seismic Design and Retrofit of Bridges*", John Wiley and Sons, New York, 704 p.
91. Rafi M. M, Nadjai, F. A., and Talamona, D., 2006, "Aspects of behaviour of CFRP reinforced concrete beams in bending", Construction and Building Materials, article in press ;
92. Razaqpur, A. G., Isgor, B. O., Greenaway, S., and Selley, A. "Concrete Contribution to the Shear Resistance of Fiber Reinforced Polymer Reinforced Concrete Members" Journal of Composites for Construction, ASCE, 2004, Vo. 8, No. 5, p. 452-460.
93. Razaqpur, A.G. and Isgor, O.B. "Proposed Shear Design Method for FRP-Reinforced Concrete Members without Stirrups", ACI Structural Journal, 2006; 103(1), p. 93-102;
94. Rizkalla, S. H., 1997, "A New Generation of Civil Engineering Structures and Bridges," Proceedings of the Third International Symposium on Non-Metallic (FRP) Reinforcement for Concrete Structures (FRPRCS-3), Sapporo, Japan, Vol. 1, pp. 113-128;
95. Saadatmanech, H., 1994, Fiber Composites for New and existing Structures, ACI Structural Journal, V.91, No. 3;
96. Santini, R., 2007, "Metodi di Calibrazione del Coefficiente Parziale di Sicurezza γ_f per Elementi in C.A. con Barre di FRP", Thesis, Dept. of Struct. Eng., Univ. of Naples, Italy;

97. Shehata, E. (1999). "*FRP for shear reinforcement in concrete structures*". Ph.D. thesis, Department of Civil and Geological Engineering, The University of Manitoba, Winnipeg, Man.
98. Shehata, E., Morphy R.,, and Rizkalla, S. (2000), "*Fibre Reinforced Polymer Shear Reinforcement for Concrete Members: Behaviour and Design Guidelines*," Canadian Journal of Civil Engineering, V. 27 (5), p. 859-872.
99. Sommese, G., 2007, "Modelli di Deformabilità per Travi in C.A. Armate con Barre in FRP", Thesis, Dept. of Struct. Eng., Univ. of Naples, Italy;
100. Sørensen, J.D., S.O. Hansen & T. Arnbjerg Nielsen, "Calibration of Partial Safety Factors for Danish Structural Codes", Proc. IABSE Conf. Safety, Risk and Reliability – Trends in Engineering,Malta, 2001, IABSE, Zürich, pp. 179-184.
101. Spitaleri, G., and Totaro, N., 2006, "Calibration of Resistance Factors for FRP Flexural Strengthening of RC Beams in the European Format", 2nd International fib Congress, June 5-8, 2006 - Naples, Italy;
102. Stratford, T. J., and Burgoyne, C. J. "Crack-Based Analysis of Concrete with Reinforcement" Magazine of Concrete Research, V. 54, 2002, p. 321-332.
103. Stratford, T. and Burgoyne, C.J. "Shear Analysis of Concrete with Brittle Reinforcement", Journal of Composites for Construction, ASCE, 2003, p. 323-330.
104. Swamy, N., and Aburawi, M. "Structural Implications of Using GFRP Bars as Concrete Reinforcement" Proceedings of the Third International Symposium on Non-Metallic (FRP) Reinforcement for Concrete Structures (FRPRCS-3), Japan Concrete Institute, Sapporo, Japan, 1997, V.2, p. 503-510.
105. Taerwe, L., 1997, "FRP Activities in Europe: Survey of Research and Applications," Proceedings of the Third International Symposium on Non-Metallic (FRP) Reinforcement for Concrete Structures (FRPRCS-3), V. 1, Japan Concrete Institute, Tokyo, Japan, pp. 59-74;

106. Tariq, M., and Newhook, J. P. “Shear Testing of FRP reinforced Concrete without Transverse Reinforcement” Proceedings of CSCE 2003-Anuual Conference, Moncton, NB, Canada, (on CD-Rom), 2003, 10p.

107. Taylor, H. P. J. "Investigation of the Forces Carried Across Cracks in Reinforced Concrete Beams in Shear by Interlock of Aggregate." 42.447, Cement and Concrete Association, London, 1970;

108. Tepfers, R., “Tensile lap splices with confining reinforcement,” Contribution to the International Conference on Bond in Concrete, Paisley, Scotland, June 14th-l6th 1982, pp. 318-330;

109. Theriault, M., and Benmokrane, B., 1998, “Effects of FRP Reinforcement Ratio and Concrete Strength on Flexural Behavior of Concrete Beams”, Journal of Composites for Construction, Vol. 2, No. 1, pp.7-16;

110. Tottori, S., and Wakui, H. “Shear capacity of RC and PC beams using FRP reinforcement”. ACI SP-138. Edited by A. Nanni and C. Dolan. American Concrete Institute, Detroit, Mich., 1993, p. 615–631;

111. Toutanji H. A., M. Saafi, “Flexural Behavior of Concrete Beams Reinforced with Glass Fiber-Reinforced Polymer (GFRP) Bars”, ACI Structural Journal/September-October 2000;

112. Toutanji H., and Deng, Y., 2003, “Deflection and crack-width prediction of concrete beams reinforced with glass FRP rods”, Construction and Building Materials, 17, pp. 69-74;

113. Tureyen, A. K., and Frosch, R. J. “Shear Tests of FRP-Reinforced Concrete Beams without Stirrups” ACI Structural Journal, V. 99, No. 4, 2002, p.427-434.

114. Tureyen, A. K. and Frosch, R. J. “Concrete Shear Strength: Another Perspective”, ACI Structural Journal, V. 100, No. 5, 2003, p.609-615.

115. Vijay, P. V., Kumar, S. V., and GangaRao, H. V. S. "Shear and Ductility Behavior of Concrete Beams Reinforced with GFRP Rebars" Advanced Composite Materials in Bridges and Structures, Montreal, Quebec, 1996, p. 217-227.

116. Walraven, J. C. "Fundamental Analysis of Aggregate Interlock." Journal of the Structural Division, Proceedings of the American Society of Civil Engineering, 107 (No. ST11), 1981. p. 2245-2269;

117. Whitehead, P.A. and Ibell, T.J. (2005), "*Novel Shear Reinforcement for Fiber-Reinforced Polymer-Reinforced and Prestressed Concrete*", ACI Structural Journal, V.102, No. 2, p. 286-294.

118. Yost, J. R. "Fiber reinforced plastic grids for the structural reinforcement of concrete beams" PhD dissertation, University of New Hampshire, Durham, N.H., 1993;

119. Yost, J. R., Gross, S. P., and Dinehart, D. W. "Shear Strength of Normal Strength Concrete Beams Reinforced with Deformed GFRP Bars" Journal of Composites for Construction, ASCE, 2001, V. 5, No. 4, p. 263-275.

120. Yost, J. R., Gross, S. P., and Dinehart, D. W., 2003, "Effective Moment of Inertia for Glass Fiber-Reinforced Polymer-Reinforced Concrete Beams", ACI Structural Journal, V. 100, No. 6;

121. Zhao, W., Maruyama, K., and Suzuki, H. "Shear behaviour of concrete beams reinforced by FRP rods as longitudinal and shear reinforcement" Non-metallic (FRP) reinforcement for concrete structures. Proceedings of the Second International RILEM Symposium (FRPRCS-2). Edited by L. Taerwe. E & FN Spon, London, Great Britain, 1995, p. 352–359.

122. Zhao, W., Pilakoutas, K., Waldron, P. "FRP Reinforced Concrete: Calculations for Deflections", Non-metallic (FRP) Reinforcement for Concrete Structures (FRPRCS-3), Vol., 2, p. 511–518, Japan Concrete Institute, 1997a;

123. Zhao, W., Pilakoutas, K. and Waldron, P. "FRP Reinforced Concrete: Cracking Behaviour and Determination", Non-metallic (FRP) Reinforcement for Concrete Structures (FRPRCS-3), Vol. 2, p. 439–446, Japan Concrete Institute, 1997b;

Appendix A: DESIGN CASES

Design case **CA.dB.bA.R0.5.G** means:
f_c = nominal value **A**;
d = nominal value **B**;
b = nominal value **A**;
ρ_f/ρ_{fb} = **0.5**;
reinforcement type = **G**FRP

Table 1 - Material Properties and Fabrication Descriptors for FRP-RC Beams

No.	Design Case	M_r [KN·m]	Mean μ_{Mr}	Standard Deviation σ_{Mr}	Bias λ_{MF}	COV V_{MF} [%]
1	CA.dA.bA.R0,1.G	3,65	4,37	0,51	1,20	11,76
2	CB.dA.bA.R0,1.G	6,75	8,08	0,95	1,20	11,74
3	CA.dA.bB.R0,1.G	57,11	69,32	6,91	1,21	9,97
4	CB.dA.bB.R0,1.G	105,41	127,92	12,75	1,21	9,97
5	CA.dB.bA.R0,1.G	20,62	25,01	2,51	1,21	10,02
6	CB.dB.bA.R0,1.G	38,05	46,18	4,57	1,21	9,90
7	CA.dB.bB.R0,1.G	322,12	393,06	37,91	1,22	9,65
8	CB.dB.bB.R0,1.G	594,57	725,56	69,90	1,22	9,63
9	CA.dA.bA.R0,2.G	7,30	8,72	1,02	1,20	11,71
10	CB.dA.bA.R0,2.G	13,47	16,11	1,90	1,20	11,77
11	CA.dA.bB.R0,2.G	114,00	138,42	13,68	1,21	9,89
12	CB.dA.bB.R0,2.G	210,43	255,06	25,20	1,21	9,88
13	CA.dB.bA.R0,2.G	41,16	49,95	4,96	1,21	9,94
14	CB.dB.bA.R0,2.G	75,96	92,00	9,17	1,21	9,97
15	CA.dB.bB.R0,2.G	643,05	784,15	74,99	1,22	9,56
16	CB.dB.bB.R0,2.G	1186,94	1446,30	138,46	1,22	9,57
17	CA.dA.bA.R0,3.G	10,92	13,06	1,52	1,20	11,65
18	CB.dA.bA.R0,3.G	20,15	24,05	2,83	1,19	11,77
19	CA.dA.bB.R0,3.G	170,61	206,79	20,48	1,21	9,90
20	CB.dA.bB.R0,3.G	314,91	381,40	37,45	1,21	9,82
21	CA.dB.bA.R0,3.G	61,59	74,63	7,38	1,21	9,89
22	CB.dB.bA.R0,3.G	113,68	137,69	13,51	1,21	9,81
23	CA.dB.bB.R0,3.G	962,33	1173,20	111,29	1,22	9,49
24	CB.dB.bB.R0,3.G	1776,27	2161,80	204,70	1,22	9,47
25	CA.dA.bA.R0,4.G	14,51	17,34	2,03	1,19	11,70
26	CB.dA.bA.R0,4.G	26,79	31,95	3,69	1,19	11,55
27	CA.dA.bB.R0,4.G	226,79	274,70	26,72	1,21	9,73
28	CB.dA.bB.R0,4.G	418,61	505,99	48,68	1,21	9,62
29	CA.dB.bA.R0,4.G	81,87	99,09	9,73	1,21	9,82
30	CB.dB.bA.R0,4.G	151,12	182,50	17,68	1,21	9,68
31	CA.dB.bB.R0,4.G	1279,25	1558,00	144,91	1,22	9,30
32	CB.dB.bB.R0,4.G	2361,23	2867,20	265,84	1,21	9,27
33	CA.dA.bA.R0,5.G	18,07	21,53	2,50	1,19	11,59
34	CB.dA.bA.R0,5.G	33,35	39,57	4,59	1,19	11,59

35	CA.dA.bB.R0,5.G	282,35	341,05	32,65	1,21	9,57
36	CB.dA.bB.R0,5.G	521,16	627,25	59,64	1,20	9,51
37	CA.dB.bA.R0,5.G	101,93	123,13	11,93	1,21	9,68
38	CB.dB.bA.R0,5.G	188,14	226,40	21,57	1,20	9,53
39	CA.dB.bB.R0,5.G	1592,62	1933,80	179,22	1,21	9,27
40	CB.dB.bB.R0,5.G	2939,64	3558,70	323,44	1,21	9,09
41	CA.dA.bA.R0,6.G	21,56	25,60	2,96	1,19	11,56
42	CB.dA.bA.R0,6.G	39,80	46,96	5,36	1,18	11,41
43	CA.dA.bB.R0,6.G	336,90	406,13	38,00	1,21	9,36
44	CB.dA.bB.R0,6.G	621,85	745,06	67,13	1,20	9,01
45	CA.dB.bA.R0,6.G	121,62	146,48	13,76	1,20	9,39
46	CB.dB.bA.R0,6.G	224,49	269,27	24,50	1,20	9,10
47	CA.dB.bB.R0,6.G	1900,35	2304,40	204,71	1,21	8,88
48	CB.dB.bB.R0,6.G	3507,65	4232,20	357,34	1,21	8,44
49	CA.dA.bA.R0,7.G	24,97	29,35	3,38	1,18	11,51
50	CB.dA.bA.R0,7.G	46,09	53,21	5,94	1,15	11,16
51	CA.dA.bB.R0,7.G	390,20	466,37	41,54	1,20	8,91
52	CB.dA.bB.R0,7.G	720,23	846,71	62,31	1,18	7,36
53	CA.dB.bA.R0,7.G	140,86	168,40	15,21	1,20	9,03
54	CB.dB.bA.R0,7.G	260,00	305,86	23,29	1,18	7,61
55	CA.dB.bB.R0,7.G	2200,99	2647,40	221,37	1,20	8,36
56	CB.dB.bB.R0,7.G	4062,57	4811,90	311,04	1,18	6,46
57	CA.dA.bA.R0,8.G	28,33	32,56	3,79	1,15	11,65
58	CB.dA.bA.R0,8.G	52,29	58,02	6,32	1,11	10,90
59	CA.dA.bB.R0,8.G	442,67	516,75	43,94	1,17	8,50
60	CB.dA.bB.R0,8.G	817,07	922,51	57,42	1,13	6,22
61	CA.dB.bA.R0,8.G	159,80	187,06	15,99	1,17	8,55
62	CB.dB.bA.R0,8.G	294,96	334,00	21,68	1,13	6,49
63	CA.dB.bB.R0,8.G	2496,92	2936,80	228,94	1,18	7,80
64	CB.dB.bB.R0,8.G	4608,79	5247,50	252,39	1,14	4,81
65	CA.dA.bA.R0,9.G	31,64	35,09	4,16	1,11	11,86
66	CB.dA.bA.R0,9.G	58,39	61,81	6,68	1,06	10,81
67	CA.dA.bB.R0,9.G	494,31	557,16	45,76	1,13	8,21
68	CB.dA.bB.R0,9.G	912,40	981,52	55,96	1,08	5,70
69	CA.dB.bA.R0,9.G	178,45	201,83	16,88	1,13	8,36
70	CB.dB.bA.R0,9.G	329,38	355,52	21,31	1,08	6,00
71	CA.dB.bB.R0,9.G	2788,23	3169,20	233,68	1,14	7,37
72	CB.dB.bB.R0,9.G	5146,49	5582,50	230,35	1,08	4,13
73	CA.dA.bA.R0,95.G	33,27	36,20	4,35	1,09	12,01
74	CB.dA.bA.R0,95.G	61,41	63,45	6,83	1,03	10,76
75	CA.dA.bB.R0,95.G	519,83	574,47	46,70	1,11	8,13
76	CB.dA.bB.R0,95.G	959,49	1007,50	55,70	1,05	5,53
77	CA.dB.bA.R0,95.G	187,66	208,09	17,27	1,11	8,30
78	CB.dB.bA.R0,95.G	346,38	364,92	21,21	1,05	5,81
79	CA.dB.bB.R0,95.G	2932,15	3264,30	239,29	1,11	7,33
80	CB.dB.bB.R0,95.G	5412,13	5729,30	224,75	1,06	3,92
81	CA.dA.bA.R1.G	34,89	37,19	4,48	1,07	12,04
82	CB.dA.bA.R1.G	64,40	65,02	7,01	1,01	10,78
83	CA.dA.bB.R1.G	545,14	590,23	48,01	1,08	8,13
84	CB.dA.bB.R1.G	1006,21	1031,30	56,22	1,02	5,45

85	CA.dB.bA.R1.G	196,79	213,82	17,65	1,09	8,25
86	CB.dB.bA.R1.G	363,24	373,78	21,52	1,03	5,76
87	CA.dB.bB.R1.G	3074,92	3357,20	242,44	1,09	7,22
88	CB.dB.bB.R1.G	5675,64	5867,50	223,06	1,03	3,80
89	CA.dA.bA.R1,1.G	36,30	39,12	4,11	1,08	10,52
90	CB.dA.bA.R1,1.G	67,00	68,04	6,28	1,02	9,23
91	CA.dA.bB.R1,1.G	567,20	619,68	44,18	1,09	7,13
92	CB.dA.bB.R1,1.G	1046,93	1078,30	49,29	1,03	4,57
93	CA.dB.bA.R1,1.G	204,76	224,66	16,36	1,10	7,28
94	CB.dB.bA.R1,1.G	377,94	390,91	18,80	1,03	4,81
95	CA.dB.bB.R1,1.G	3199,36	3521,90	224,42	1,10	6,37
96	CB.dB.bB.R1,1.G	5905,34	6127,70	209,15	1,04	3,41
97	CA.dA.bA.R1,2.G	37,63	40,68	4,33	1,08	10,65
98	CB.dA.bA.R1,2.G	69,45	70,64	6,53	1,02	9,25
99	CA.dA.bB.R1,2.G	587,93	644,61	45,18	1,10	7,01
100	CB.dA.bB.R1,2.G	1085,20	1119,20	49,29	1,03	4,40
101	CA.dB.bA.R1,2.G	212,24	233,69	16,74	1,10	7,16
102	CB.dB.bA.R1,2.G	391,76	405,91	19,06	1,04	4,70
103	CA.dB.bB.R1,2.G	3316,31	3664,40	229,46	1,10	6,26
104	CB.dB.bB.R1,2.G	6121,20	6360,20	199,81	1,04	3,14
105	CA.dA.bA.R1,25.G	38,26	41,44	4,42	1,08	10,67
106	CB.dA.bA.R1,25.G	70,62	71,91	6,59	1,02	9,17
107	CA.dA.bB.R1,25.G	597,86	656,26	45,94	1,10	7,00
108	CB.dA.bB.R1,25.G	1103,51	1138,70	49,95	1,03	4,39
109	CA.dB.bA.R1,25.G	215,83	238,11	17,04	1,10	7,16
110	CB.dB.bA.R1,25.G	398,37	412,73	19,32	1,04	4,68
111	CA.dB.bB.R1,25.G	3372,28	3731,50	234,76	1,11	6,29
112	CB.dB.bB.R1,25.G	6224,51	6471,70	198,34	1,04	3,06
113	CA.dA.bA.R1,3.G	38,88	42,14	4,50	1,08	10,69
114	CB.dA.bA.R1,3.G	71,76	73,11	6,71	1,02	9,18
115	CA.dA.bB.R1,3.G	607,51	668,01	46,76	1,10	7,00
116	CB.dA.bB.R1,3.G	1121,33	1156,80	50,63	1,03	4,38
117	CA.dB.bA.R1,3.G	219,31	242,29	17,28	1,10	7,13
118	CB.dB.bA.R1,3.G	404,80	419,68	19,50	1,04	4,65
119	CA.dB.bB.R1,3.G	3426,71	3795,40	239,45	1,11	6,31
120	CB.dB.bB.R1,3.G	6324,98	6577,30	199,74	1,04	3,04
121	CA.dA.bA.R1,35.G	39,48	42,83	4,57	1,08	10,66
122	CB.dA.bA.R1,35.G	72,87	74,25	6,83	1,02	9,20
123	CA.dA.bB.R1,35.G	616,90	678,86	47,84	1,10	7,05
124	CB.dA.bB.R1,35.G	1138,67	1175,60	51,25	1,03	4,36
125	CA.dB.bA.R1,35.G	222,70	246,03	17,57	1,10	7,14
126	CB.dB.bA.R1,35.G	411,06	426,30	19,69	1,04	4,62
127	CA.dB.bB.R1,35.G	3479,70	3858,60	241,58	1,11	6,26
128	CB.dB.bB.R1,35.G	6422,79	6681,30	202,63	1,04	3,03
129	CA.dA.bA.R1,4.G	40,07	43,53	4,66	1,09	10,71
130	CB.dA.bA.R1,4.G	73,96	75,32	6,97	1,02	9,25
131	CA.dA.bB.R1,4.G	626,05	689,70	48,15	1,10	6,98
132	CB.dA.bB.R1,4.G	1155,56	1193,50	51,99	1,03	4,36
133	CA.dB.bA.R1,4.G	226,01	249,96	17,92	1,11	7,17
134	CB.dB.bA.R1,4.G	417,16	432,81	19,90	1,04	4,60

135	CA.dB.bB.R1,4.G	3531,33	3915,10	245,55	1,11	6,27
136	CB.dB.bB.R1,4.G	6518,09	6781,60	203,84	1,04	3,01
137	CA.dA.bA.R1,5.G	41,20	44,80	4,81	1,09	10,73
138	CB.dA.bA.R1,5.G	76,04	77,47	7,11	1,02	9,17
139	CA.dA.bB.R1,5.G	643,69	709,39	49,96	1,10	7,04
140	CB.dA.bB.R1,5.G	1188,11	1227,30	52,97	1,03	4,32
141	CA.dB.bA.R1,5.G	232,37	257,35	18,50	1,11	7,19
142	CB.dB.bA.R1,5.G	428,91	445,03	20,57	1,04	4,62
143	CA.dB.bB.R1,5.G	3630,81	4032,60	253,14	1,11	6,28
144	CB.dB.bB.R1,5.G	6701,70	6978,10	207,97	1,04	2,98
145	CA.dA.bA.R1,6.G	42,27	45,90	4,95	1,09	10,79
146	CB.dA.bA.R1,6.G	78,03	79,50	7,38	1,02	9,28
147	CA.dA.bB.R1,6.G	660,51	728,21	51,49	1,10	7,07
148	CB.dA.bB.R1,6.G	1219,15	1259,80	54,67	1,03	4,34
149	CA.dB.bA.R1,6.G	238,44	264,00	19,14	1,11	7,25
150	CB.dB.bA.R1,6.G	440,11	456,97	21,00	1,04	4,60
151	CA.dB.bB.R1,6.G	3725,66	4143,10	260,91	1,11	6,30
152	CB.dB.bB.R1,6.G	6876,78	7162,00	211,89	1,04	2,96
153	CA.dA.bA.R1,7.G	43,30	47,15	5,08	1,09	10,77
154	CB.dA.bA.R1,7.G	79,92	81,48	7,58	1,02	9,31
155	CA.dA.bB.R1,7.G	676,58	746,77	52,55	1,10	7,04
156	CB.dA.bB.R1,7.G	1248,83	1291,30	56,25	1,03	4,36
157	CA.dB.bA.R1,7.G	244,25	270,89	19,58	1,11	7,23
158	CB.dB.bA.R1,7.G	450,83	468,13	21,56	1,04	4,61
159	CA.dB.bB.R1,7.G	3816,34	4244,50	269,08	1,11	6,34
160	CB.dB.bB.R1,7.G	7044,15	7337,70	217,20	1,04	2,96
161	CA.dA.bA.R1,8.G	44,29	48,26	5,21	1,09	10,80
162	CB.dA.bA.R1,8.G	81,74	83,35	7,74	1,02	9,28
163	CA.dA.bB.R1,8.G	691,98	764,18	54,23	1,10	7,10
164	CB.dA.bB.R1,8.G	1277,26	1321,00	57,67	1,03	4,37
165	CA.dB.bA.R1,8.G	249,81	277,24	20,09	1,11	7,25
166	CB.dB.bA.R1,8.G	461,09	478,85	22,04	1,04	4,60
167	CA.dB.bB.R1,8.G	3903,22	4343,30	275,21	1,11	6,34
168	CB.dB.bB.R1,8.G	7204,52	7506,50	222,22	1,04	2,96
169	CA.dA.bA.R1,9.G	45,23	49,30	5,31	1,09	10,77
170	CB.dA.bA.R1,9.G	83,49	85,18	7,91	1,02	9,29
171	CA.dA.bB.R1,9.G	706,77	780,86	55,30	1,10	7,08
172	CB.dA.bB.R1,9.G	1304,55	1349,50	58,94	1,03	4,37
173	CA.dB.bA.R1,9.G	255,14	283,25	20,65	1,11	7,29
174	CB.dB.bA.R1,9.G	470,94	489,33	22,65	1,04	4,63
175	CA.dB.bB.R1,9.G	3986,64	4435,80	282,29	1,11	6,36
176	CB.dB.bB.R1,9.G	7358,49	7668,70	229,12	1,04	2,99
177	CA.dA.bA.R2,0.G	46,14	50,35	5,47	1,09	10,86
178	CB.dA.bA.R2,0.G	85,17	86,87	8,09	1,02	9,32
179	CA.dA.bB.R2,0.G	721,00	796,97	56,77	1,11	7,12
180	CB.dA.bB.R2,0.G	1330,81	1376,90	60,31	1,03	4,38
181	CA.dB.bA.R2,0.G	260,28	289,15	21,06	1,11	7,28
182	CB.dB.bA.R2,0.G	480,42	499,08	23,16	1,04	4,64
183	CA.dB.bB.R2,0.G	4066,87	4530,60	290,32	1,11	6,41
184	CB.dB.bB.R2,0.G	7506,57	7826,20	235,35	1,04	3,01

185	CA.dA.bA.R2,1.G	47,02	51,29	5,62	1,09	10,96
186	CB.dA.bA.R2,1.G	86,79	88,54	8,25	1,02	9,32
187	CA.dA.bB.R2,1.G	734,70	812,84	58,32	1,11	7,17
188	CB.dA.bB.R2,1.G	1356,10	1403,00	61,93	1,03	4,41
189	CA.dB.bA.R2,1.G	265,23	294,81	21,67	1,11	7,35
190	CB.dB.bA.R2,1.G	489,55	508,79	23,68	1,04	4,65
191	CA.dB.bB.R2,1.G	4144,16	4617,80	295,42	1,11	6,40
192	CB.dB.bB.R2,1.G	7649,24	7976,40	239,06	1,04	3,00
193	CA.dA.bA.R2,2.G	47,87	52,23	5,74	1,09	11,00
194	CB.dA.bA.R2,2.G	88,35	90,17	8,43	1,02	9,35
195	CA.dA.bB.R2,2.G	747,92	827,98	59,34	1,11	7,17
196	CB.dA.bB.R2,2.G	1380,50	1428,70	62,65	1,03	4,38
197	CA.dB.bA.R2,2.G	270,00	300,47	22,04	1,11	7,34
198	CB.dB.bA.R2,2.G	498,36	518,23	24,15	1,04	4,66
199	CA.dB.bB.R2,2.G	4218,73	4704,00	302,29	1,12	6,43
200	CB.dB.bB.R2,2.G	7786,89	8120,60	244,24	1,04	3,01
201	CA.dA.bA.R2,3.G	48,68	53,21	5,82	1,09	10,93
202	CB.dA.bA.R2,3.G	89,86	91,75	8,58	1,02	9,35
203	CA.dA.bB.R2,3.G	760,69	842,24	60,49	1,11	7,18
204	CB.dA.bB.R2,3.G	1404,08	1453,20	64,04	1,03	4,41
205	CA.dB.bA.R2,3.G	274,61	305,42	22,51	1,11	7,37
206	CB.dB.bA.R2,3.G	506,87	527,31	24,63	1,04	4,67
207	CA.dB.bB.R2,3.G	4290,78	4788,20	308,38	1,12	6,44
208	CB.dB.bB.R2,3.G	7919,88	8259,40	248,33	1,04	3,01
209	CA.dA.bA.R2,4.G	49,48	54,06	5,95	1,09	11,01
210	CB.dA.bA.R2,4.G	91,32	93,28	8,76	1,02	9,40
211	CA.dA.bB.R2,4.G	773,05	856,54	61,88	1,11	7,22
212	CB.dA.bB.R2,4.G	1426,89	1476,90	65,25	1,04	4,42
213	CA.dB.bA.R2,4.G	279,07	310,55	22,88	1,11	7,37
214	CB.dB.bA.R2,4.G	515,11	535,66	24,99	1,04	4,67
215	CA.dB.bB.R2,4.G	4360,48	4866,00	314,46	1,12	6,46
216	CB.dB.bB.R2,4.G	8048,52	8391,30	256,11	1,04	3,05
217	CA.dA.bA.R2,5.G	50,24	54,93	6,02	1,09	10,95
218	CB.dA.bA.R2,5.G	92,73	94,78	8,88	1,02	9,37
219	CA.dA.bB.R2,5.G	785,02	869,88	63,18	1,11	7,26
220	CB.dA.bB.R2,5.G	1448,97	1500,30	66,79	1,04	4,45
221	CA.dB.bA.R2,5.G	283,39	315,24	23,32	1,11	7,40
222	CB.dB.bA.R2,5.G	523,08	544,21	25,48	1,04	4,68
223	CA.dB.bB.R2,5.G	4427,98	4943,40	320,87	1,12	6,49
224	CB.dB.bB.R2,5.G	8173,12	8528,30	257,64	1,04	3,02
225	CA.dA.bA.R2,6.G	50,98	55,72	6,12	1,09	10,98
226	CB.dA.bA.R2,6.G	94,10	96,15	9,01	1,02	9,37
227	CA.dA.bB.R2,6.G	796,62	883,36	64,41	1,11	7,29
228	CB.dA.bB.R2,6.G	1470,39	1521,90	67,45	1,04	4,43
229	CA.dB.bA.R2,6.G	287,58	320,19	23,74	1,11	7,41
230	CB.dB.bA.R2,6.G	530,81	552,26	25,94	1,04	4,70
231	CA.dB.bB.R2,6.G	4493,42	5019,40	327,20	1,12	6,52
232	CB.dB.bB.R2,6.G	8293,91	8654,20	265,14	1,04	3,06
233	CA.dA.bA.R2,7.G	51,70	56,57	6,25	1,09	11,05
234	CB.dA.bA.R2,7.G	95,43	97,44	9,19	1,02	9,43

235	CA.dA.bB.R2,7.G	807,88	895,45	65,03	1,11	7,26
236	CB.dA.bB.R2,7.G	1491,17	1544,40	68,99	1,04	4,47
237	CA.dB.bA.R2,7.G	291,64	325,09	24,28	1,11	7,47
238	CB.dB.bA.R2,7.G	538,31	560,32	26,38	1,04	4,71
239	CA.dB.bB.R2,7.G	4556,93	5097,40	331,42	1,12	6,50
240	CB.dB.bB.R2,7.G	8411,13	8779,60	268,86	1,04	3,06

Table 2 - Material Properties and Fabrication descriptors for FRP-RC Slabs

No.	Design Case	M_r [KN·m]	Mean μ_{Mr}	Standard Deviation σ_{Mr}	Bias λ_{MF}	COV V_{MF} [%]
1	CA.dA.R0,1.G	3,17	3,68	0,67	1,16	18,11
2	CB.dA.R0,1.G	5,86	6,80	1,23	1,16	18,12
3	CA.dB.R0,1.G	19,83	23,76	2,76	1,20	11,63
4	CB.dB.R0,1.G	36,60	43,85	5,09	1,20	11,61
5	CA.dC.R0,1.G	50,76	61,32	6,42	1,21	10,47
6	CB.dC.R0,1.G	93,70	113,24	11,72	1,21	10,35
7	CA.dA.R0,2.G	6,33	7,34	1,34	1,16	18,23
8	CB.dA.R0,2.G	11,69	13,55	2,48	1,16	18,33
9	CA.dB.R0,2.G	39,59	47,36	5,47	1,20	11,56
10	CB.dB.R0,2.G	73,07	87,45	10,16	1,20	11,61
11	CA.dC.R0,2.G	101,34	122,47	12,70	1,21	10,37
12	CB.dC.R0,2.G	187,05	225,65	23,39	1,21	10,37
13	CA.dA.R0,3.G	9,48	10,97	2,01	1,16	18,28
14	CB.dA.R0,3.G	17,50	20,20	3,71	1,15	18,36
15	CA.dB.R0,3.G	59,24	70,87	8,18	1,20	11,55
16	CB.dB.R0,3.G	109,34	130,60	15,14	1,19	11,60
17	CA.dC.R0,3.G	151,65	183,05	18,79	1,21	10,26
18	CB.dC.R0,3.G	279,92	337,19	34,97	1,20	10,37
19	CA.dA.R0,4.G	12,60	14,56	2,68	1,16	18,44
20	CB.dA.R0,4.G	23,26	26,78	4,91	1,15	18,34
21	CA.dB.R0,4.G	78,75	94,03	10,81	1,19	11,49
22	CB.dB.R0,4.G	145,35	173,26	19,74	1,19	11,39
23	CA.dC.R0,4.G	201,59	242,97	24,82	1,21	10,22
24	CB.dC.R0,4.G	372,10	447,13	45,57	1,20	10,19
25	CA.dA.R0,5.G	15,69	18,08	3,36	1,15	18,57
26	CB.dA.R0,5.G	28,95	33,27	6,14	1,15	18,47
27	CA.dB.R0,5.G	98,04	116,84	13,36	1,19	11,43
28	CB.dB.R0,5.G	180,96	214,90	24,46	1,19	11,38
29	CA.dC.R0,5.G	250,98	301,67	30,70	1,20	10,18
30	CB.dC.R0,5.G	463,25	554,86	55,75	1,20	10,05
31	CA.dA.R0,6.G	18,72	21,41	4,04	1,14	18,85
32	CB.dA.R0,6.G	34,55	39,06	7,53	1,13	19,28
33	CA.dB.R0,6.G	116,98	138,97	15,79	1,19	11,37
34	CB.dB.R0,6.G	215,92	254,53	28,66	1,18	11,26
35	CA.dC.R0,6.G	299,47	358,87	35,74	1,20	9,96
36	CB.dC.R0,6.G	552,76	658,41	63,39	1,19	9,63
37	CA.dA.R0,7.G	21,68	24,44	4,84	1,13	19,81
38	CB.dA.R0,7.G	40,01	44,07	9,00	1,10	20,42

39	CA.dB.R0,7.G	135,49	159,05	18,27	1,17	11,49
40	CB.dB.R0,7.G	250,08	288,13	31,17	1,15	10,82
41	CA.dC.R0,7.G	346,85	411,82	39,94	1,19	9,70
42	CB.dC.R0,7.G	640,21	746,96	63,29	1,17	8,47
43	CA.dA.R0,8.G	24,59	26,99	5,65	1,10	20,93
44	CB.dA.R0,8.G	45,39	47,97	10,40	1,06	21,69
45	CA.dB.R0,8.G	153,70	176,10	20,01	1,15	11,36
46	CB.dB.R0,8.G	283,71	313,79	33,25	1,11	10,59
47	CA.dC.R0,8.G	393,48	456,63	42,73	1,16	9,36
48	CB.dC.R0,8.G	726,29	813,21	62,38	1,12	7,67
49	CA.dA.R0,9.G	27,46	29,02	6,34	1,06	21,83
50	CB.dA.R0,9.G	50,69	51,12	11,47	1,01	22,43
51	CA.dB.R0,9.G	171,64	189,81	21,90	1,11	11,54
52	CB.dB.R0,9.G	316,80	333,60	34,57	1,05	10,36
53	CA.dC.R0,9.G	439,39	491,73	45,66	1,12	9,28
54	CB.dC.R0,9.G	811,02	864,80	62,76	1,07	7,26
55	CA.dA.R0,95.G	28,88	29,95	6,69	1,04	22,34
56	CB.dA.R0,95.G	53,31	52,47	11,93	0,98	22,74
57	CA.dB.R0,95.G	180,50	195,71	22,72	1,08	11,61
58	CB.dB.R0,95.G	333,16	342,47	35,56	1,03	10,38
59	CA.dC.R0,95.G	462,07	506,46	46,94	1,10	9,27
60	CB.dC.R0,95.G	852,88	887,67	63,83	1,04	7,19
61	CA.dA.R1,0.G	30,29	30,80	6,97	1,02	22,62
62	CB.dA.R1,0.G	55,90	53,79	12,23	0,96	22,73
63	CA.dB.R1,0.G	189,28	200,93	23,76	1,06	11,82
64	CB.dB.R1,0.G	349,38	350,82	36,11	1,00	10,29
65	CA.dC.R1,0.G	484,57	520,30	48,04	1,07	9,23
66	CB.dC.R1,0.G	894,41	908,97	65,01	1,02	7,15
67	CA.dA.R1,1.G	31,51	32,33	7,03	1,03	21,74
68	CB.dA.R1,1.G	58,16	56,35	12,11	0,97	21,49
69	CA.dB.R1,1.G	196,94	211,17	21,63	1,07	10,24
70	CB.dB.R1,1.G	363,52	367,07	32,58	1,01	8,87
71	CA.dC.R1,1.G	504,18	546,90	43,59	1,08	7,97
72	CB.dC.R1,1.G	930,60	950,83	56,48	1,02	5,94
73	CA.dA.R1,2.G	32,66	33,68	7,46	1,03	22,15
74	CB.dA.R1,2.G	60,29	58,49	12,62	0,97	21,57
75	CA.dB.R1,2.G	204,14	219,56	22,63	1,08	10,31
76	CB.dB.R1,2.G	376,81	381,36	33,66	1,01	8,83
77	CA.dC.R1,2.G	522,61	568,69	45,50	1,09	8,00
78	CB.dC.R1,2.G	964,62	986,55	58,03	1,02	5,88
79	CA.dA.R1,25.G	33,21	34,24	7,59	1,03	22,17
80	CB.dA.R1,25.G	61,31	59,40	12,85	0,97	21,64
81	CA.dB.R1,25.G	207,59	223,63	23,08	1,08	10,32
82	CB.dB.R1,25.G	383,16	387,99	34,35	1,01	8,85
83	CA.dC.R1,25.G	531,43	579,14	46,38	1,09	8,01
84	CB.dC.R1,25.G	980,90	1003,90	59,19	1,02	5,90
85	CA.dA.R1,3.G	33,75	34,86	7,74	1,03	22,20
86	CB.dA.R1,3.G	62,30	60,41	13,13	0,97	21,73
87	CA.dB.R1,3.G	210,94	227,60	23,39	1,08	10,28
88	CB.dB.R1,3.G	389,35	394,11	34,76	1,01	8,82

89	CA.dC.R1,3,G	540,00	588,98	46,84	1,09	7,95
90	CB.dC.R1,3.G	996,73	1020,50	59,68	1,02	5,85
91	CA.dA.R1,35.G	34,27	35,47	7,90	1,03	22,28
92	CB.dA.R1,35.G	63,26	61,39	13,35	0,97	21,75
93	CA.dB.R1,35.G	214,20	231,14	24,08	1,08	10,42
94	CB.dB.R1,35.G	395,37	400,33	35,33	1,01	8,83
95	CA.dC.R1,35.G	548,36	598,37	47,70	1,09	7,97
96	CB.dC.R1,35.G	1012,10	1036,80	60,92	1,02	5,88
97	CA.dA.R1,4.G	34,78	35,97	8,05	1,03	22,38
98	CB.dA.R1,4.G	64,20	62,31	13,61	0,97	21,84
99	CA.dB.R1,4.G	217,38	234,63	24,24	1,08	10,33
100	CB.dB.R1,4.G	401,24	406,34	35,68	1,01	8,78
101	CA.dC.R1,4.G	556,49	607,36	48,56	1,09	7,99
102	CB.dC.R1,4.G	1027,20	1052,50	61,35	1,02	5,83
103	CA.dA.R1,5.G	35,76	36,99	8,29	1,03	22,42
104	CB.dA.R1,5.G	66,01	64,11	14,04	0,97	21,90
105	CA.dB.R1,5.G	223,50	241,59	25,19	1,08	10,43
106	CB.dB.R1,5.G	412,54	418,18	36,84	1,01	8,81
107	CA.dC.R1,5.G	572,17	625,11	50,15	1,09	8,02
108	CB.dC.R1,5.G	1056,10	1082,50	62,99	1,02	5,82
109	CA.dA.R1,6.G	36,70	38,07	8,54	1,04	22,43
110	CB.dA.R1,6.G	67,73	65,63	14,42	0,97	21,97
111	CA.dB.R1,6.G	229,34	248,05	25,88	1,08	10,43
112	CB.dB.R1,6.G	423,32	429,07	37,81	1,01	8,81
113	CA.dC.R1,6.G	587,12	642,09	51,82	1,09	8,07
114	CB.dC.R1,6.G	1083,70	1111,30	64,76	1,03	5,83
115	CA.dA.R1,7.G	37,59	39,02	8,80	1,04	22,57
116	CB.dA.R1,7.G	69,38	67,23	14,73	0,97	21,91
117	CA.dB.R1,7.G	234,92	254,49	26,56	1,08	10,43
118	CB.dB.R1,7.G	433,62	439,41	38,92	1,01	8,86
119	CA.dC.R1,7.G	601,41	658,31	53,30	1,09	8,10
120	CB.dC.R1,7.G	1110,10	1137,70	66,29	1,02	5,83
121	CA.dA.R1,8.G	38,44	39,86	8,99	1,04	22,56
122	CB.dA.R1,8.G	70,96	69,04	15,09	0,97	21,85
123	CA.dB.R1,8.G	240,27	260,28	27,35	1,08	10,51
124	CB.dB.R1,8.G	443,49	449,58	39,79	1,01	8,85
125	CA.dC.R1,8.G	615,10	673,46	54,43	1,09	8,08
126	CB.dC.R1,8.G	1135,30	1164,10	68,17	1,03	5,86
127	CA.dA.R1,9.G	39,27	40,81	9,21	1,04	22,56
128	CB.dA.R1,9.G	72,48	70,48	15,47	0,97	21,95
129	CA.dB.R1,9.G	245,41	266,06	28,01	1,08	10,53
130	CB.dB.R1,9.G	452,97	459,26	41,02	1,01	8,93
131	CA.dC.R1,9.G	628,24	688,99	55,74	1,10	8,09
132	CB.dC.R1,9.G	1159,60	1189,40	69,88	1,03	5,88
133	CA.dA.R2,0.G	40,06	41,60	9,44	1,04	22,70
134	CB.dA.R2,0.G	73,93	71,81	15,82	0,97	22,03
135	CA.dB.R2,0.G	250,35	271,23	28,56	1,08	10,53
136	CB.dB.R2,0.G	462,09	468,54	41,57	1,01	8,87
137	CA.dC.R2,0.G	640,89	702,63	57,32	1,10	8,16
138	CB.dC.R2,0.G	1182,90	1213,40	71,02	1,03	5,85

139	CA.dA.R2,1.G	40,82	42,36	9,69	1,04	22,88
140	CB.dA.R2,1.G	75,34	73,16	16,07	0,97	21,97
141	CA.dB.R2,1.G	255,10	276,76	29,22	1,08	10,56
142	CB.dB.R2,1.G	470,87	477,25	42,86	1,01	8,98
143	CA.dC.R2,1.G	653,07	716,52	58,64	1,10	8,18
144	CB.dC.R2,1.G	1205,40	1237,10	73,05	1,03	5,91
145	CA.dA.R2,2.G	41,55	43,05	9,81	1,04	22,79
146	CB.dA.R2,2.G	76,69	74,47	16,47	0,97	22,11
147	CA.dB.R2,2.G	259,69	281,52	29,84	1,08	10,60
148	CB.dB.R2,2.G	479,34	486,13	43,38	1,01	8,92
149	CA.dC.R2,2.G	664,82	728,98	60,16	1,10	8,25
150	CB.dC.R2,2.G	1227,10	1259,20	74,16	1,03	5,89
151	CA.dA.R2,3.G	42,26	43,98	10,04	1,04	22,82
152	CB.dA.R2,3.G	78,00	76,01	16,75	0,97	22,03
153	CA.dB.R2,3.G	264,13	286,76	30,34	1,09	10,58
154	CB.dB.R2,3.G	487,53	494,62	44,48	1,01	8,99
155	CA.dC.R2,3.G	676,17	742,34	60,78	1,10	8,19
156	CB.dC.R2,3.G	1248,10	1281,40	75,89	1,03	5,92
157	CA.dA.R2,4.G	42,95	44,71	10,25	1,04	22,92
158	CB.dA.R2,4.G	79,27	77,00	17,01	0,97	22,09
159	CA.dB.R2,4.G	268,42	291,46	31,06	1,09	10,66
160	CB.dB.R2,4.G	495,45	502,79	45,08	1,01	8,97
161	CA.dC.R2,4.G	687,16	754,96	61,99	1,10	8,21
162	CB.dC.R2,4.G	1268,30	1301,70	77,18	1,03	5,93
163	CA.dA.R2,5.G	43,61	45,42	10,40	1,04	22,91
164	CB.dA.R2,5.G	80,50	78,35	17,35	0,97	22,15
165	CA.dB.R2,5.G	272,58	296,08	31,49	1,09	10,64
166	CB.dB.R2,5.G	503,12	510,27	45,76	1,01	8,97
167	CA.dC.R2,5.G	697,79	766,45	63,24	1,10	8,25
168	CB.dC.R2,5.G	1288,00	1322,10	78,51	1,03	5,94
169	CA.dA.R2,6.G	44,26	46,08	10,50	1,04	22,79
170	CB.dA.R2,6.G	81,69	79,48	17,61	0,97	22,16
171	CA.dB.R2,6.G	276,60	300,43	31,87	1,09	10,61
172	CB.dB.R2,6.G	510,55	518,20	46,62	1,01	9,00
173	CA.dC.R2,6.G	708,11	778,44	64,53	1,10	8,29
174	CB.dC.R2,6.G	1307,00	1342,10	79,97	1,03	5,96
175	CA.dA.R2,7.G	44,88	46,72	10,73	1,04	22,97
176	CB.dA.R2,7.G	82,84	80,60	17,96	0,97	22,28
177	CA.dB.R2,7.G	280,51	305,13	32,56	1,09	10,67
178	CB.dB.R2,7.G	517,77	525,42	47,35	1,01	9,01
179	CA.dC.R2,7.G	718,11	789,33	65,50	1,10	8,30
180	CB.dC.R2,7.G	1325,50	1361,60	81,18	1,03	5,96

VITA

Raffaello Fico was born in the city of Naples, Italy. He earned his Bachelor of Civil Engineering degree from the University of Naples "Federico II" in October 2004, carrying out his thesis at the University of Missouri-Rolla (USA), titled "*Bridge Deck Construction with Internal FRP Reinforcement*" (April-August 2004). He will be graduating with the degree of Doctor of Philosophy in Materials and Structures Engineering in December 2007.